

FINAL PUBLISHABLE JRP REPORT

JRP-Contract number	IND05		
JRP short name	MEPROVISC		
JRP full title	Dynamic mechanical properties and long-term deformation behaviour of viscous materials		
Version numbers of latest contracted Annex Ia and Annex Ib against which the assessment will be made	Annex Ia:	V1.0	
	Annex Ib:	V1.0	
Period covered (dates)	From	01/10/2011	To 30/09/2014
JRP-Coordinator			
Name, title, organisation	Nigel Jennett, Dr. NPL		
Tel:	020 8943 6641		
Email:	nigel.jennett@npl.co.uk		
JRP website address	http://projects.npl.co.uk/meprovisc		
Other JRP-Partners	INRIM, Italy BAM, Germany PTB, Germany CSM, Switzerland NGFE, United Kingdom Schwarz, Germany		
REG1-Researcher (associated Home Organisation)	Norbert Schwarzer Schwarzer Norbert, Germany	Start date: 01 Oct 2011 Duration: 36 months	
REG2-Researcher (associated Home Organisation)	Cagatay Basdogan Koc University, Turkey	Start date: 01 Oct 2012 Duration: 24 months	
REG3-Researcher (associated Home Organisation)	Andrew Bushby Queen Mary University of London, United Kingdom	Start date: 01 Oct 2012 Duration: 24 months	

Report Status: PU Public

TABLE OF CONTENTS

1 Executive Summary 3

2 Project context, rationale and objectives 4

3 Research results 6

3.1 Traceable measurement of instrument drift 6

3.1.1 Stability of Instrumented Indentation Apparatus 6

3.1.1.1 Development of a Jamin Interferometer system to calibrate displacement..... 6

3.1.1.2 The demonstration of the IIT system stability 12

3.1.2 Calibration for IIT dynamic testing 13

3.1.3 Calibration of stylus based profilometer..... 15

3.1.3.1 In-situ characterisation of the probing force of stylus profilometers 16

3.1.3.2 Measurement of the effective stiffness and (vertical) dynamic performance of stylus profilometers . 18

3.1.3.3 Calibration of the tip radius of a diamond stylus 19

3.2 Dimension and mechanical property measurement of viscous materials – data generation. 23

3.2.1 Indentation creep measurement..... 23

3.2.2 Indentation dynamic measurement 23

3.2.3 Tensile testing on the polymers..... 24

3.2.4 Evaluation of Relaxation time as a function of temperature and relative humidity 24

3.2.5 Evaluation of the stress-relaxation response and degradation using Infrared spectroscopy 27

3.2.6 Sensitivity study of oscillation measurement methods..... 30

3.2.7 Practice in the determination of the absolute surface deformation of polymer specimen under sliding contact 32

3.2.8 Indentation creep at elevated temperatures on virgin PVC 34

3.3 Development of new analysis methods for measurement of dimensions and mechanical properties of viscous materials. 34

3.3.1 The development of the VE model for indentation creep test analysis 34

3.3.2 The development of the VE model for indentation dynamic test analysis..... 36

3.3.3 The development of the VE model for the polymer under sliding contact..... 38

3.3.4 Modeling of the surface deformation of SU-8 under sliding contact 40

3.3.5 Viscoelastic model used in 2D Finite Element analysis 41

3.3.6 Viscoelastic model used in 3D Finite Element analysis 45

3.4 Case Studies 45

3.4.1 Case study 1: Correction of step height measurement obtained using commercially available tactile probe methods 45

3.4.2 Case study 2: Nano-Indentation Visco-Elastic Characterisation of Elastomers for Creep Prediction of Automotive Timing Belts..... 50

3.5 Certified reference materials 53

3.6 Summary of research results 53

4 Actual and potential impact 54

5 Website address and contact details 55

6 List of publications..... 55

1 Executive Summary

Introduction

There is an immediate industrial need for new and validated measurement methods that are able to map the dimensional and mechanical properties of viscous materials with high-resolution. Viscous materials (such as polymers) continuously deform over time. This makes polymeric parts subject to dimension change that limits their useful lifetime. Current measurement methods are invalid because they assume a time independent material response. This project provided validated indentation and contact measurement methods to measure the shape, mechanical properties and deformation rate of viscous materials.

The Problem

A wide range of industrial products incorporate viscous materials (polymeric components), to improve cost-effectiveness, reduce weight and improve performance. For example, polymeric components can be used to manufacture lighter cars, reducing fuel consumption and CO₂ emissions, whilst also improving mechanical efficiency in components such as bearings and drive belts. However, the lifetime and performance of polymeric components is limited by their long-term deformation behaviour, as progressive deformation may alter their properties. Yet, before this project, prevailing measurement methods only measured short-term behaviour and assumed long-term stability - no methods were available for accurately measuring the long-term properties of viscous materials. To develop higher-performance, more competitive products, European industry therefore required methods to accurately measure the behaviour of viscous materials throughout their lifetime.

Specifically, more stable measurement instruments were required that could reduce measurement drift (a reduction in instrument accuracy over time) in order to distinguish drift from genuine nano-level deformation changes. New standardised measurement methods could then be developed using the new high-stability instruments, traceable to SI measurement unit definitions. The accurate interpretation of measurement results often requires complex modelling, yet the current models were too simplistic to simulate long-term deformation. New analysis techniques were required to better understand accuracy and uncertainty in long-term measurements of deformation. Suitable materials, with established properties, were also needed, to be used as reference materials from which measurement instruments could be calibrated.

The Solution

This project has developed methods of obtaining accurate time dependent properties of materials that are reproducible not only by indentation instruments but also by independent test methods. It has also developed and validated new measurement methods for high-resolution dimensional, mechanical property and deformational behaviour mapping of viscous materials based upon tactile probe (mechanical contact) methods. The approach of this project has been to target physical properties of materials that can be equally accessed and measured by independent methods and in units traceable to the SI.

The project addressed new measurement methods based upon mechanical contact and demonstrated their capability and reproducibility for high-resolution dimensional and mechanical property mapping of viscous materials in a number of industrial case studies. A key advance was to achieve a step improvement in the characterisation of the dimensional drift in metrological platforms and measurement systems. New and improved analysis techniques have been developed and validated to describe contacts with viscous materials. These have been used to improve measurement procedures and correction routines for contact-based dimensional measurement of visco-elastic materials, expressing outputs as property values traceable to the SI. The new validated measurement methods have been used to develop a specification for and identify a list of candidate certified reference materials, for which there is a demand from the polymer and life science industries.

Impact

The findings of the project has influenced the design of the future instrumented nano-indentation systems being developed by Anton Paar and Micro Materials Ltd, two of the European leading instrument developer in this field. The results obtained through the project have been used to understand the long term perform of polymeric products in two companies. The long term creep data has been used by SDS Limited to predict the life expectancy of their drainage structures. NGF Europe has used the ability to accurately measure the latex components in the timing belt and to give confidence of the improved designs to provide longer service life in automotive applications. The test procedures have been taken up by the ISO TC164/SC3 committees as new

work items for development of new standards, which will increase the uptake of these methods in the future. The identification of candidate reference materials for indentation creep and dynamic testing will also benefit the indentation community. An improved analytical solution for visco-elastic analysis was developed and a Matlab based programme has made available for users of nano-indentation equipment. More complex models was also developed by Schwarz from the output of this project, which are now commercially available via their website and consultancy services they provide.

2 Project context, rationale and objectives

Therefore the key aims of the project were to:

- Improve the characterisation of the dimensional drift in metrological platforms and measurement systems (used in the measurement of viscous materials). It is important to understand which component of the measurement is due to instrument drift over time which is a systematic error of the instrument and which component is due to the material true response, i.e. the data you actually want. In order to carry out this characterization, the project had to develop a novel highly stable differential (Jamin) optical interferometer with low noise, high sampling rate electronics.
- Write measurement procedures and correction routines for contact-based dimensional measurement. The current state of the art for dimensional measurement using tactile probes is entirely optimised for purely elastic contacts and cannot cope with visco-elastic or visco-plastic materials at all. Using current methods on viscous materials results in an order of magnitude increase in measurement uncertainty (error). The development of step-height artefacts and the procedures to use them in stylus profilometry, coordinate measurement machines (CMM) with touch-trigger probes and scanned probe microscopy (SPM), will enable a significant reduction of uncertainty in dimensional measurement
- Develop validated methods to obtain the mechanical properties of visco-elastic materials as property values traceable to the SI. By providing the traceability of the force and displacement calibration of the testing machine, the mechanical properties can be derived absolutely without referencing to a primary instrument.
- Develop improved analysis methods to describe contacts with viscous materials, and validate these methods. Increasing the complexity of the viscous-elastic model to be able to better simulate the response of soft polymers Viscoelastic materials exhibit both viscous and elastic characteristics when undergoing deformation. Various models are needed in order to determine their stress and strain interactions, which commonly use a combination of springs and dashpots to simulate elastic and viscous components respectively. Compared to the simply Voigt model which only consists of a Newtonian damper and Hookean elastic spring connected in parallel, the three-element standard linear solid (SLS) model is more accurate in predicting polymeric material responses by having an extra spring element to simulate the immediate elastic response. In reality, polymers are believed to be a mixture of many different springs and dashpots. This means when polymers are going through a deformation process, different parts of the polymer chains will response at different speed, hence contribute more than one time constant. The SLS model oversimplifies this process by allowing only one time constant, which is highly related to the experimental creep time. During a creep experiment, over time, longer time constant is activated which will dominate the calculated results when using SLS model for simulation. This will require the users to choose the creep time carefully when design their experiments, which they normally have lack of knowledge. In order to describe the polymer deformation response more accurately, the SLS model is expanded to an element Kelvin model by having more springs and dashpots.
- Demonstrate applicability of the methods in a number of industrial case studies, work with SDS limited demonstrated the ability to distinguish mechanical property differences between products manufactured from recycled or virgin feedstock.
- Develop a specification for and identify a list of candidate certified reference materials, for which there is a strong demand, inter alia from the polymer and life science industries.

This project enables the integration of effort across EU centres of excellence to address a pressing industrial need. This project has established collaboration with all of the leading instrumented indentation manufacturers in the world. The resulting alignment of effort shares out the necessary tasks between partners, which reduces duplication at national level. This project not only brings together a critical mass of instrumentation to solve the

technical challenges, but also enables evaluation of the developed solutions to ensure the widest possible impact on existing commercial equipment and corresponding user bases. Working together across the EU builds the necessary consensus for a standards acceptance, before even submission of a NWIP. This will act to speed up the standardisation process. The project benefits from active involvement of industrial end users, which will demonstrate the applicability and efficacy of the solutions developed in the project. This will accelerate adoption of the technology and the consequent benefits of accelerated innovation and improved sustainability and competitiveness in EU industry.

Objectives:

1. To develop traceable measurement methods of instrument drift in order to clearly distinguish instrument drift from material viscosity.
2. To develop and validate methods for the measurement of dimensional and mechanical properties of viscous materials when in contact or stressed. These properties include: shape or dimension, elastic modulus (complex or multi-component) and viscosity (time constant).
3. To develop new analysis methods (standard protocols & algorithms) for the measurement of dimensions and mechanical properties of viscous materials to demonstrate modulus measurements from all methods

In addition the project will demonstrate the applicability of the methods in a number of industrial case studies and develop a specification for and identify a list of candidate certified reference materials.

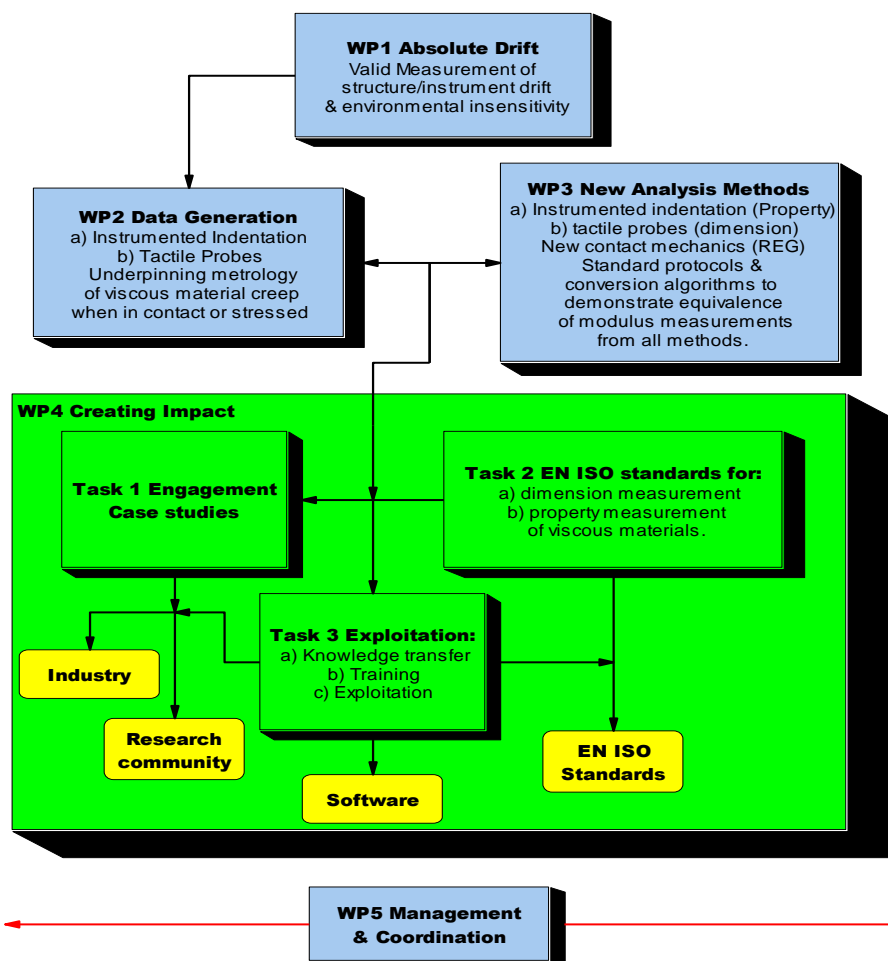


Figure 1: Relationship of work-packages and scientific and technological objectives to project main challenges.

3 Research results

3.1 Traceable measurement of instrument drift

3.1.1 Stability of Instrumented Indentation Apparatus

In order to understand the viscous behaviour of a material, one must first understand how the measurement instrument will behave when held under a constant load or position for long periods of time in particular how reliable is the obtained data. These load and displacement data are then used to derive properties parameterise to describe the materials behaviour. One key requirement is to calibrate the displacement of the measurement instrument at the length-scale that match the measurement request. In this project, this was carried out using an optical interferometer system.

3.1.1.1 Development of a Jamin Interferometer system to calibrate displacement

There is a growing demand for higher accuracy displacement measurements at small scales (nanometre to micrometre range), driven by commercial trend to make material component smaller and more compact. To accurately measurement the dimensions at these small length scales, the optical interferometry is proven to be a good candidate [1]. In this project, the NPL Plane Mirror Differential Optical interferometer has been modified at NPL, a field programmable gate array (FPGA) fringe counting system developed to run on a LabVIEW platform and its performance rigorously assessed against the x-ray interferometer. This modified Jamin Interferometer was then used to calibrate the displacement of the nano-indentation apparatus at PTB and BAM.

a. Interferometer operating principle

The NPL plane mirror interferometer is shown in Figure 2. It is designed to be used in conjunction with a helium neon laser, either stabilised or unstabilised depending on the application. Polarised light with a wavelength of 632.8 nm in air enters the Jamin Interferometer block and is incident on the quadrature coated beamsplitter (QCBS). The beamsplitter splits the light into two components, one of which is reflected off a quadrature coating which retards the phase by $\pi/4$ with respect to the transmitted beam.

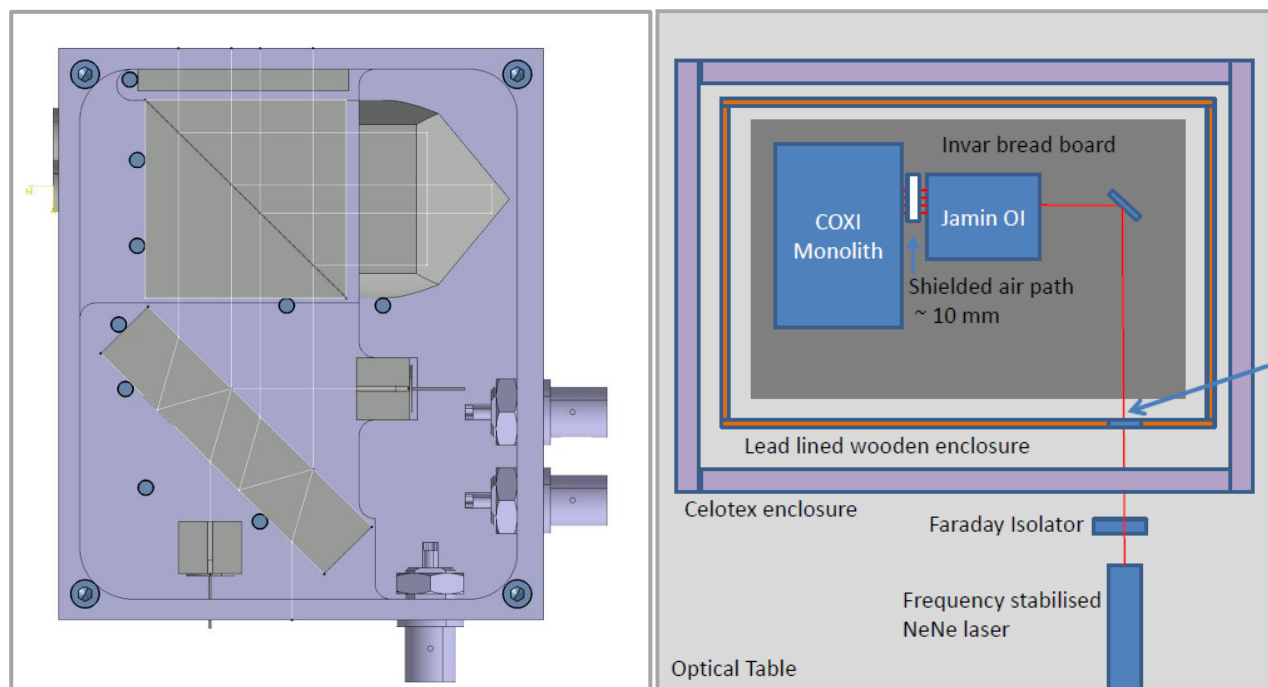


Figure 2 Left: the schematic diagram of the NPL Plane Mirror Differential Optical Interferometer; Right: the setup to check stability of interferometer against an X-ray interferometer.

The two beams leave the QCBS and enter the polarising beam splitter (PBS). The polarization of the incoming beam is aligned so as to transmit both beams through the PBS and to fall onto the measurement reference

and sample mirrors from which the beams are reflected back into the interferometer. In doing so, the beams pass through the quarter wave plate twice, which has the effect of rotating the polarisation of the light by $\pi/4$. These beams are therefore reflected by the polarizing beamsplitters onto the cube corner where they are displaced, but retro-reflected back onto the polarising beam splitter. The beams are incident on the mirrors again, but displaced from their original positions such that the inner two beams shown in Figure 2 belong to one path and the other two to the other. After reflection from the mirrors the beams are re-transmitted by the polarising beam splitter and recombine at the Jamin beamsplitter. Two beams are produced with, in the ideal case, a $\pi/4$ phase difference between them (sine and cosine) and contain information about the displacement of the moving mirror.

b. Data collection

The intensity of the beams is measured using photodiodes 1 and 2. Photodiode 3 measures the intensity of the laser beam and this signal can be used to correct for any variations in laser beam intensity. Both beams have a D.C offset and their phase difference is not exactly $\pi/4$ owing to imperfections in the beam splitter ratio and stray reflections in the interferometer. Signals from the photodiodes are converted from current to voltage using transimpedance amplifiers and normalised using the intensity reference signal from photodiode 3. The signals are then 'conditioned' to have an amplitude ± 9.5 V giving a resolution of 0.7 pm and are acquired by a National Instruments FPGA card. This ensures that most of the dynamic range of the analogue to digital converters (ADCs) is used, but allows some scope for any changes in the amplitude of the signals. Data is acquired from the interferometer by the ADCs at a frequency of 200 kHz. Software on the FPGA process the data and obtains a value for the phase of the beam and hence a displacement. As mentioned above, the two signals from the photodiodes will not be exactly in quadrature. The usual method for correcting for this is to use a Heydemann correction [2]. There are several options for implementing this; the first and simplest is to obtain data for calculation of the Heydemann correction parameters prior to use of the interferometer by cycling through an optical fringe and to use this data during the operation of the interferometer. This assumes that the errors in the optical signal, i.e. deviation from quadrature, caused by signal amplitude and alignment remain constant. Although this may not be the case, any changes should be assumed to be small. The other alternative is to continually update the Heydemann correction as the optical interferometer measures displacements equivalent to multiple fringes. The processing required for this is beyond the requirements of a single FPGA card. To overcome this limitation, it is necessary to determine the revised Heydemann parameters on the pc and download them onto the FPGA. Figure 3 is a schematic diagram of the data collection process and Figure 4 shows the results of processing some data using a fixed Heydemann correction and a real time Heydemann correction. The scan was 100 μm in steps of 100 nm generated by a high precision servo controlled translation stage moving at 120 micrometres per minute.

c. Validation of noise level

In order to measure the noise level one could expect in an optimal experimental configuration, the optical interferometer was aligned against the x-ray interferometer (as shown in Figure 2). The x-ray interferometer (XRI) is made from a single crystal of silicon and a piezo actuator can be used to move one of the mirrors to allow setting up of the interferometer. Once this has been done the piezo actuator is brought out of contact and the x-ray interferometer is effectively a fixed mirror. Moving the mirror during the setup of the optical interferometer ensures optimal alignment of the interferometer and adjustment of the electronics, to measure the noise level and stability of the electronics and interferometer, the interferometer was aligned to the x-ray interferometer. A Fourier Transform of the optical interferometer signal shows the noise level to be ± 12.4 pm at 100 kHz. The noise level on the optical interferometer signal (which also includes a component for any vibration of the XRI) when illuminated with a stabilized laser and aligned to the x-ray interferometer. Figure 5 shows the actual drift in nanometres corrected for changes in refractive index using the modified Edlen equations [3]. The total drift was of the order of 600 pm corresponding to 0.16 pm per minute. The largest drift rate during this period was 1 pm/minute and the smallest was 0.006 pm/minute. The drift measurement was carried out in a well-controlled laboratory environment at NPL (low vibration, highly stable mirror block, low noise, a separate control room to house all the power supplies, a double thermal enclosure, etc); therefore, this level of stability represents the "best case" scenario. It is not a representation of the stability of a typical setup, but demonstrates the maximum achievable stability.

d. A portable Jamin interferometer system

NPL then made the updated Jamin interferometer portable in a package suitcase as shown in Figure 6. This allowed an easy transportation of the system to provide displacement calibration to other organisations /institutes to provide traceability to NPL’s x-ray interferometer. This device was then used to calibration the instrumented indentation tester (such as the Hysitron T950 TriboIndenter at PTB in Germany); the setup varies depending on any particular system; and the setup in PTB is shown in Figure 7.

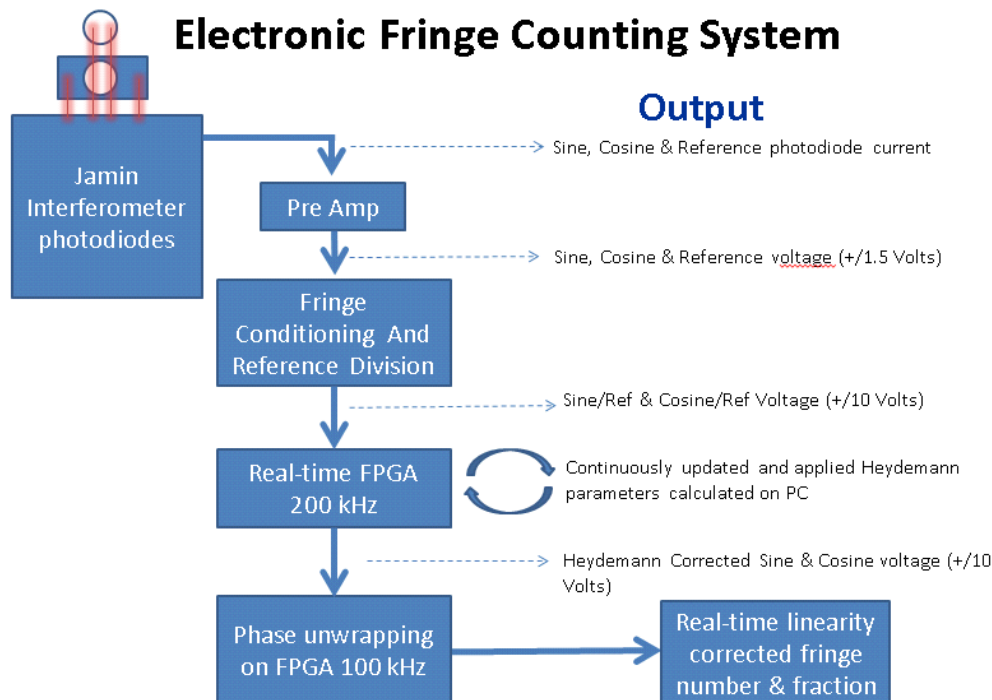


Figure 3. Schematic of the data processing and collection routines used by the FPGA fringe counting software.

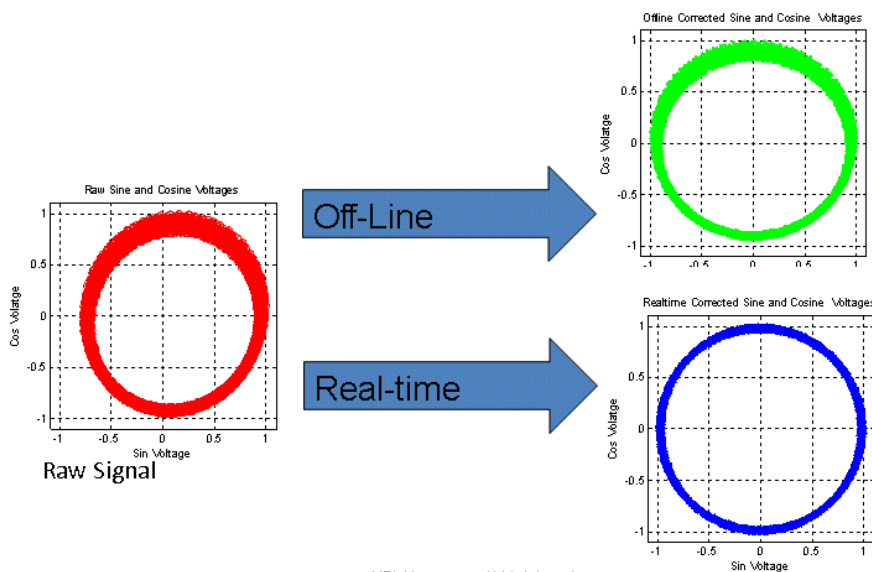


Figure 4 Showing the benefits of a real-time constantly updating Heydemann Correction (Blue), against an averaged Off-Line Correction (Green), of raw signal (red).

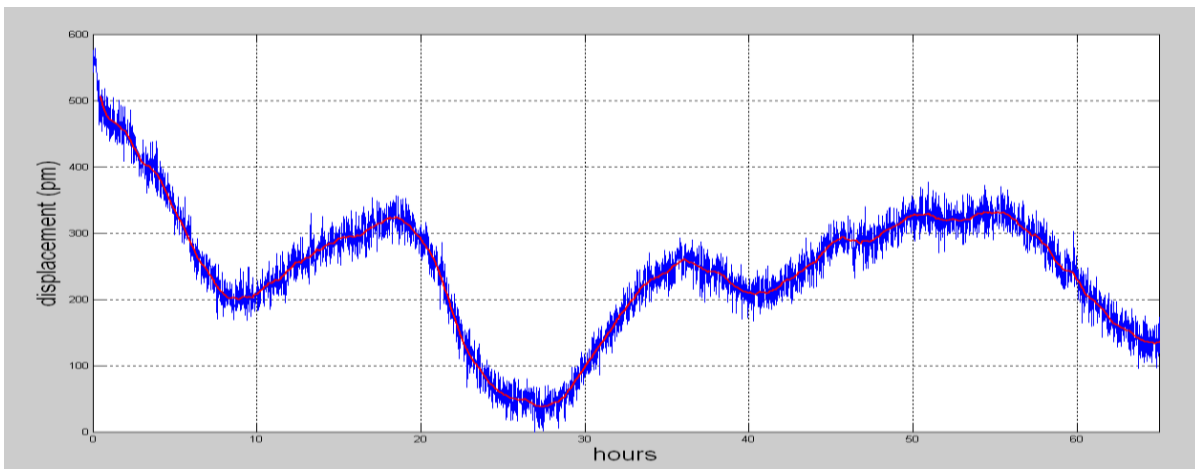
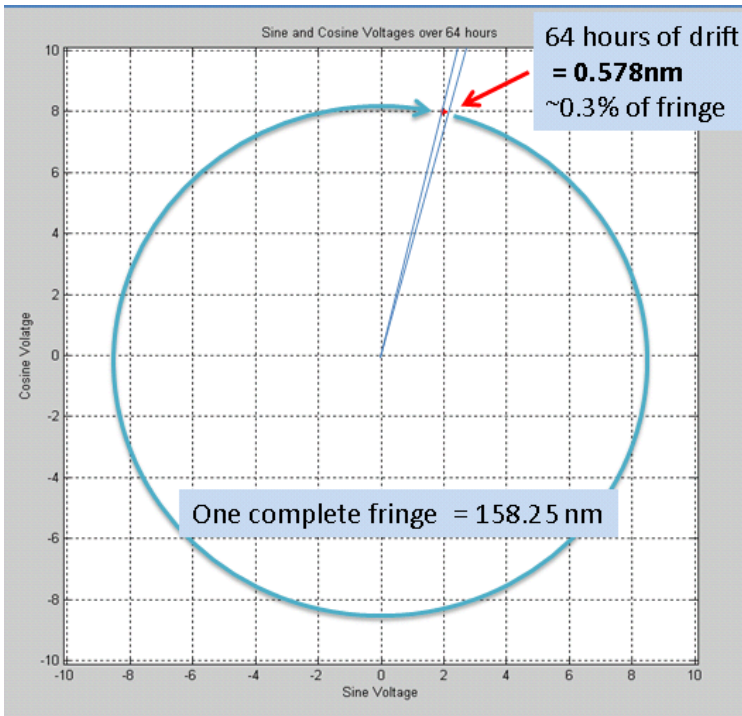


Figure 5 Showing the drift detected in the system over 64 hours for a frequency stabilised free space laser feed against the COXI monolith. The COXI monolith is a highly stable single crystal interferometer with two movable mirrors. The observed max drift rate in 64 hours is 0.062nm/hour, which is equivalent to 1.033 pm/min.



Figure 6 A portable Jamin interferometer system was developed at NPL.

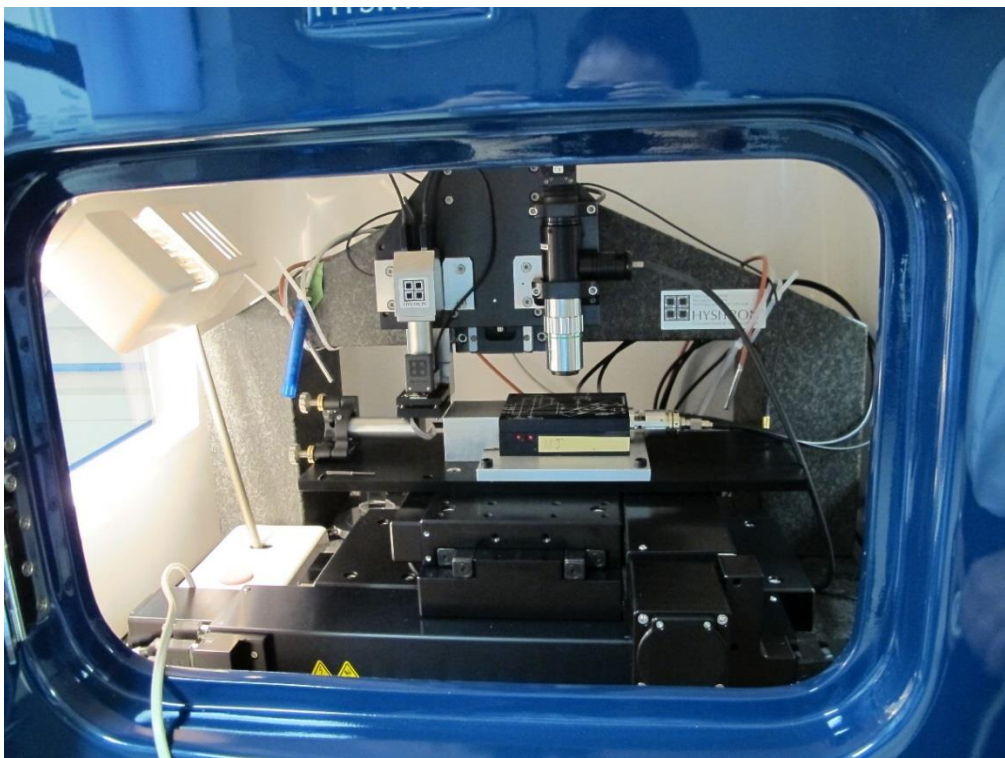


Figure 7 The set-up of the Jamin interferometer system for displacement of the Hysitron T950 TriboIndenter at PTB.

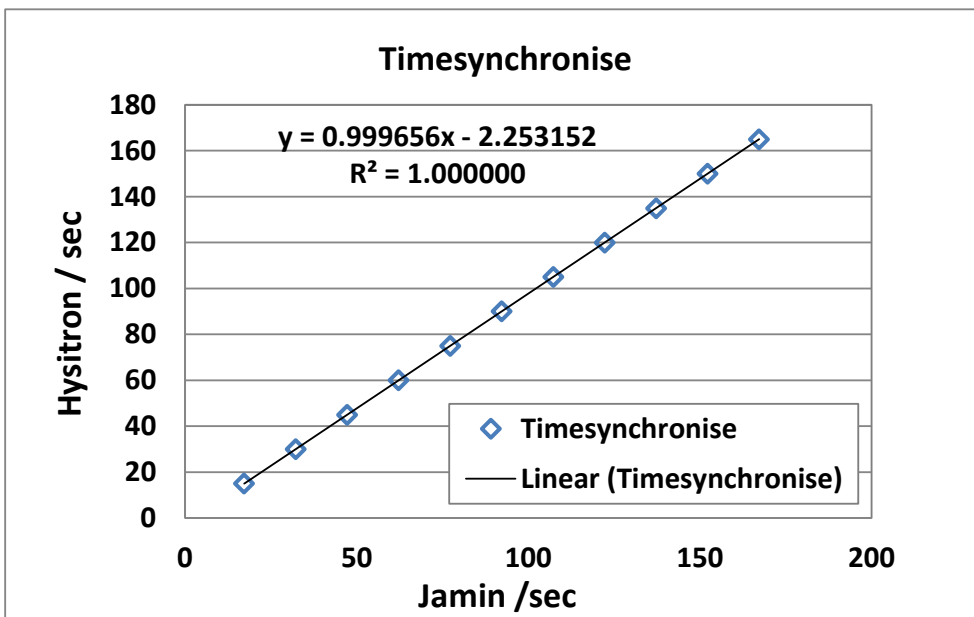
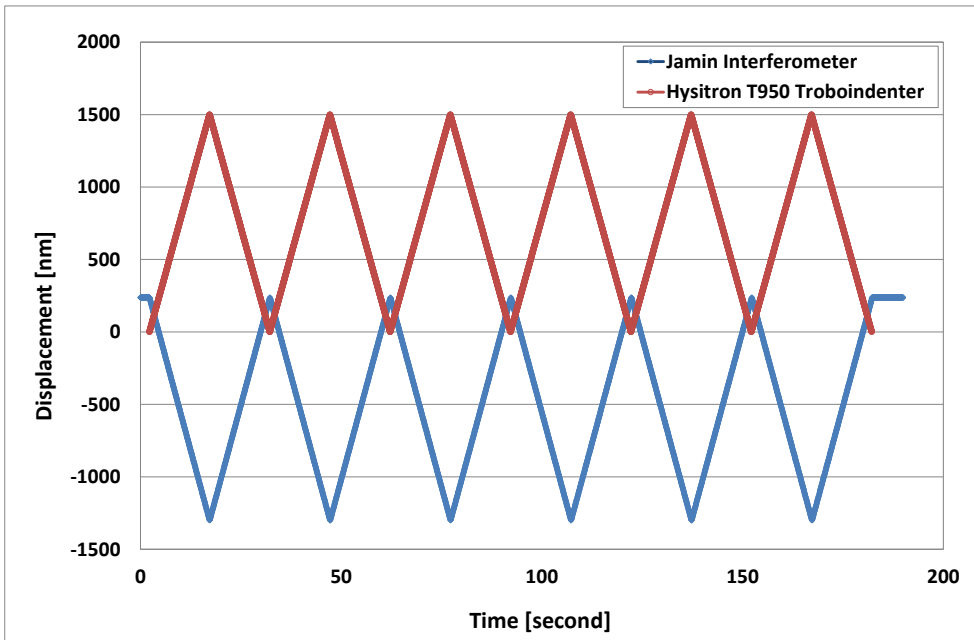


Figure 8 The displacement calibration of the Hysitron T950 TribolIndenter using the Jamin interferometer.

Displacement calibration was essential for instrumented indentation testing to obtain validated data. For such a calibration, a mirror is attached to the indenter shaft which was driven by an actuator. The mirror was then moved across the travel range, the moving displacement was recorded by the interferometer. According to ISO 14577, at least three repeating cycles should be used for calibration the displacement measuring device; in this study, six cycles were carried out. By comparing the two data sets, a calibration can be done. The obtained calibration results of the Hysitron T950 TribolIndenter are shown in Figure 8. The displacement calibration error was found to be 2.5 % between the Jamin data and the Hysitron data. This error should be used to update the system calibration values.

3.1.1.2 The demonstration of the IIT system stability

An Ultra Nanoindentation Tester (UNHT, CSM Instruments SA, now Anton Paar) was used in this study, located in a laboratory environment with temperature variation to be smaller than $\pm 0.1^{\circ}\text{C}$ (Nano-mechanics Lab, National Physical Laboratory, Teddington, UK). The UNHT features a unique design of dual indenters; one indenter is used for indentation while the other one is providing active surface referencing, to minimise thermal drift and frame compliance in real experimental time [4]. CSM supported NPL to check the long-term stability of the UNHT by doing long creep indentation testing on reference materials. A synthetic single crystal diamond was used to check the stability of the UNHT. Diamond is probably the most popular choice for indenter materials especially when operating at room temperatures. A spherical diamond indenter ($R=5\ \mu\text{m}$) was used to make an elastic contact under the force of 1 mN and hold for 100 hours as shown in Figure 9, which is believed is the longest nano-indentation creep experiment ever reported. The thermal drift rate of 0.01 pm/second from the synthetic single crystal diamond was calculated from the whole displacement data of the constant force holding period, this extremely low drift is detecting a movement at atomic level.

The thermal drift rate of 0.01 pm/second from the synthetic single crystal diamond was calculated from the whole displacement data of the constant force holding period; therefore, it is heavily averaged. There is a possibility that the short term thermal fluctuation (at the time scale of tens of seconds) is likely to be cancelled out when fitting a very long creep data. In order to investigate this, the displacement data was cut into small segments of only 60 seconds, same time as a normal indentation creep test would take. The drift rate was then calculated for every segment as plotted in Figure 10. It was found that the short term drift could be as high as 5 pm/second; this is still a very low drift rate for a normal indentation testing, but significantly higher than the 0.01 pm/second obtained from the whole dataset. This raises a question of what is the best time scale to calculate the thermal drift when conducting indentation creep test. One recommendation given here is that the time scale for calculating the thermal drift should be similar to the performed indentation test. Two orders of magnitude difference in the estimated thermal drift may exist if the wrong set of data is chosen.

The measured low thermal drifts provide strong evidence to confirm that the UNHT system has extremely good long term stability in the laboratory environment for this study. The dual indenter design of the UNHT is a top referencing system, compared to other IIT systems available in the market; this unique feature cuts down the frame loop; the use of ZeroDur® glass also reduces the thermal sensitivity with temperature. The results reposted here suggest that such a system can provide extremely good stability for long term indentation creep testing when located in a well-controlled environment. Ultra-stability enables collection of valid, low-uncertainty, long-term creep data – orders of magnitude longer than previously possible, which allows the investigation of longer-term indentation creep study using instrumented indentation.

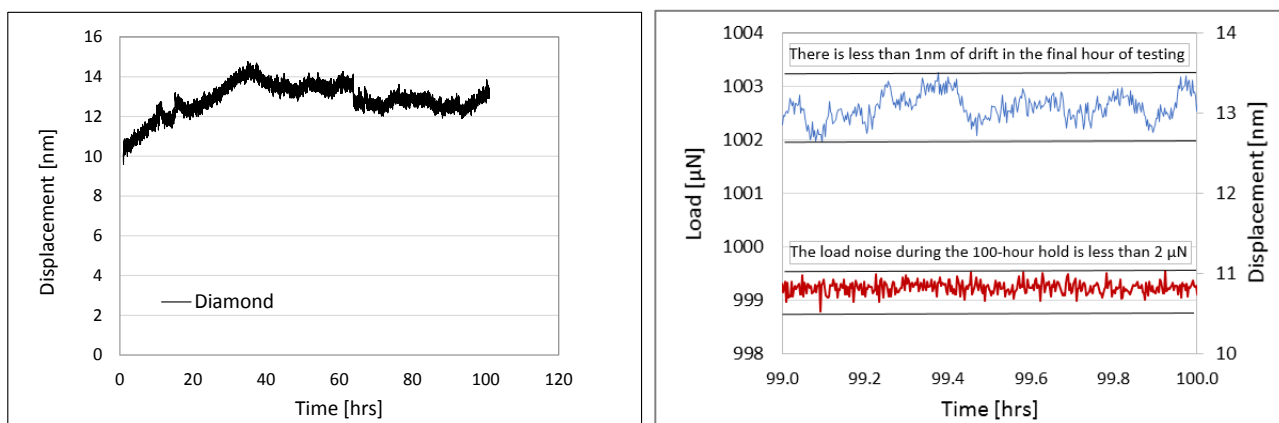


Figure 9 The 100 hour indentation creep on a piece of synthetic single crystal diamond using a spherical indenter ($R=5\ \mu\text{m}$).

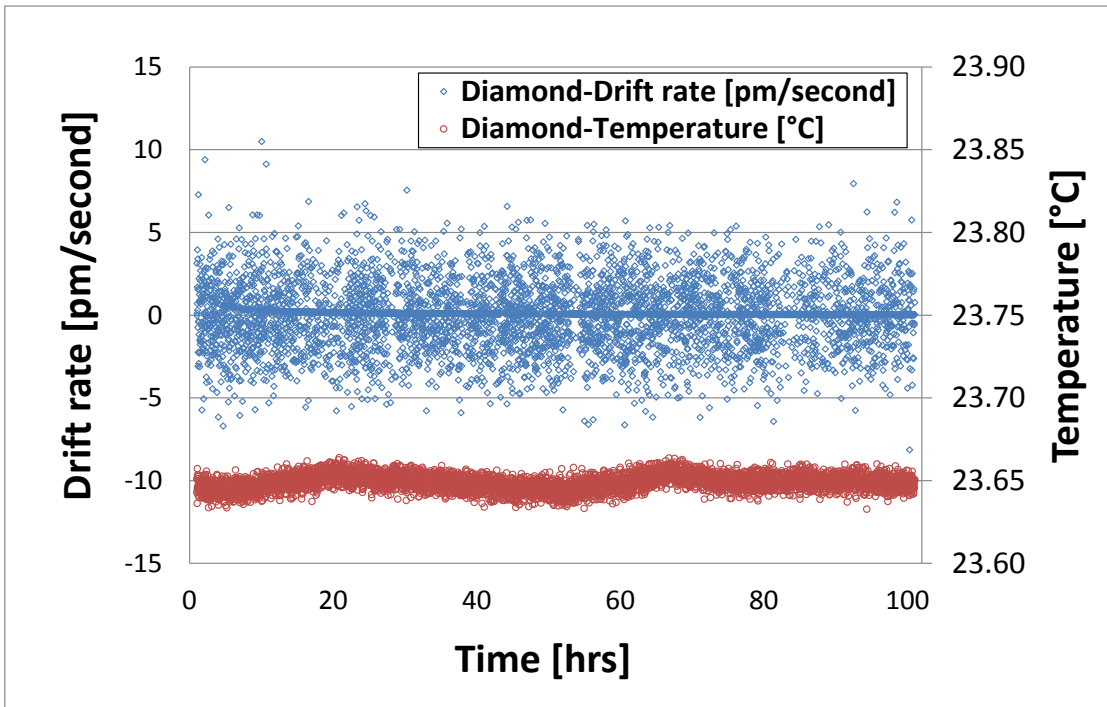


Figure 10 Left axis: the drift rate calculated from the data obtained from the synthetic diamond for every 60 seconds data showing a much higher short term drift rate compared to the 0.01 pm/second drift rate calculation using the whole date set. Right axis: the temperature of the UNHT chamber showing the temperature variation during the creep experiment is about $\pm 0.01^{\circ}\text{C}$.

3.1.2 Calibration for IIT dynamic testing

During basic instrumented indentation testing usually contact force and displacement penetration are measured continuously. Using dynamic testing in addition a small oscillation is superimposed on the semi-static force, and a frequency-specific amplifier is used to measure the response of the indenter. Typically, the amplitude of the force oscillation is controlled (increased) such that the amplitude h_0 of the displacement oscillation remains constant. As an example of an oscillating test system, Figure 11 shows the measuring head of a Nano Indenter G200 (XP or DCM) located in BAM.

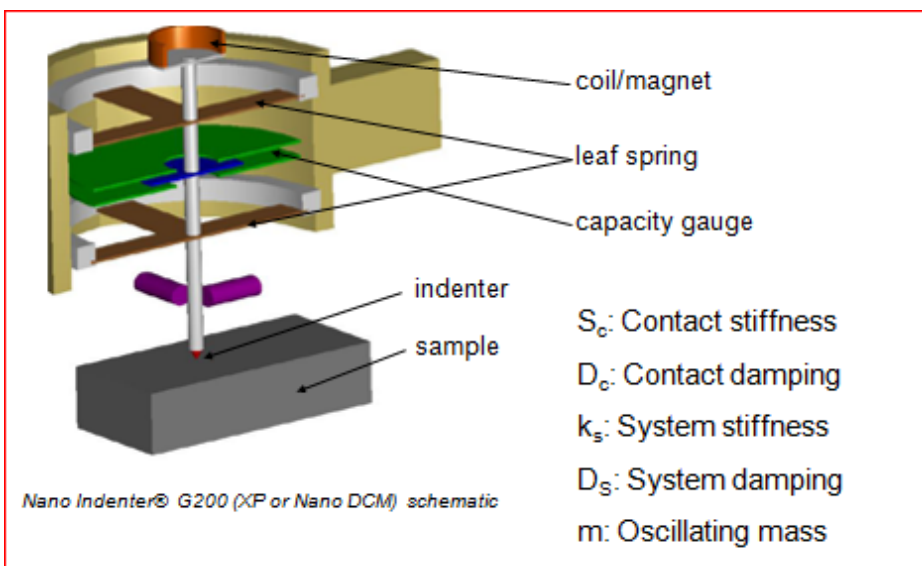


Figure 11 Measuring head of an Nano Indenter G200 (XP or DCM).

Such an oscillating system in contact with the sample can be modelled using a simple harmonic oscillator and taking in to account system stiffness k , system damping D and oscillating mass m as shown in Figure 12. For the calibration of the measurement of dynamic force and displacement amplitude it is assumed, that the results of the calibration for semi-static measurement can be applied. Usually the measurement of phase angle is not calibrated. The values for dynamic system stiffness, dynamic system damping and oscillating mass must be estimated additionally using measurements on a free hanging indenter. Figure 13 shows an example of dynamic compliance obtained by BAM, as measured for free oscillating measuring heads of Nano DCM. By fitting this curve, the Dynamic system stiffness k_s , dynamic system damping D_s and oscillating mass m can be determined.

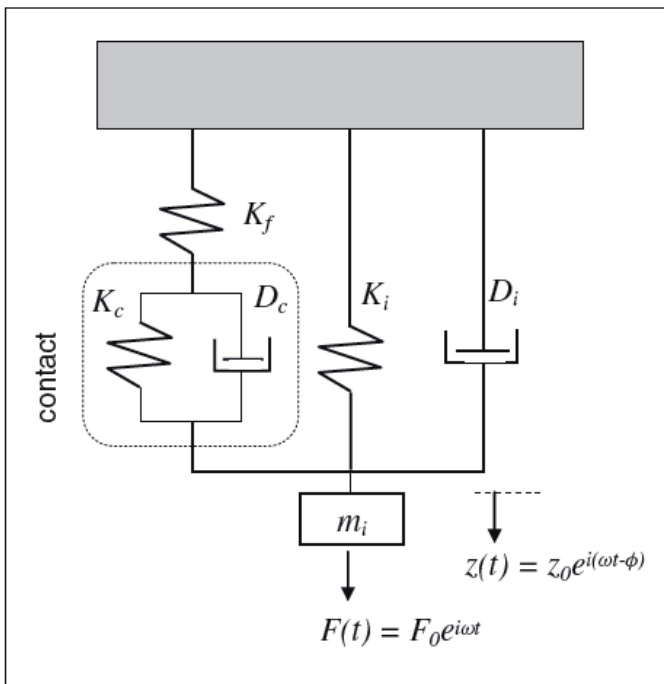


Figure 12 Model of oscillating system in contact with the sample.

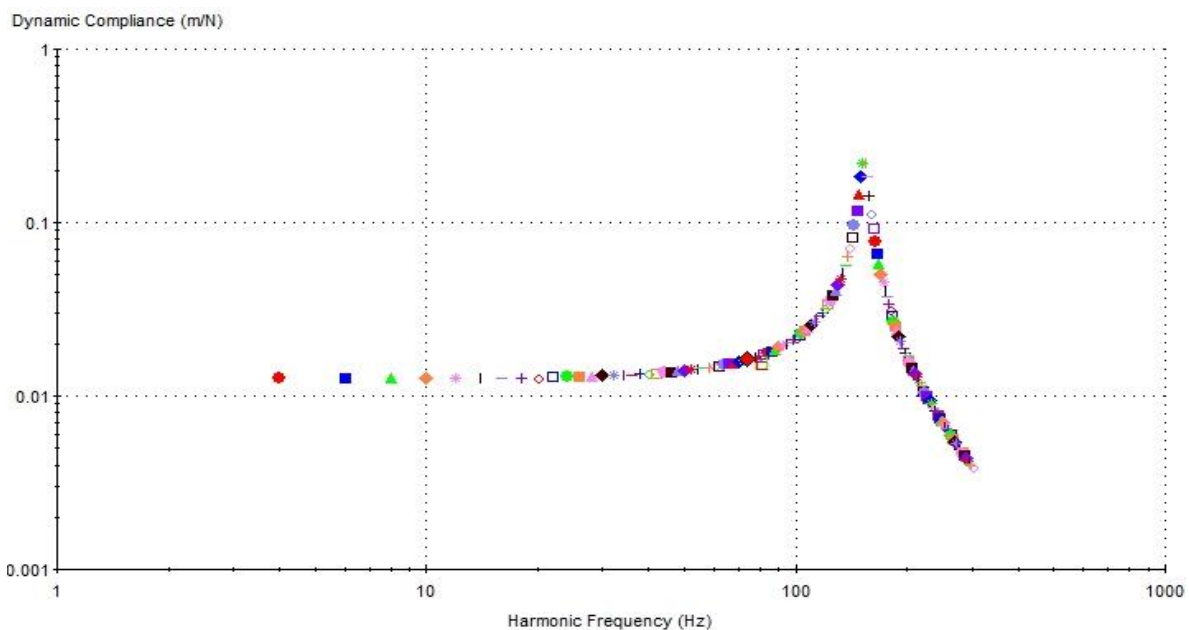


Figure 13 Measured compliance for the Nano DCM. Compliance was measured with the indenter hanging free in the center of the displacement range.

To evaluate the stability of calibration, the stability of dynamic system stiffness k_s , system dumping D_s and oscillating mass m under different environmental conditions (temperature, air pressure and humidity) was investigated. The temperature in the test box (T_{box}) was changed systematically in the range from 22 °C to 29 °C. Because a controlled change of temperature keeping air pressure and humidity constant was not possible, the calibrated values for k_s , D_s and m together with actual values for the temperature in the box, the pressure in the lab and the relative humidity have been recorded over three months. The relative humidity in the lab was between 34 % and 37 % for all calibrations. It was found that these calibration values were indeed influenced by the environmental temperature and air pressure. As a result, it is strongly recommended to perform a calibration of dynamic system stiffness, dynamic system dumping and dynamic mass just before conducting the dynamic tests on the sample under investigation.

3.1.3 Calibration of stylus based profilometer

Cost-effective polymers have long been applied in micro-system technology for forming various micro- and nano-structures [5], including micro-optics like micro-lens arrays, diffractive micro-optical elements, and micro-actuators and -sensors like micro-grippers and micro-x-y stages, etc. In many cases, the functionality of these photo resist micro-structures is, to a large extent, determined by the geometrical dimensions of these structures. As for quantitative dimensional characterization of polymer microstructures, currently available dimensional measurement methods and instruments suffer usually from technical difficulties. Most photo resists are usually transparent. As a result, photo resist structures cannot be easily measured by optical methods including imaging and non-imaging systems. The specimens' low reflectance is the most important reason for strong systematic deviations. On the contrary, contact stylus-based profilometry, whose measurement results are, in general, independent of the physical, electrical and optical properties of the material under test, should be in general an ideal choice for the quantitative determination of the dimensions of structures made of polymer. However, at least compared with silicon-based functional materials for microsystems, photo resists generally have relatively weak mechanical properties (low Young's modulus, weak tensile strength and hardness) and usually additionally a noticeable viscosity. Consequently, large systematic measurement deviations appear when photo resist macro- and micro-structures are characterized by contact-based stylus profilometry [6]. To improve the measurement accuracy of stylus profilometry for soft specimens, one of the natural approaches would be to model the surface deformations of soft specimens under tactile scan, and then to compensate for these systematic deviations as demonstrated in Figure 14.

The measurement results of typical stylus probe methods for determination of the dimensions of specimens, which consist of several different materials, especially of viscous materials, usually demonstrate considerably large deviation. Detailed analysis of the error sources within stylus step-height measurement method/system reveals that the potential dimensional measurement error is jointly determined by the mechanical properties of the substrate and of the viscous material and by the measurement conditions of the stylus instrument in use. Good understanding of the characteristics of a stylus instrument used for step height measurement would lay a solid foundation for the next working points of this project. This calibration work was carried out by PTB including the following fundamental characterizations:

- Determination of the form error (and equivalent radius) of the stylus tip in use
- Calibration of the contact force generated by a stylus instrument
- Characterization of the probe sensing system of the stylus instrument in use
- Characterization of the dynamic performance of the stylus instrument

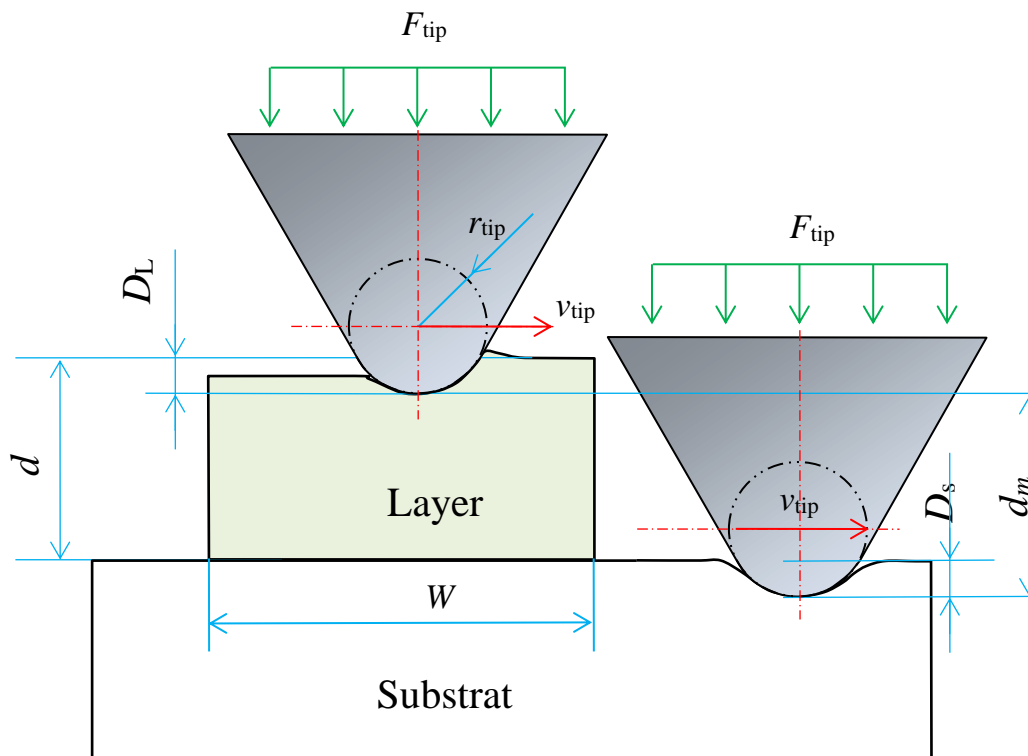


Figure 14: Step height measurement of a viscous material on a substrate with a stylus instrument. Large errors in the measured step height d_m occur because viscous materials deform more than the substrate ($d_s \ll d_{vm}$), where t is the thickness of the polymer layer at zero-probing force, t_m the measured layer thickness (step height) under a probing force F_{tip} and a tip radius r_{tip} .

3.1.3.1 In-situ characterisation of the probing force of stylus profilometers

The probing force applied on a specimen under test is one of the most important factors for modelling the measurement deviations of tactile profilometry. In most commercial profilometers the correct probing force will only be generated when the surface under test is scanned. Therefore the in-situ determination of the probing force becomes one of the preconditions for high precision force calibration of tactile profilometers. In this project, a cantilever-based force transfer standard [7] and a micro-machined nano-force actuator have been employed for this purpose. The fundamental principle of the cantilever-based force calibration system is shown in Figure 15.

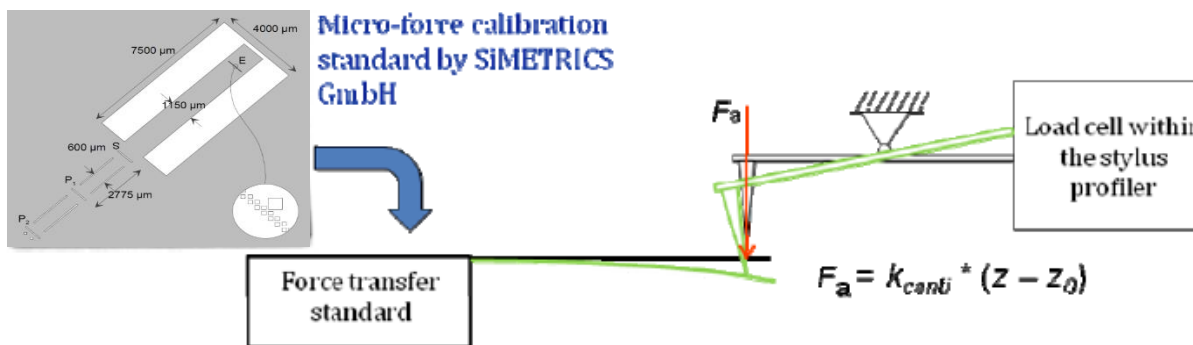


Figure 15 Fundamental principle of the cantilever-based force calibration system using a cantilever-based micro-force transfer standard

To further verify the probing force in the low-force region, a micromachined nanoforce actuator recently developed by PTB is applied to characterize the probing force of a contact stylus profilometer. To demonstrate the feasibility of the in-situ force characterisation approach shown in Figure 16 (a), a prototype of the PTB nanoforce actuator (b) is positioned under the stylus of the Tencor profilometer. With our selfdeveloped stiffness calibration system, the fundamental specifications of the nanoforce prototype have been found to be: $k_{MEMS} = 31.6 \text{ N/m}$, and $s_{MEMS} = 328.0 \text{ nm/V}$.

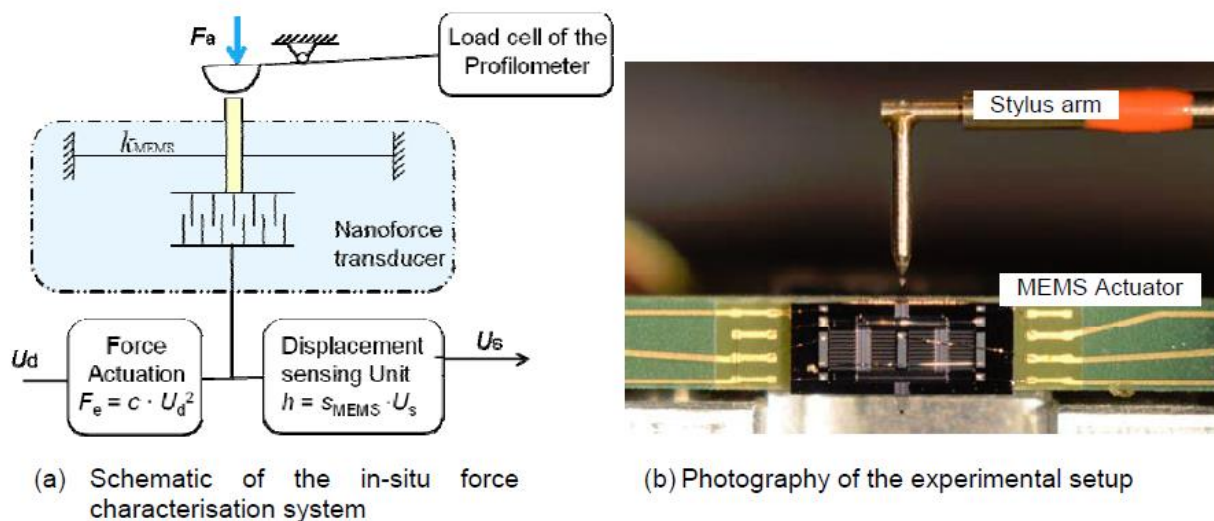


Figure 16 In-situ calibration of the probing force of a contact stylus profilometer using a micro-machined nano-force actuator: (a), a prototype of the PTB nanoforce actuator (b) is positioned under the stylus of the Tencor profilometer.

The preliminary calibration result of the probing force of a Tencor P11 (KLA-Tencor, USA) is demonstrated in Figure 17, which reveals that the profilometer Tencor P11 has a quite good force linearity ($\sim 1.2\%$) and a relatively small offset ($-1.95 \mu\text{N}$).

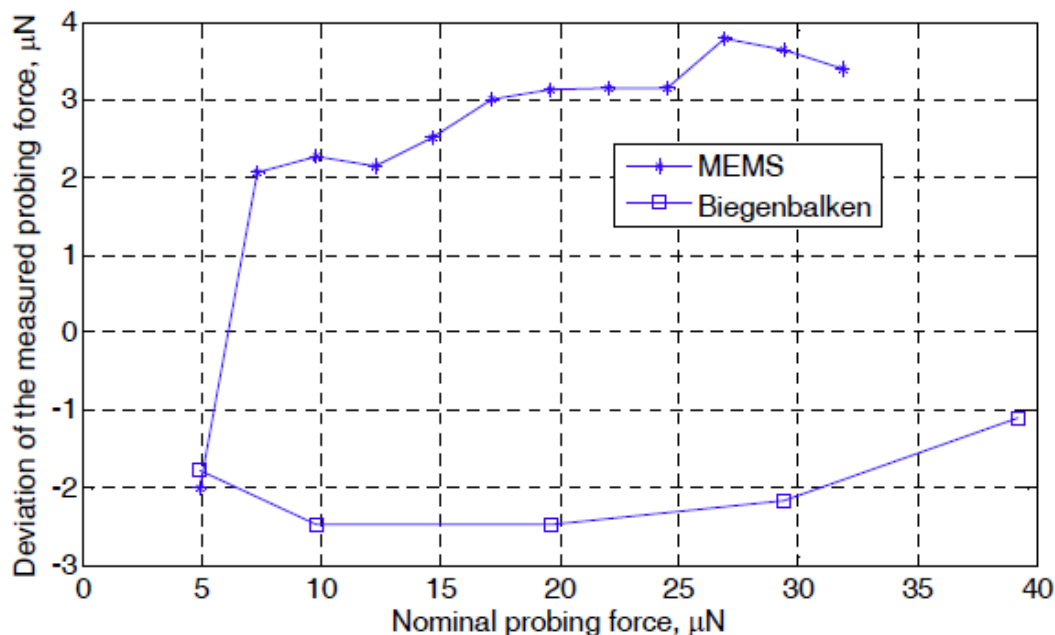


Figure 17 Comparison between the measured probing force of a contact stylus profilometer using a reference cantilever based force transfer standard and a MEMS nanoforce sensor, respectively.

3.1.3.2 Measurement of the effective stiffness and (vertical) dynamic performance of stylus profilometers

In-situ determination of the effective stiffness and (vertical) dynamic performance of a commercial stylus profilometer is one of the most challenging tasks within this project, due to the limited vertical working distance/space, lack of necessary (electronic) signal input/output from the instrument, and quite weak spring constant of the suspending system of the vertical sensing unit of the instrument. Here the nanoforce transducer detailed in section 3.2.1 is chosen to characterise both static parameter (i.e. vertical stiffness of the stylus tester) and dynamic performances (i.e. resonance frequency and Q-value) of the stylus profilometer, since the MEMS-based transducer features:

1. Small geometrical size, therefore can be conveniently integrated into any of currently available commercial stylus profilometers,
2. Active force actuation and displacement sensing with resolution down to several nN and subnanometer, respectively, consequently needs no (signal) feedback from commercial stylus instruments,
3. Capability of quantitative characterisation of the stiffness of cantilever-like mechanical force sensors with wide range (e.g. from 0.1 N/m to 50 N/m)
4. Much higher resonant frequency compared with that of almost all stylus instruments.

a. Stiffness calibration

When the nanoforce transducer is applied for stiffness calibration, the calibration system can be simplified as in the Figure 18 with a typical calibration procedure described as below:

1. The MEMS force actuator is firstly moved by the drive signal to realize self-calibration without touching the stylus tip and to compensate for the circumstance influence (e.g. variation of the relative humidity within the measurement system, temperature deviation, etc.)
2. The stylus tip is then brought into contact to the MEMS actuator with an appropriate probing force
3. The drive signal V_D is then applied to the force actuator to move the actuator and the stylus together, and then the slopes load is determined
4. Finally the stiffness of the stylus instrument can be evaluated as $K_{stylus} = (S_{load}/S_{free} - 1) * K_{MEMS}$

From experiments the stiffness of the stylus instrument Tencor P11 is determined to 0.23 ± 0.03 N/m.

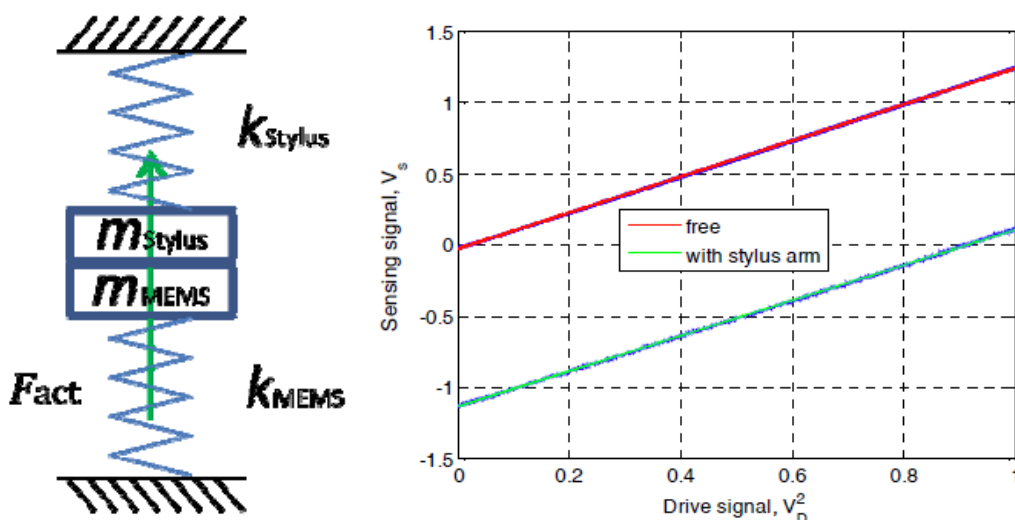


Figure 18 Left: mechanical model of the spring constant calibration system. Right: typical measurement result obtained for the stylus instrument Tencor P11

b. Resonance frequency

By means of varying the modulation frequency f_0 the amplitude-frequency response of the calibration system can be experimentally determined. A typical measurement curve obtained when the MEMS force actuator is coupled with a stylus instrument Tencor P11 is shown in Figure 19, from which the resonance frequency $f_{Messsys}$

is found to be 56.0 Hz. the quality factor of the surface scanning instrument is found to be 5.6, indicating that this instrument is better suitable for measurement of relatively flat surface with low scanning speed.

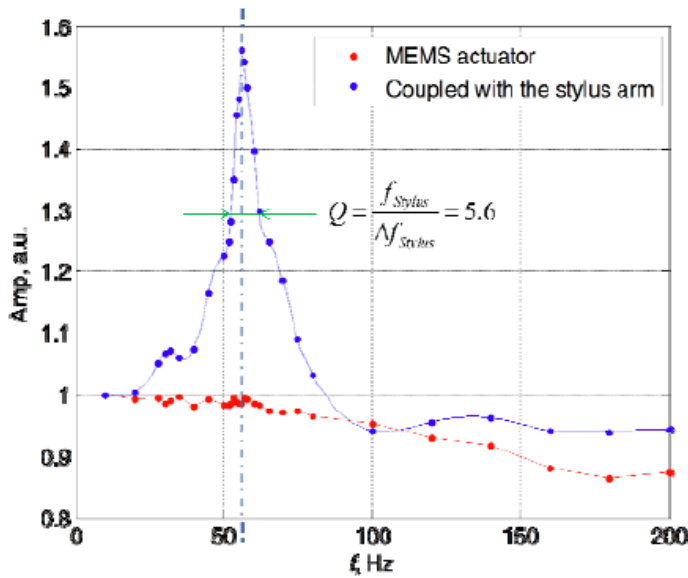


Figure 19 Measured amplitude-frequency response of the calibration system coupled with the stylus instrument Tencor P11

3.1.3.3 Calibration of the tip radius of a diamond stylus

To demonstrate the feasibility of using a reference structure to characterize the tip rounding of diamond stylus, here three methods have been employed to determine the tip radius of a stylus tip used for the stylus profilometer, including scanning electron microscopy (SEM) imaging, atomic force microscopy (AFM) imaging and calibration standards. Although the above two methods, SEM imaging and AFM surface scanning, feature high resolution, they also have disadvantages such as they are cost- and time-consuming and incompatible for in-situ calibration. Therefore, in this project, the methodology to characterize tactile stylus tips using a calibration standard is proposed.

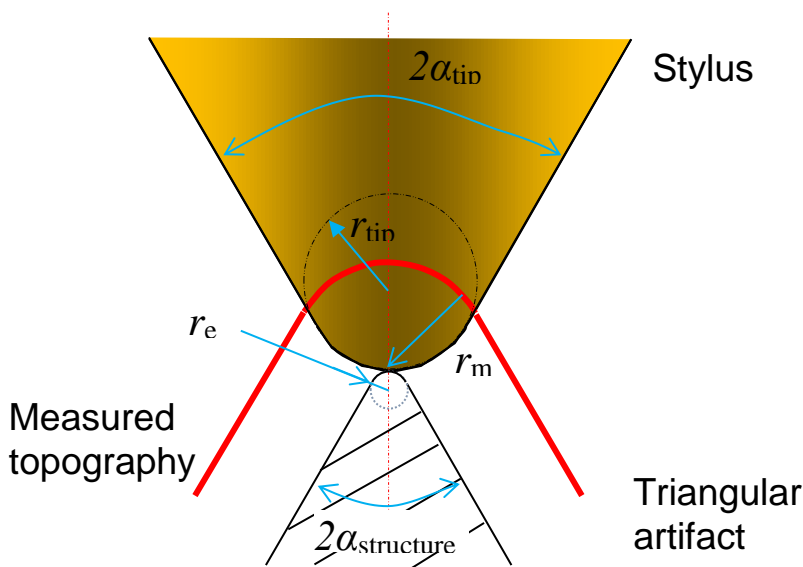


Figure 20: Determination of the tip rounding of a stylus using a reference structure.

a. SEM imaging of a diamond stylus

As demonstrated in Figure 21, SEM can help to view the topography of the stylus tips directly, however it is not easy to quantitatively evaluate the geometrical parameters of the measured stylus tips.

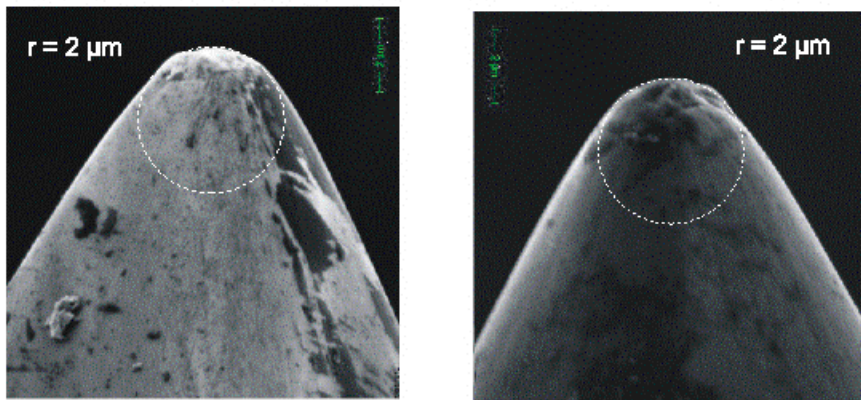
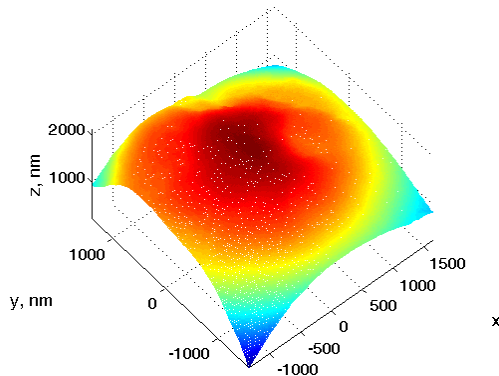


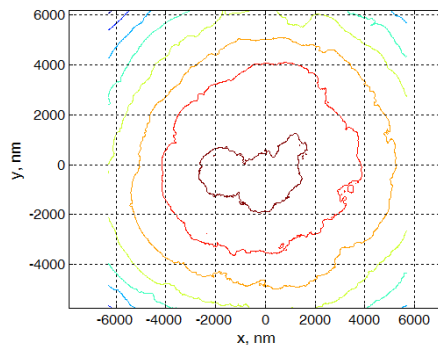
Figure 21: SEM Imaging of a stylus tip with nominal tip radius of 2 μm from two sides.

b. AFM approach

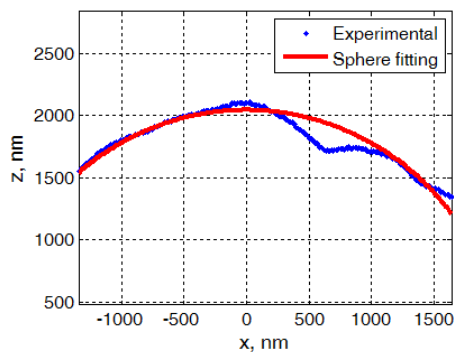
To quantitatively determine the tip parameters, atomic force microscopy has also been employed to image the 3D topography of the stylus tip, as shown in Figure 22. By means of comparing Figure 22 with Figure 21, one can see clearly that the imperfect tip surface of the 2.0 μm stylus tip is now quantitatively revealed. The further analysis indicates that the nominal tip radius of the commercial stylus tips can be reached only when the data evaluation range is large enough.



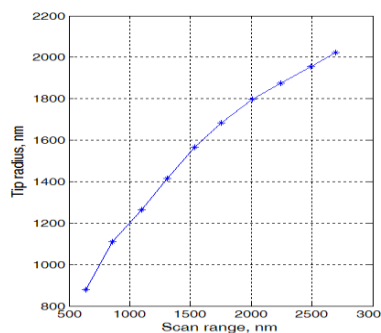
(a) 3D topography of a 2.0 μm stylus tip



(b) Contour diagram of a 2.0 μm stylus tip



(c) Cross-sectional profile of a 2.0 μm stylus tip (y = 0 μm)



(d) Evaluation of the tip radius of stylus tips on basis of AFM imaging

Figure 22 AFM imaging of a stylus tip with nominal tip radius of 2 μm

c. Tip radius characterization using a 1-D stylus tip calibration reference structures

Reference structures used for this purpose can have various forms with known dimensional specifications, e.g. sphere, rectangle or triangular form. One of the typical reference artifacts for characterization of the tip geometry of a stylus tester might be a metallic work-piece with triangular cross-section and sharp edge, as illustrated in Figure 23. Assuming that the edge rounding of the reference structure should have a radius of r_e , and the evaluated curvature of the measured topography be r_m , the tip radius of the stylus (r_{tip}) under characterization should be subtraction of these two. An appropriate reference artifact should satisfy the following requirements: first, the apex angle of a reference artifact should be at least smaller than that of the stylus tester, i.e. $\alpha_{structure} \leq \alpha_{tip}$, so that the effective region of the stylus tip rounding can be fully used for data evaluation; second, the high-order form error of the side edge and that of edge rounding should be as small as possible. As an example, the schematic of the reference structure (KNT 4050/01) as shown in Figure 23 consists of three sets of triangular structures with different apex angles, i.e. $\alpha_{artifact} = 70^\circ, 90^\circ$ and 120° , respectively, which are suitable for characterization of different diamond stylus. The edge radius of the reference structures has been carefully calibrated, with a nominal value of about $1 \mu m$. To evaluate the tip rounding of the stylus, the curved profiles around the structures' top edges are fitted with circle fitting. The experimental and fitted curves are illustrated in Figure 24 in which thick lines are fitted circular curves, and thin line with the marker “.” are experimental data, and the lateral position shifts of the three structures have been removed. A series of line scanning have been carried out. Finally, the tip radius of the measured stylus is found to be $2.02 \pm 0.31 \mu m$.

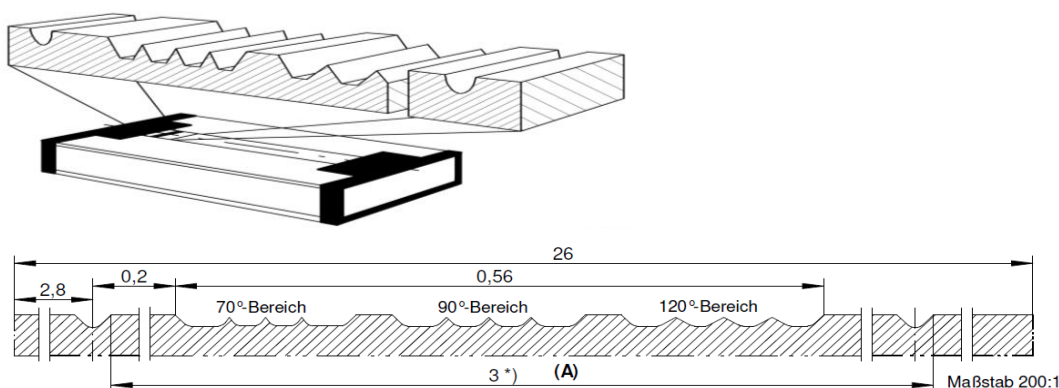


Figure 23 Schematic of the stylus tip calibration standard (KNT 4050/01, Halle Präzisions Kalibriernormale GmbH)

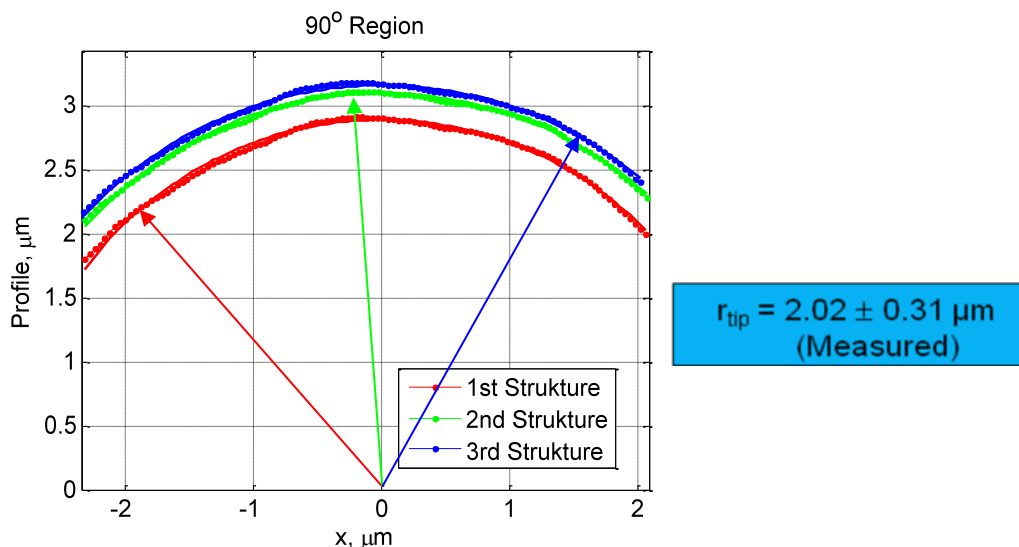


Figure 24 Evaluation of the stylus tip radius from the line profiles of reference structures.

d. Surface scanning speed of LD 120

The actual surface scanning speed of the surface profilometer has also been experimentally investigated. The Profilometer is firstly engaged onto an optical flat with a probing force of 500 μN , and then scan the flat surface with a fixed stroke length of 100 mm using different pre-defined scanning speed. The scanning time ΔT for the given stroke L_0 is recorded by a well-calibrated timer. The actual scanning speed of the surface profilometer can be calculated as the stroke length divided by the time ΔT . The measured result is shown in Figure 25. It can be seen that the profile scanner has relatively low error when the scanning speed is set to be relatively slow. However, when the scanning speed is set to up to 2000 $\mu\text{m/s}$, a speed error of about 55 % has been detected.

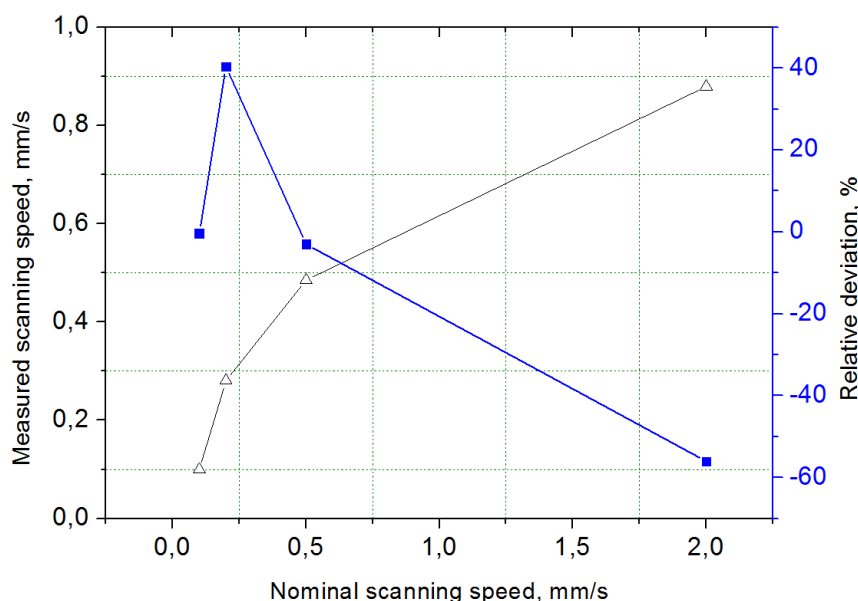


Figure 25 Experimental investigation of the scanning speed of the stylus profilometer (Marsurf LD 120).

Key research outputs and conclusions

The objective was achieved through the development of a new, highly-stable, optical interferometer system, with low-noise, high-sampling rate electronics, suitable for use in industrial settings. Optical interferometers combine and overlap light-waves to intensify the waves, creating high-resolution, accurate images, suitable for measuring changes in the shape and dimensions of viscous materials. The stability of the optical interferometer was assessed and calibrated using an X-ray interferometer at NPL, the UK's National Measurement Institute (X-ray interferometers are more accurate but less suitable for industrial conditions than an optical interferometers). The optical interferometer demonstrated a measurement drift of 0.58 nanometres (approximately the width of two atoms) over a 64 hour period, a drift rate of one proton width per second – suitably accurate for measuring long-term changes in the properties of viscous materials. The optical interferometer system was made portable, to ensure it can be used to make *in situ* measurements. Tactile probe profilometry is used in industry to measure micro surface features and other small height changes in materials, to control manufacturing and quality assurance processes. Such measurements are made using a probe, and the weight of the probe must be carefully controlled to ensure it doesn't damage the sample or cause sample build-up on the probe itself, both of which distort measurements. This is particularly difficult to achieve for polymers that can deform under the probe. New correction algorithms were successfully developed for profilometer probes, which enabled correction for distortions created during soft material surface mapping. The project team also developed well-characterised step height change reference materials and organised a comparison exercise where in which they were used by profilometry instrument manufacturers to assess instrument performance. A tactile probe profilometer ISO standard is in preparation.

3.2 Dimension and mechanical property measurement of viscous materials – data generation.

3.2.1 Indentation creep measurement

An Ultra Nanoindentation Tester (UNHT, CSM Instruments SA now Anton Paar) was used to study the indentation creep behaviours of selected polymeric materials. An example of indentation creep using a Berkovich indenter is give in Figure 26 as obtained by NPL from a commercially available material denoted PS-3 (Vishay Micro-Measurements, Raleigh, NC, USA). This material has excellent viscoelastic mechanical properties and it is highly homogeneous with very good surface finish. The extremely long indentation creep data of 30000 seconds was achieved due to the high stability of the UNHT as shown in The demonstration of the IIT system stability. The extremely long creep data also provided a better chance to obtain the instant modulus (the elastic response when a load is just applied) and the infinite modulus (the remaining elasticity when the load is held for infinite time).

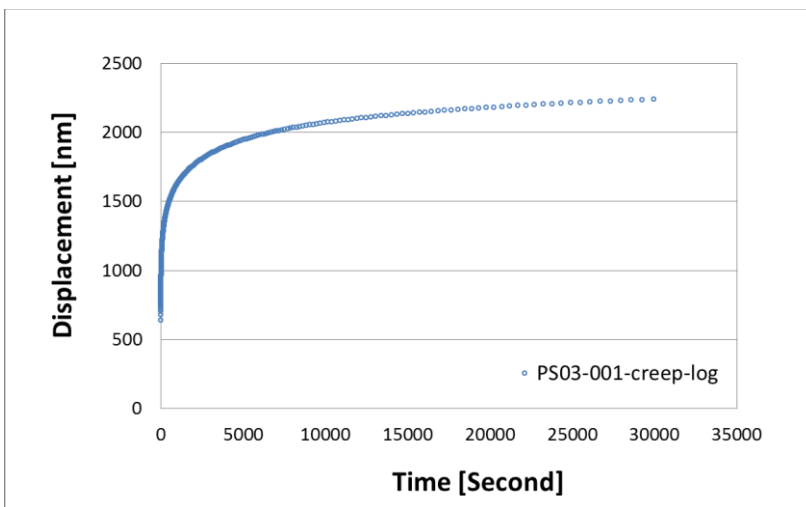


Figure 26 Long-term indentation creep on PS03-001

3.2.2 Indentation dynamic measurement

A Nano Indenter G200 was used to conduct indentation dynamic measurement on a selection of polymeric materials and an example is given in Figure 27 collected at 75 Hz as obtained by BAM.

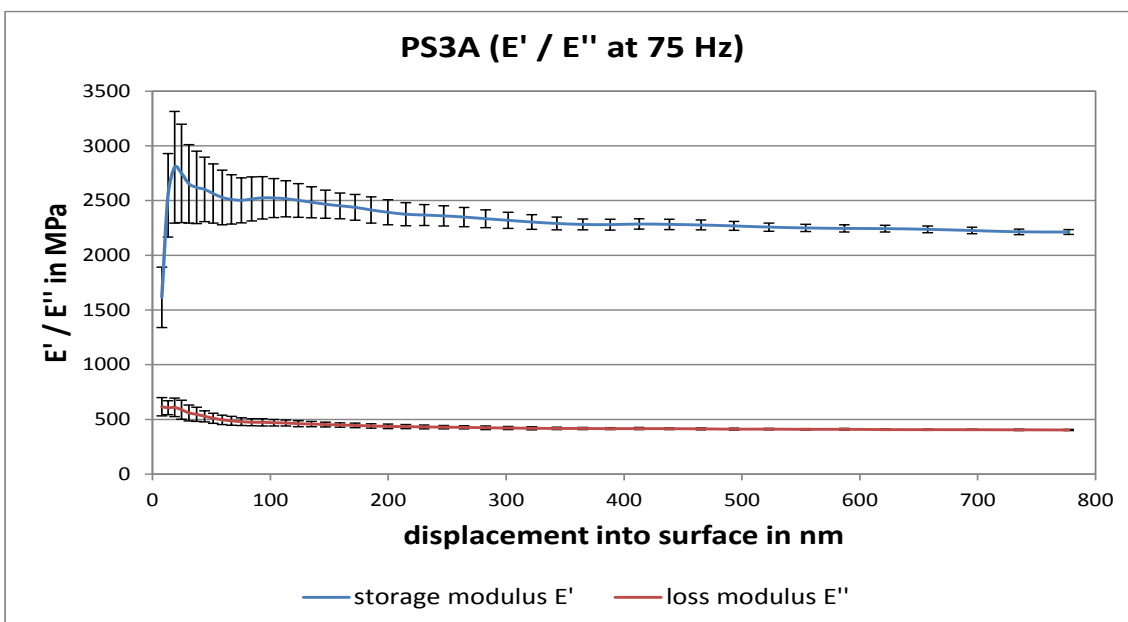


Figure 27 Indentation dynamic testing on PS03-001

3.2.3 Tensile testing on the polymers

The tensile testing experiments were carried out at INRIM. The samples before test and the results of the complete stress-strain diagram measured at a temperature of 23 ± 0.1 °C with a relative humidity of 50 ± 2 %, with a strain rate of 0.015 mm/s are given (see Figure 28). Samples have been cut in order to perform measurement until breaking. Chemical characteristics of the samples have been tested before the test and after the test.

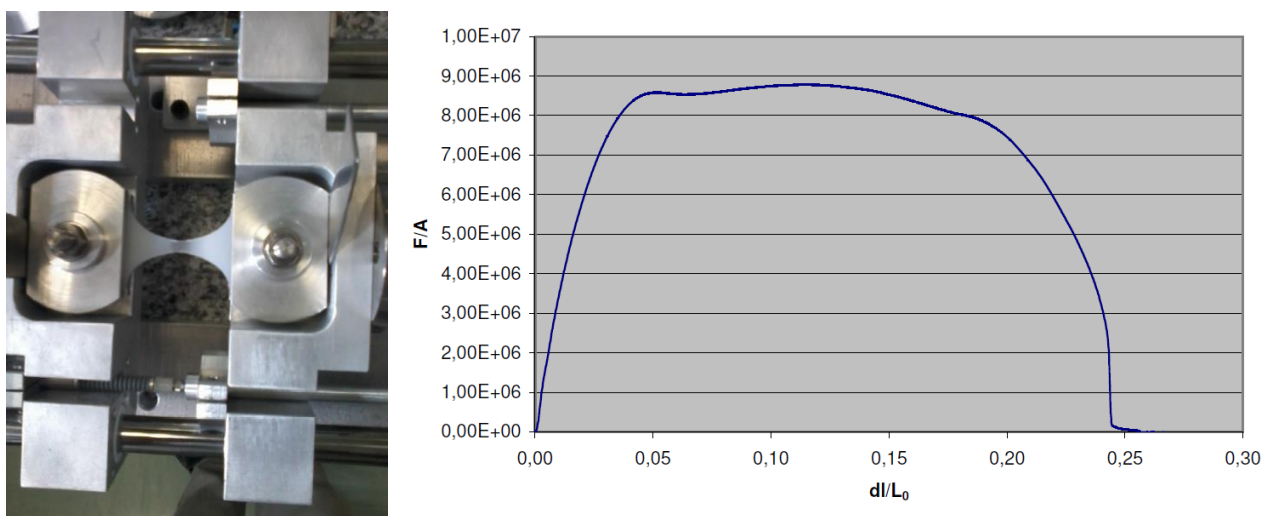


Figure 28 Tensile testing setup and results obtained on JTT sample.

3.2.4 Evaluation of Relaxation time as a function of temperature and relative humidity

The stress relaxation, as a function of temperature and relative humidity, are shown in Figure 29. Measurements have been carried out by INRIM at 18 ± 0.1 °C, 23 ± 0.1 °C and 28 ± 0.1 °C (at 25 ± 2 % and 75 ± 2 % of relative humidity) in the climatic cell (for each step of temperature 5 hours of conditioning time). Measurements have been carried out at controlled displacement: Strain rate 0.01 mm/s until 0.5 % of elongation for JHS 202, JHT 202 and JSS 202 and until 1 % of elongation for JTT 202. About 30 minutes of relaxation time for each sample was recorded. The relaxation times of the measured Force (in newton); actually, the MAX real stress ($s=F/A$), of each sample is calculated in the following table. (The MAX real stress is calculated on the basis of MAX force measured as a function of fixed elongation imposed during the measurements).

Sample	Surface Area /m ²	Measured MAX force /N					
		18 °C - 25%	23 °C - 25%	28 °C - 25%	18 °C - 75%	23 °C - 75%	28 °C - 75%
JJT-202	0,000024	-	57,12	47,80	62,16	53,62	46,92
JJS-202	0,000048	-	71,89	62,10	87,00	72,71	61,93
JHT-202	0,000031	120,41	62,92	26,10	111,70	49,73	19,52
JHS-202	0,00003	469,36	483,19	512,09	501,99	486,49	495,02

Sample	Surface Area /m ²	MAX Real Stress /MPa					
		18 °C - 25%	23 °C - 25%	28 °C - 25%	18 °C - 75%	23 °C - 75%	28 °C - 75%
JJT-202	0,000024	-	2,38	1,99	2,59	2,23	1,96
JJS-202	0,000048	-	1,50	1,29	1,81	1,51	1,29
JHT-202	0,000031	3,88	2,03	0,84	3,60	1,60	0,63
JHS-202	0,00003	15,65	16,11	17,07	16,73	16,22	16,50

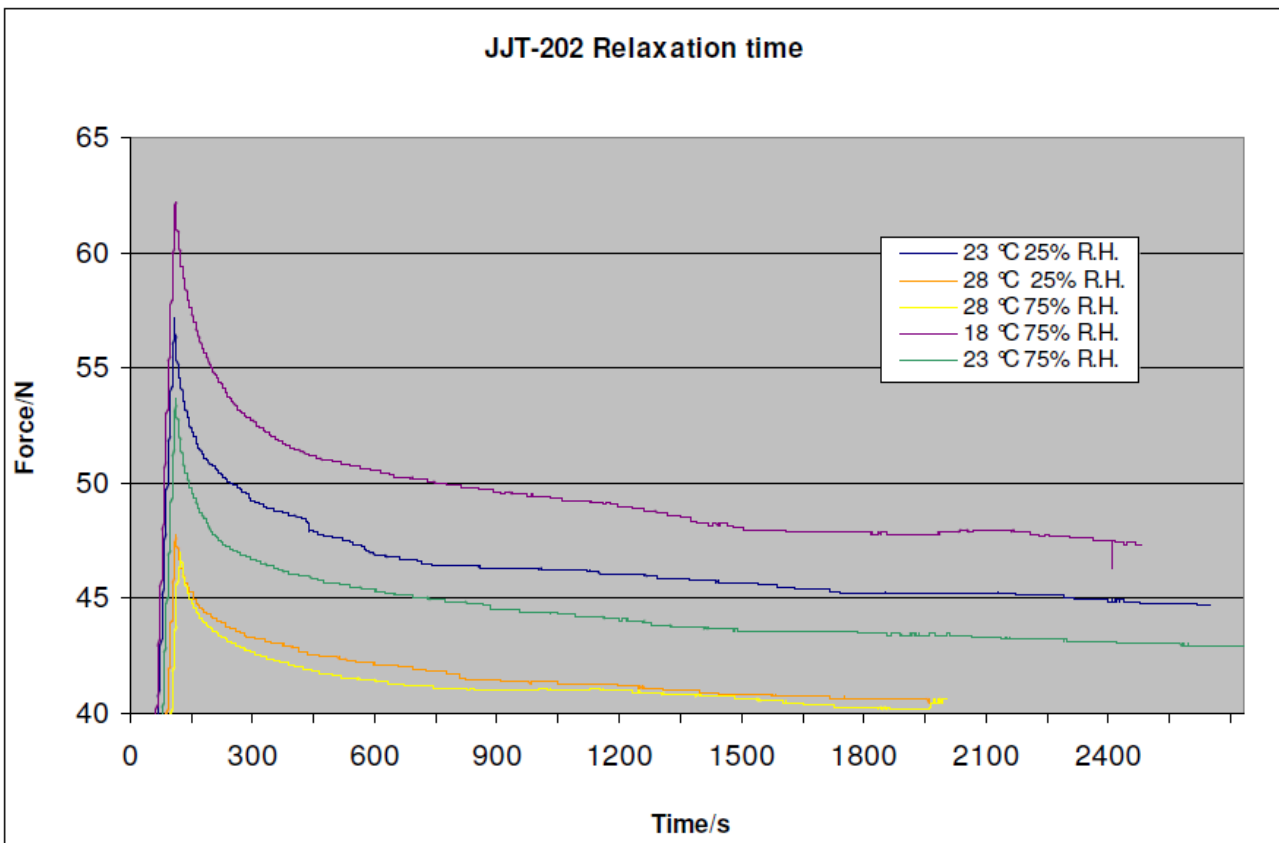


Figure 29 The relaxation time has been calculated as the time needed to MAX force to decay of 1/e (~0.37).

Since the stress-relaxation curves do not show a simple exponential behaviour, the Kohlrausch-Williams-Watts decay function (KWW) has been used:

$$\Phi(t) = \exp\left(-\frac{t}{\tau_0}\right)^\beta$$

In the Table the value of calculated relaxation times of each sample are reported:

Sample	Relaxation time /s					
	18 °C - 25%	23 °C - 25%	28 °C - 25%	18 °C - 75%	23 °C - 75%	28 °C - 75%
JJT-202		3,05E+06	8,57E+06	4,16E+05	1,24E+06	2,42E+06
JJS-202		3,51E+05	9,61E+05	3,58E+04	3,54E+05	9,52E+05
JHT-202	3,34E+03	1,33E+03	1,98E+03	1,65E+03	8,85E+02	1,96E+03
JHS-202	5,36E+07	1,94E+08	1,55E+07	2,44E+08	1,23E+09	5,58E+08

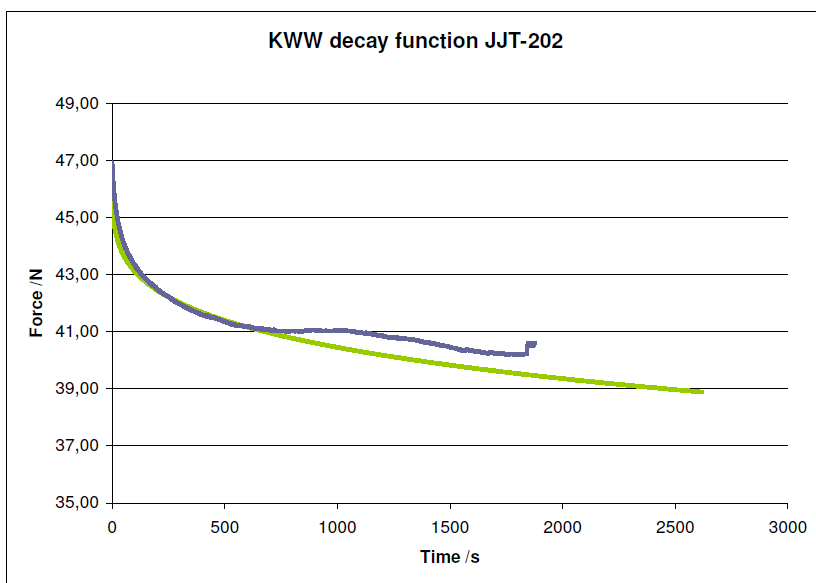


Figure 30 The use of KWW decay function to fit the JJT-202 stress-relaxation curves.

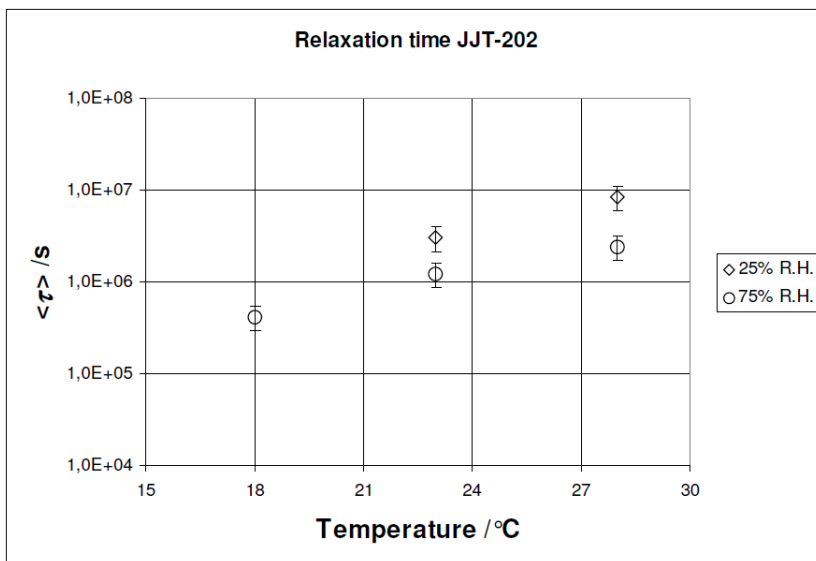


Figure 31 The relaxation time plotted as a function of temperature and relative humidity are depicted. Qualitatively relaxation time results are reported with an over-estimated uncertainty (i.e. of about 20% for JJS-202 and JHT-202 and of about 30% for JJT-202 and JHS-202).

3.2.5 Evaluation of the stress-relaxation response and degradation using Infrared spectroscopy

a. Ex-situ test

Identification of possible structural and chemical modifications on elongated materials using attenuated total reflectance (ATR) infrared spectroscopy was also performed by INRIM. ATR-infrared spectroscopy is a useful technique to study of samples showing large absorptivities in the mid-infrared spectral range. Due to the low penetration depth of the radiation experienced with this technique, mainly surface degradation can be studied. Another and more unique application of ATR-spectroscopy is optical depth profiling by which a component concentration or gradient in structural changes can be probed near the bulk material surface.

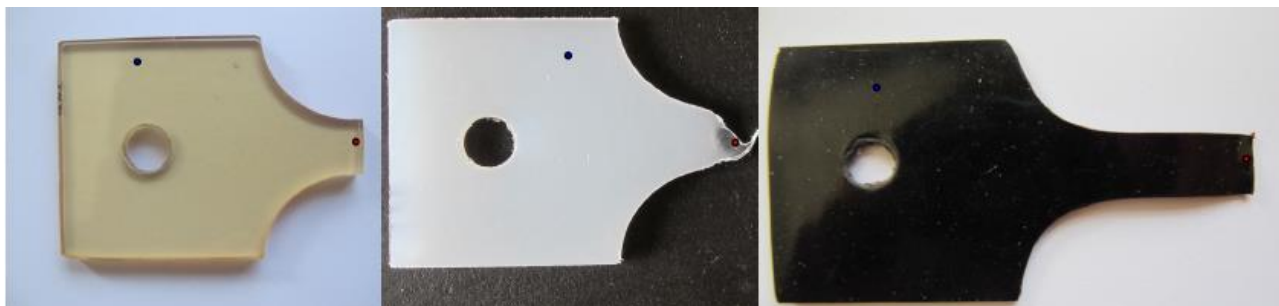


Figure 32: Example of samples of JHT, JJT and CSM, respectively from to left, in which the ATR measurement have been performed, on the as made sample (blue spots) and on the fracture (red spots)

The sample JJT has shown clearly evidence of structural modification. Since this material is composed of polyethylene that is almost completely formed by methylene groups, its infrared spectrum would be expected to consist solely of methylene stretches and bends. Four sharp peaks dominate the spectrum: The methylene stretches at 2920 and 2850 cm^{-1} and the methylene deformations at 1464 and 719 cm^{-1} (On Figure 33 the total ATR spectrum of JJT sample as made is reported). Due to the crystallinity of polyethylene, the 1464 and 719 cm^{-1} peaks are split, and additional peaks are seen at 1473 and 731 cm^{-1} . Crystallinity bands arising from inter-chain interactions of polyethylene can be observed in the splitting of the CH_2 rocking band into a pair of bands at 730 cm^{-1} and 720 cm^{-1} . The 1470 cm^{-1} band similarly exhibits crystal splitting. Qualitatively, the degree of crystallinity may be estimated from the degree of splitting of these bands. The degree of crystallinity can be determined from the ratio of 731 cm^{-1} to 719 cm^{-1} peaks. In Figure 34, reported below, the spectra collected on the as made sample (red curves) and on the deformed region (pink curves) of JJT samples show clearly that the degree of crystallinity is lower, or almost absent, in the deformed region, that became transparent, indicating, like it is reported in literature, the presence of amorphous polyethylene.

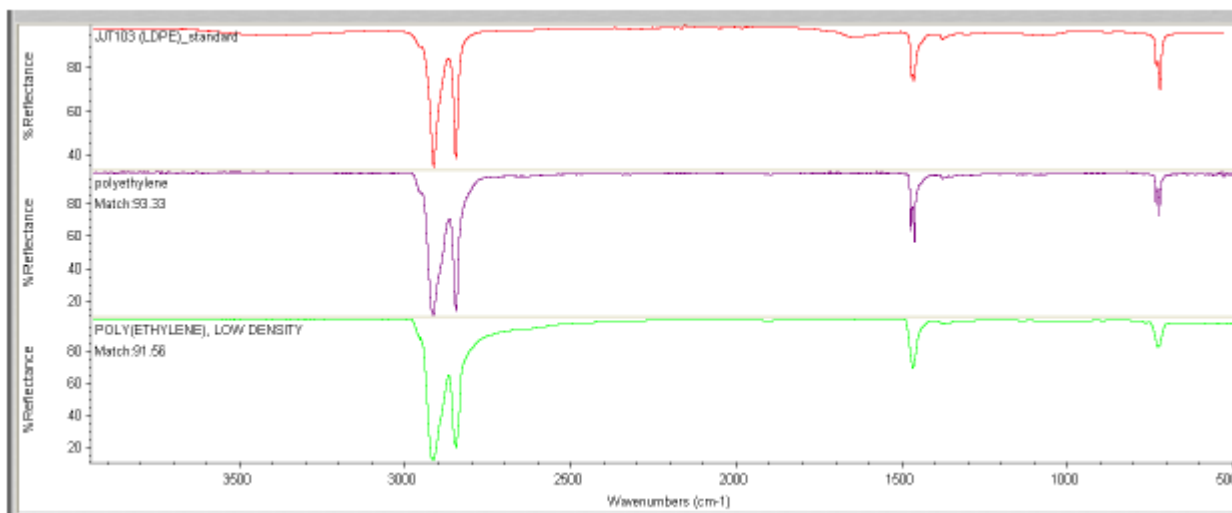


Figure 33: ATR spectrum of JJT sample with the relative match of the library

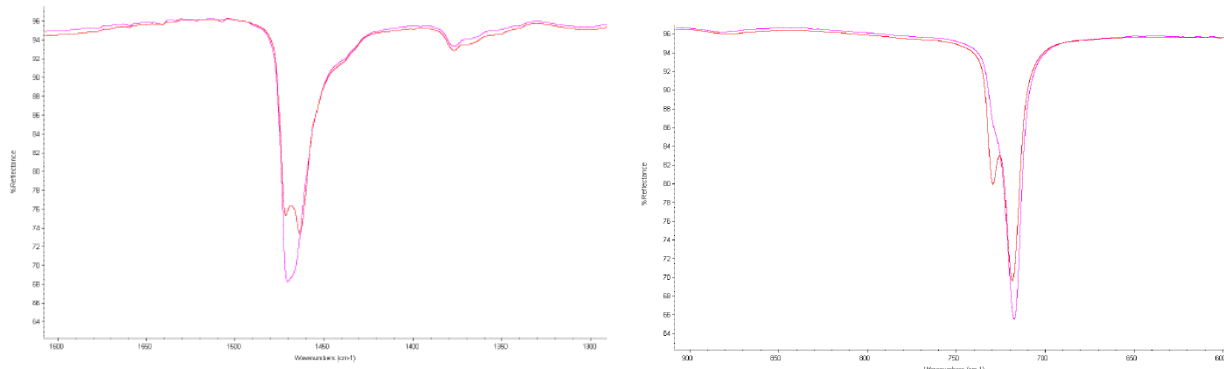


Figure 34: Left: the disappearing of the split bending band at 1470 cm⁻¹ on the fracture zone (pink curve); Right: the disappearing of the split rocking band around 725 cm⁻¹ on the fracture zone (pink curve)

b. In-situ test

Since the FTIR/ATR technique is not suitable for the main purpose of this task (i.e. investigation during the elongation of the samples on the chemical degradation) other techniques have been taken in account. In particular Near-infrared Spectroscopy (NIR) technique can be used since it is widely employed as online monitoring analysis for quality control in industrial process owing to availability of external sensor easy to use (fiber optic). On the contrary the information on chemical structure are obtained by the overtone frequencies mode of the infrared (IR) active band, and as a consequence, not all the IR band are active in the NIR region; nevertheless, for some cases, they are sufficient to get the needed information. Particularly evident was the case of Polyethylene (JJT And JJS sample). In this case the simplicity of the polymer molecule has made possible the investigation on crystalline/amorphous transition of the materials during the elongation test. The experimental apparatus used for this measurement at INRIM are shown in Figure 35. NIR Measures have been performed using a THERMO scientific Antaris II NIR analyzer equipped with fiber optic probe (the light spot visible on the pictures).

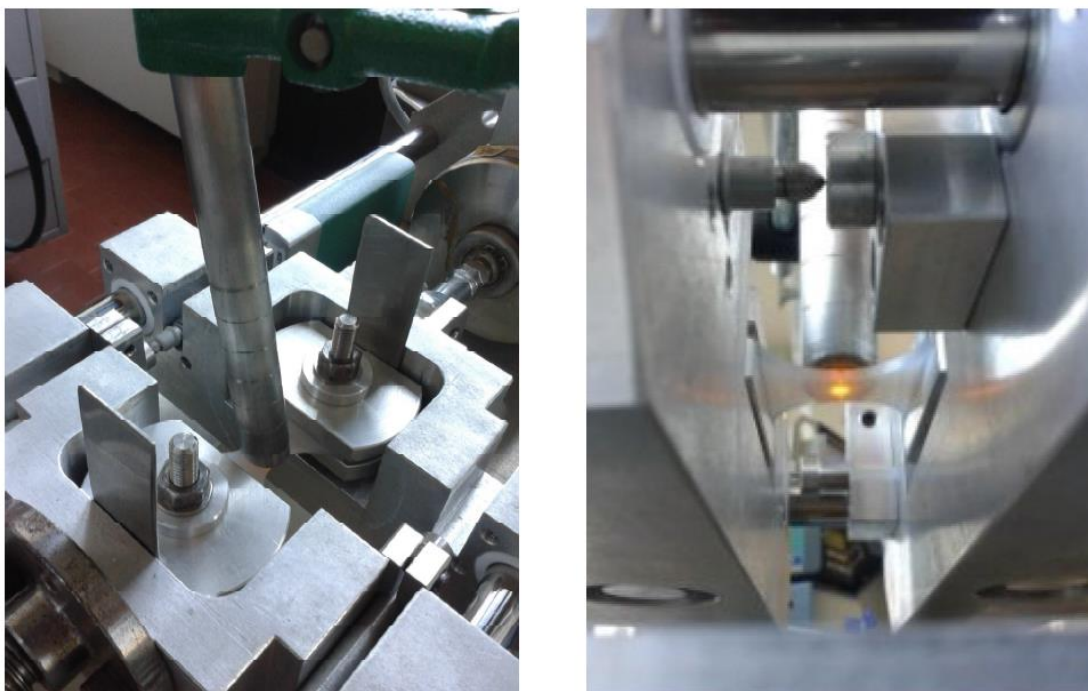


Figure 35: NIR experimental apparatus for analysis during elongation test. In order to induce a reproducible deformation two nicks have preliminary performed on the sample.

Since the instrument can acquire a spectrum by overlapping 32 or 64 scans, this would require a fixed time (> 5 s) to carry out the analysis, so the measurements have been performed discretely, i.e. each 0.25 mm of extension a spectrum has been acquired, in order to obtain a series of NIR spectra strictly linked to the mechanical behaviour of the sample. Measurements of chemical degradation in extension, until 10 % of elongation (7 mm), have been performed only on Polyethylene samples (JJS and JJT), since in previous analysis relevant variations have been observed. By comparing these curve with continuous curves (of the complete stress-strain diagrams) a consistent behavior is observed.

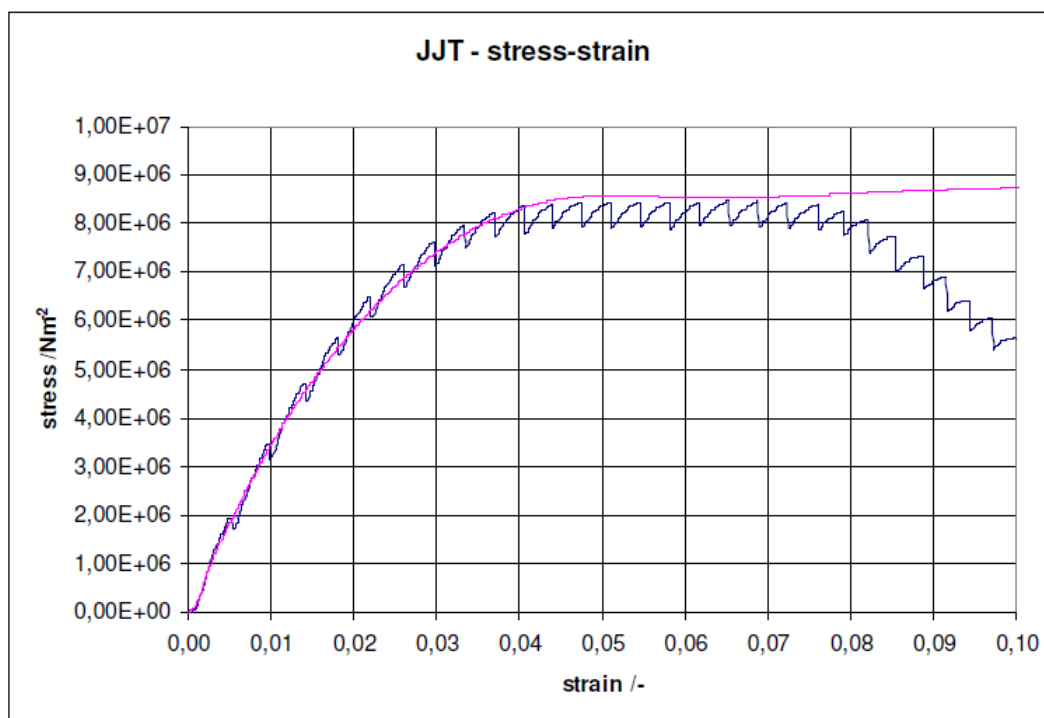


Figure 36: stress strain curve of the JJT sample performed during NIR investigation. The pink curve shows the well agreement with fit model.

At the onset of the tensile test the stress gradually increases, reflecting the elastic deformation of the sample. Further stretching of the sample causes the plastic deformation, which results in the irreversible variation of the structure. The deformation finally ends up with the breaking of the sample. Polyethylene samples often show a complex supermolecular structure consisting of folded-chain crystal lamellae embedded in a liquid-like amorphous matrix. It is believed that adjacent lamellae are linked with so-called amorphous tie-chain molecules. Because of differences in mechanical properties, even under a common macroscopic deformation, each phase is often subjected to a different level of local mechanical stimuli. For example, crystalline structure generally makes a material strong, but it also makes it brittle. The amorphous structure, on the other hand, give a polymer toughness, that is, the ability to bend without breaking. The generation of such different deformation behaviors may be closely associated with the co-existence of the crystalline and amorphous structures. Thus the analysis of the corresponding NIR spectra becomes important to derive the in-depth understanding of deformation at the submolecular level. In the case of polyethylene the overtone bands in the NIR region may easily be calculated as multiples of the wavenumber where a fundamental vibrational mode absorbs energy. Thus for a peak at 2890 cm^{-1} , the first overtone might be expected at 1730 nm and the second overtone at 1153 nm. In particular the peaks around 1730 and 1760 nm have been related from the literature, to the degree of crystallinity even if the question is still debated [8].

Figure 37 below shows the curves acquired in this region of the spectrum is reported. For clarity all the spectra showed are related to step of 0.5 mm and on the right bottom square is also showed the raw data of the elongation test, in order to make easier to relate the spectra to the macroscopic change induced into the sample. One of the issue related to this technique is due to the fact that during the elongation test the thickness of the sample decreases causing a variation of the baseline reference spectrum taken at the start of the measurement. A possible solution is to use a thick sample. As it seems from these results on Polyethylene

(JJT), the NIR technique allows to detect in particular the transition from plastic behaviour (just after the tensile strength point) to breaking strength point. Qualitatively a relevant intensity decrease can be systematically observed around 0.07 of strain in JJT sample.

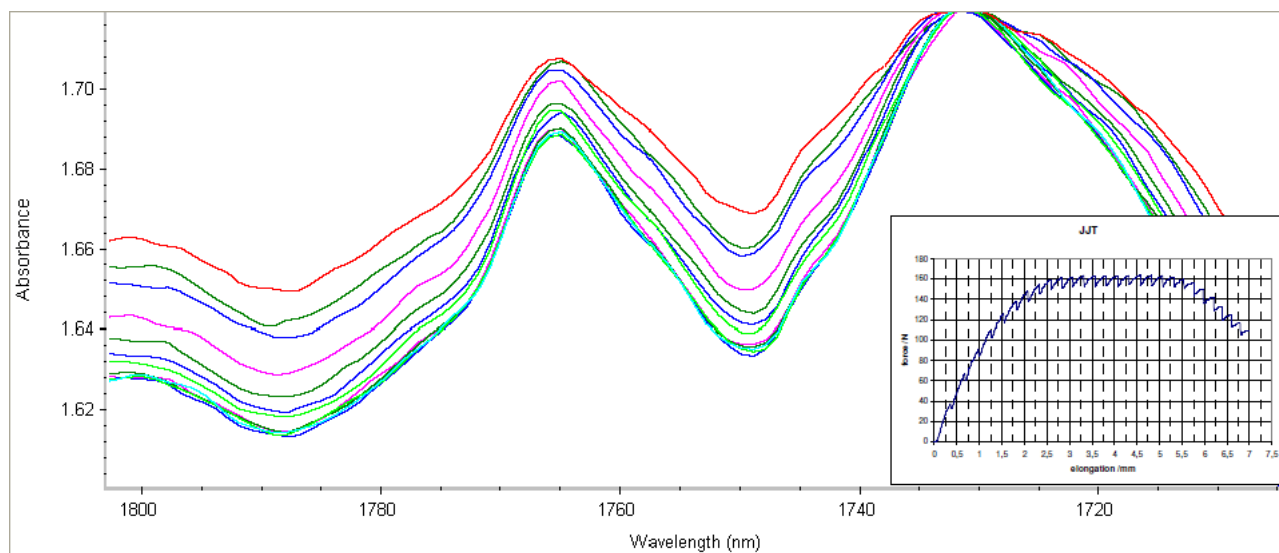


Figure 37: Series of NIR spectra acquired for the sample JJT. The red curve correspond to the as made sample. After each step of 0.5 mm the intensity of the band especially the one at 1760 nm decrease. Relevant variation of the intensity are evident comparing the red curve to the pink curve (2.0 mm of elongation, around the transition from elastic to plastic region) and to the light green curve (4.0 mm of elongation, around the transition from plastic to break region)

3.2.6 Sensitivity study of oscillation measurement methods

In order to check the suitability and the effectiveness of the measurement, preliminary tests have been carried out on JHS, JHT, JJS and JJT materials. performed by using measurements based on ultrasonic filed. This was carried out using piezoelectric transducer applied on the specimen surfaces, and allowed whether the instrumentation sensitivity is enough to detect the signals to be verified. Measurements have been carried out on the basis of two different measurement methods:

- the “pulse-echo” method, chosen to measure wave propagation speed in isotropic and homogeneous materials; this technique uses only one transducer, working as transmitter and receiver.
- the “through transmission” technique, chosen for solids with high absorption properties and for non-homogeneous solids. In this technique, two transducers are used, one working as transmitter and the other one as receiver.



Figure 38: Series Cylindrical-shaped samples, and thickness measurement

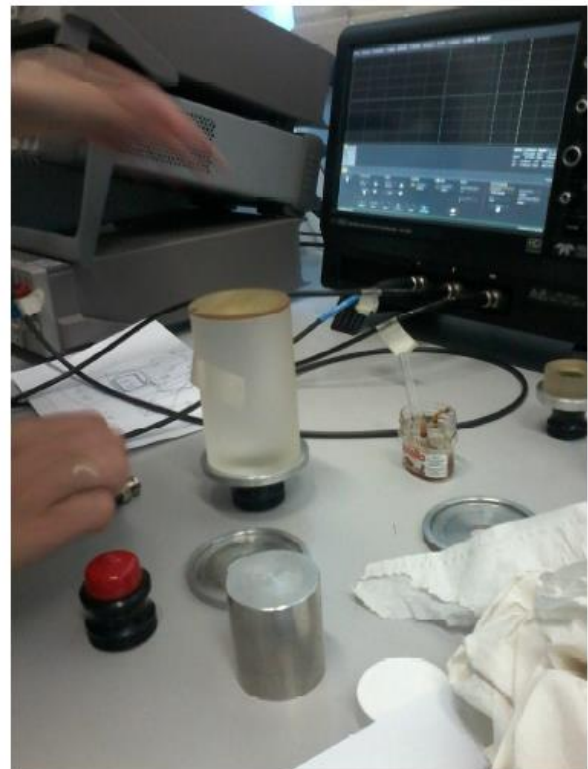
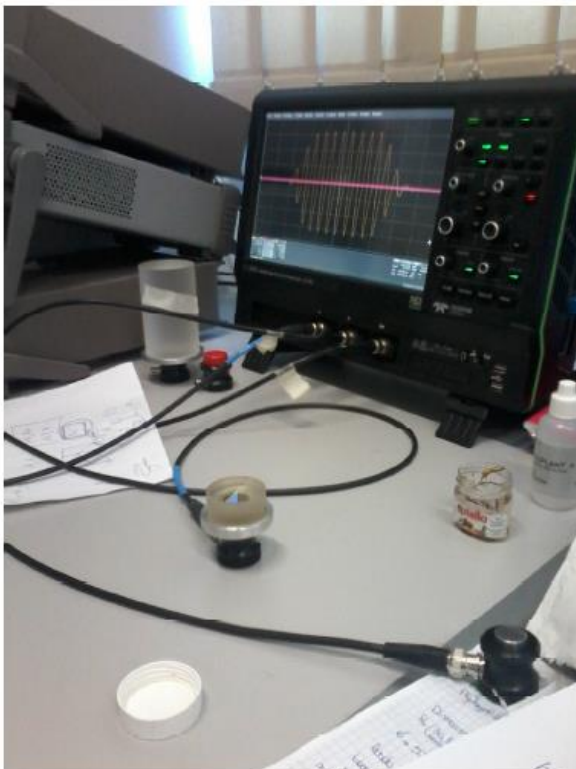


Figure 39: Preliminary tests of longitudinal and shear waves speed measurements.

In order to generate the pulses, which produce longitudinal and transverse elastic waves in the solid, contact piezoelectric ultrasonic transducers have been used. A proper “buffer rod” is allocated between the sample and the transducer in order to prevent the effect of acoustic near field on the measurement. The mechanical properties of the buffer rod (in glass) used are widely known. Besides, in the contact points between the sensible element of the transducer and the rod, and between the rod and the sample a thin layer of a proper coupling fluids (e.g. glycerin or silicon oil) is applied. The transducers used are Panametrics Video Scan V108 with a diameter of 19.05 mm for longitudinal waves and V150 with a diameter of 12.7 mm for transverse waves. The transducers resonance frequency is 5 MHz. In order to excite the transducer to emit longitudinal or transverse waves, a Pulsar–receiver Panametrics PR5800 is used. The transducers are assembled on a particular support that guarantees a good coupling between the sample and the transducers and, in the case of “through transmission” method, also a good alignment between the two transducers.

Material	Long. speed /ms ⁻¹	Trav. speed /ms-1	Young's Mod. /GPa	Shear Mod. /GPa	Poisson ratio
JHS	2636,6	1124	4,09	1,47	0,39
JHT	2301,5	1018	3,15	1,14	0,38
JJS	2026,1	700	1,28	0,45	0,43
JJT	2021,4	700	1,27	0,44	0,43

Taking an average isobaric specific heat capacities as about 0.35 for JHS and JHT (such as EP) and 0.55 for JJS and JJT (such as low density PE) and an average coefficient of dilatation α as about 0.00008 and 0.0002, it is possible to observe that only JHS sample fulfil the relation. Dynamic moduli measured from sound speed are about 1 order of magnitude greater than static moduli, measured from tensile test.

The values of Young’s modulus obtained by sound speed measurements are in general greater than the values of Young’s modulus measured by tensile test methods, as expected in the case of excitation at very high frequency in viscoelastic materials. Only the behaviour of JHS is similar to a quasi-perfect elastic material and the differences between Young’s modulus determined from dynamic methods and static methods can be justified on the basis of the differences between isothermal and isentropic behaviour.

E_d is the dynamic (isentropic) Young Modulus, E_s is the static (isothermal) Young Modulus

	E dynamic	E static	c_p	α	ρ	E dyn	diff %
JHS	4,09E+09	3,45E+09	0,35	0,00008	1166,72	4,00E+09	2,1
JHT	3,15E+09	3,50E+08	0,35	0,00008	1101,66	3,55E+08	88,7
JJS	1,28E+09	3,20E+08	0,55	0,0002	914,6	3,42E+08	73,3
JJT	1,27E+09	2,70E+08	0,55	0,0002	907,7	2,86E+08	77,5

3.2.7 Practice in the determination of the absolute surface deformation of polymer specimen under sliding contact

With the surface scanning strategy, one can relatively easily obtain the relative surface deformation of polymer under different probing force, i.e.

$$\Delta D_L = D_L(F_{tip}) - D_L(F_{ref})$$

As shown in Figure 40, the relative surface deformation ΔD_L will become negative when the probing force F_{tip} is smaller than F_{ref} .

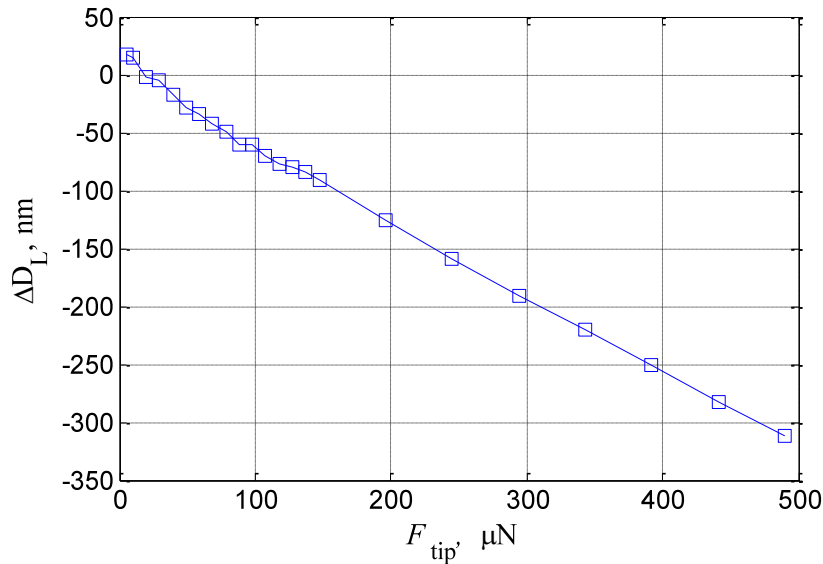


Figure 40: Relative surface deformation of Polymer Ormocomp with respect to different probing forces. (The surface scanning specifications: $r_{tip} = 2 \mu\text{m}$, $v_{tip} = 50 \mu\text{m/s}$, $F_{ref} = 20 \mu\text{N}$)

In the case of absolute surface deformation demanded, it's necessary to deduce the absolute deformation under the reference probing force, i.e. $D_L(F_{ref})$. As a result, the measurement data in can be recalculated, and the relationship between the relative deformation ΔD_L and $F_{tip}^{2/3}$ in elastic deformation region is depicted in Figure 41. With the help of linear regression, i.e. $fLinearPar = polyfit(F_{tip}^{2/3}, \Delta D_L, 1)$, the following equation can be determined:

$$\begin{cases} D_L(F_{ref}) = fLinearPar(2) \\ K_e = \left(\pi \cdot E^* \cdot r_{tip}^{\frac{1}{2}} \right)^{-\frac{2}{3}} = fLinearPar(1) \end{cases}$$

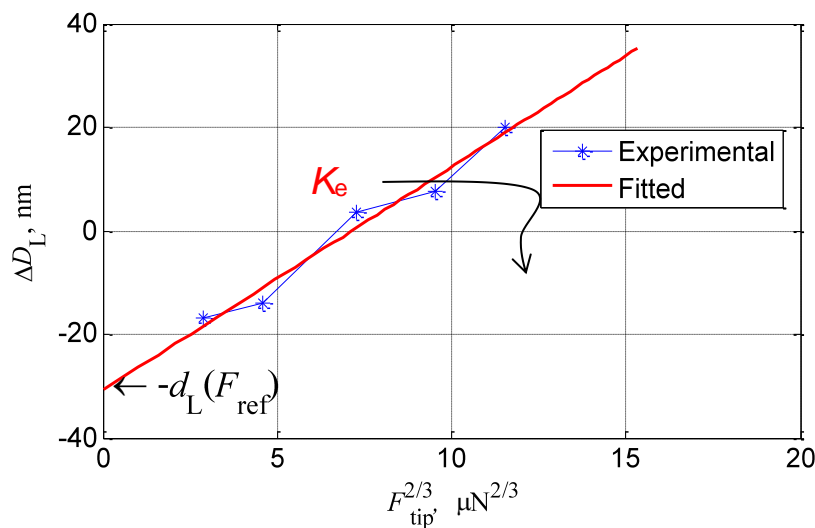


Figure 41: Relationship between the relative deformation ΔD_L and $F_{tip}^{2/3}$ in elastic deformation region.

3.2.8 Indentation creep at elevated temperatures on virgin PVC

A NanoTest instrumented indentation system was used to perform a feasibility study on virgin PVC as a function of temperature. The results are shown in Figure 42.

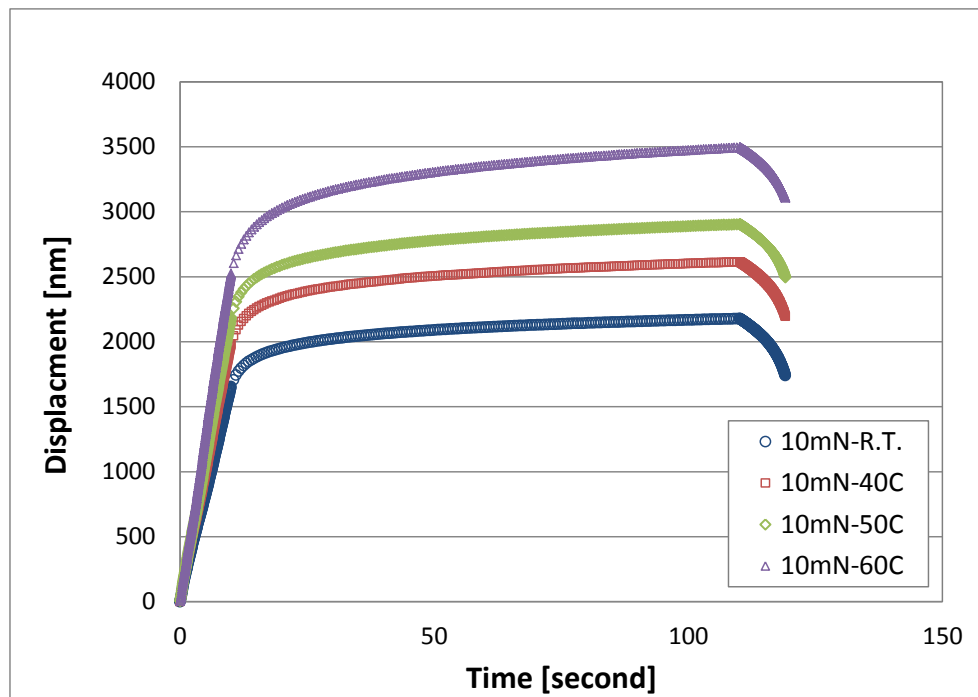


Figure 42: Indentation creep data obtained at different temperatures: R.T., 40°C, 50°C and 60°C.

Key research outputs and conclusions

After the reduction in measurement drift achieved in objective 1, changes in the mechanical and dimensional properties of viscous materials can be measured. Indentation creep testing, a technique that measures properties of a sample under pressure, was used to measure changes in shape and dimension, and to assess the elasticity and viscosity of samples. The objective was achieved through the development of a capability at NPL for long-duration, ultra-stable indentation creep measurements, using a UNHT nano-indenter (from [Anton Paar Ltd](#)). Displacement rates as low as 20 femtometres per second over a 66 hour period were demonstrated (less than two atomic nucleus widths per second), one of the longest nano-indentation creep tests ever performed.

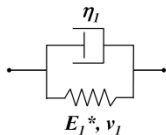
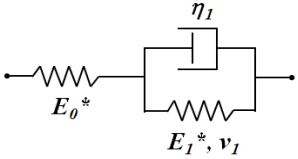
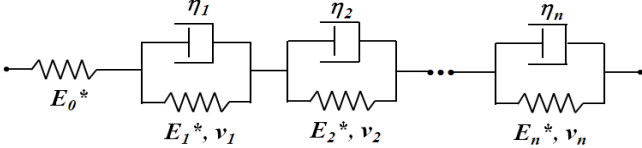
3.3 Development of new analysis methods for measurement of dimensions and mechanical properties of viscous materials.

3.3.1 The development of the VE model for indentation creep test analysis

Viscoelastic materials exhibit both viscous and elastic characteristics when undergoing deformation. NPL and KU investigated how various measurements on polymers can be integrated via a universal model to obtain their viscoelastic material properties. Various models were developed in order to determine their stress and strain interactions, which commonly use a combination of springs and dashpots to simulate elastic and viscous components respectively. Compared to the simply Voigt model which only consists of a Newtonian damper and Hookean elastic spring connected in parallel, the three-element standard linear solid (SLS) model is more accurate in predicting polymeric material responses by having an extra spring element to simulate the immediate elastic response. The SLS model is commonly used in interpreting indentation creep experimental data as it is able to represent both low viscosity materials and the dominantly elastic nature of high viscosity or crystalline materials.

In reality, polymers are believed to be a mixture of many different springs and dashpots. This means when polymers are going through a deformation process, different parts of the polymer chains will respond at different speeds, hence contributing more than one time constant. The SLS model oversimplifies this process by allowing only one time constant, which is highly related to the experimental creep time. During a creep experiment, over time, longer time constants are activated which will dominate the calculated results when using the SLS model for simulation. This will require the users to choose the creep time carefully when designing their experiments, which they normally have a lack of knowledge. In order to describe the polymer deformation response more accurately, the SLS model is expanded to an n-element Kelvin model by having more springs and dashpots as shown in Table 1.

Table 1 Description of various kinematic models

Kinematic model	Schematic representation and creep function
<p>Voigt model</p>	 $J(t) = \frac{1}{E_1^*} \left[1 - \exp\left(\frac{-t}{\tau_1}\right) \right]$
<p>standard linear solid (SLS) model</p>	 $J(t) = \frac{1}{E_0^*} + \frac{1}{E_1^*} \left[1 - \exp\left(\frac{-t}{\tau_1}\right) \right]$
<p>n-element Kelvin model</p>	 $J(t) = \frac{1}{E_0^*} + \sum \frac{1}{E_i^*} \left[1 - \exp\left(\frac{-t}{\tau_i}\right) \right]$

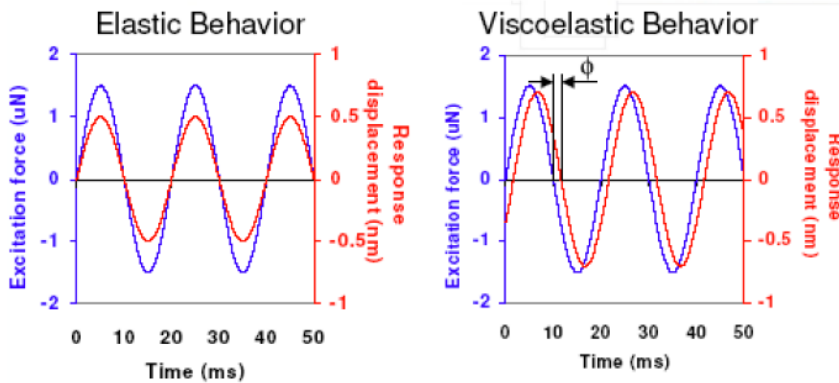
A research study was conducted to evaluate the material properties of polychloroprene (Neoprene) rubber with an array of characterization experiments performed at the nano and meso scales. These experiments were performed by four different research groups independently on the same rubber samples: relaxation results performed by KU, Berkovich nano-indentation performed by NPL, flat punch creep nano-indentation performed by QMUL and uniaxial testing performed by INRIM and. The VE models were then used to obtain the viscoelastic parameters as a comparison between different measurement techniques. NPL and KU studied the optimum of the number of elements in such a generalised Kelvin model to obtain the best fit to the indentation creep curve. As a result, a joint article is in preparation.

3.3.2 The development of the VE model for indentation dynamic test analysis

Indentation dynamic measurement (also called continuous stiffness measurement) is a technique to continuously measure the stiffness of the contact without the need for discrete unloading cycles. This is achieved by imposing a very small AC signal of known frequency on the applied indentation force DC signal. By comparing the phase and amplitude of the displacement oscillation with the imposed force oscillation, the materials response could be obtained at each point of the force-displacement data.

During basic instrumented indentation testing usually contact force and displacement penetration are measured continuously. Using dynamic testing an additional small oscillation is superimposed on the semi-static force, and a frequency-specific amplifier is used to measure the response of the indenter. Typically, the amplitude F_0 of the force oscillation is controlled (increased) such that the amplitude h_0 of the displacement oscillation remains constant as described by the equations below:

$$F(t) = F_0 e^{i\omega t + \phi} \quad h(t) = h_0 e^{i\omega t}$$



Such an oscillating system in contact with the sample can be modeled using a simple harmonic oscillator and taking in to account system stiffness k_s , system damping D_s and oscillating mass m . A kinematic model was developed by NPL to interpret the measured results, as shown in Figure 43 incorporating both instrument and sample properties. The main advantage of this method is that it gives access to measure viscoelastic behaviour with a time constant at least three orders of magnitude smaller than the conventional method.

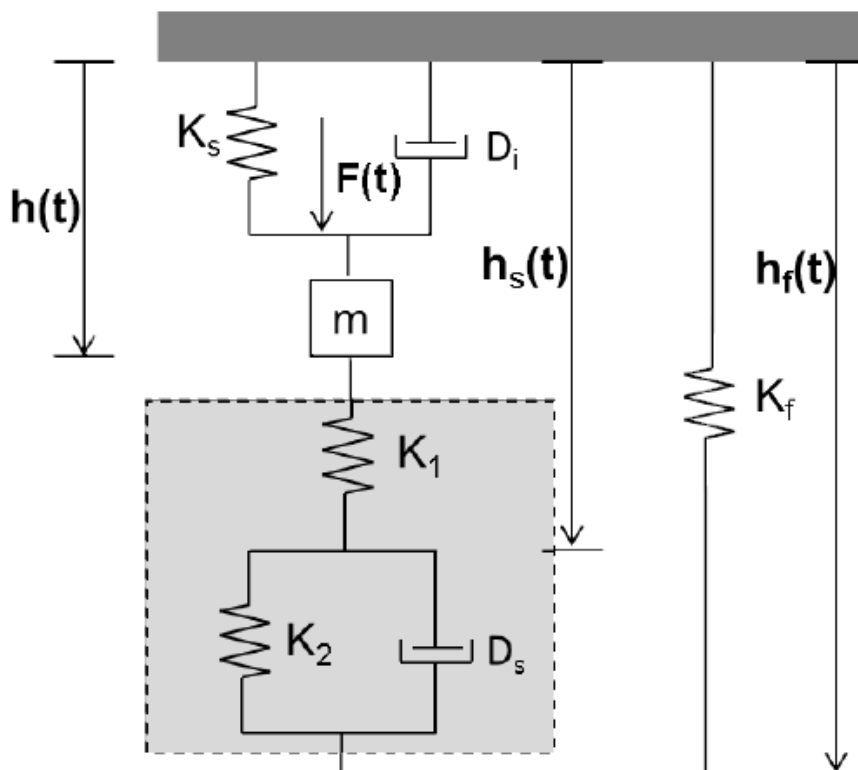


Figure 43 Schematic representation of the components of a typical indentation dynamic model: K_s , D_i and m represent, respectively, the stiffness, damping coefficient and mass of the indenter; and K_f represents the stiffness of the loading frame. The shaded, dashed box shows the three-element model describing the contact dynamics.

Table 2 Measured values together with the uncertainties used for the calculation of u_{Sc} for a measurement on PC Description obtained by BAM:

Measured value		Uncertainty		
h_o (m)	0,000000005	u_{h_o} (m)	1E-10	From semi-static calibration
F_o (N)	0,00002	u_{F_o} (N)	0,000001	From semi-static calibration
f (Hz)	75	u_f (Hz)	0,1	Estimated
ϕ (°)	15	u_ϕ (°)	0,1	Estimated
m (kg)	0,000941	u_{k_s} (N/m)	0,48	Standard deviation from repeated calibrations
k_s (N/m)	89,803	u_m (kg)	0,000001	Standard deviation from repeated calibrations
A_c (nm ²)	17130267,77	u_{A_c} (nm ²)	856510	From semi-static calibration

An estimation of the uncertainty of E' was done for all materials being under investigation in the project. The results of this estimate are given in Table 3. The values for storage modulus have the highest uncertainty for Neopren and SBR. The main source of this uncertainty is the uncertainty of zero point determination because of high surface roughness and low material stiffness. Using IIT creep and DMA tests can be provided with a high local resolution. Results of IIT creep and DMA tests are strongly dependent on experimental conditions.

For comparison experimental conditions must be strictly controlled and reported. Only results of tests under identical conditions can be compared. Using different models the change of displacement with time during creep can be evaluated. Storage and loss modulus can be estimated using the simple model of linear harmonic oscillator. In general the estimation of storage and loss modulus from creep data is possible. A comparison is only useful if adequate experimental conditions and models are used. Also in this case a first comparison shows no agreement.

Table 3 Results of estimation of uncertainty of dynamic testing for all materials under investigation in the project as obtained by BAM.

Material	E', GPa	U E', Gpa	U E', %
PS3A	1,949	0,005	0,25
PS8A	4,4	0,019	0,45
CSM	0,082	0,002	1,41
LDPE	0,383	0,007	1,78
Neopren	0,098	0,003	2,87
SBR	0,094	0,006	6,35

Exp. conditions	Creep data	Calculation using creep data	Results of dynamic testing
$F_{max} = 1 \text{ mN}$ $r = 0,1 \text{ mN/s}$ $t_0 = 10 \text{ s}$	Creep 3020 s $E_0 = 91,95 \text{ MPa}$ $E_1 = 730,22 \text{ MPa}$ $\tau = 592,33 \text{ s}$	$E'(10\text{Hz}) = 122 \text{ MPa}$ $E''(10\text{Hz}) = 0,0002 \text{ MPa}$ $E'(75\text{Hz}) = 122 \text{ MPa}$ $E''(75\text{Hz}) = 0,00003 \text{ MPa}$	$E'(10\text{Hz}) = (309 \pm 13) \text{ MPa}$ $E''(10\text{Hz}) = (50 \pm 2) \text{ MPa}$ $E'(75\text{Hz}) = (405 \pm 11) \text{ MPa}$ $E''(75\text{Hz}) = (107 \pm 2) \text{ MPa}$
$F_{max} = 1 \text{ mN}$ $r = 0,1 \text{ mN/s}$ $t_0 = 10 \text{ s}$	Creep 1020 s $E_0 = 113,19 \text{ MPa}$ $E_1 = 755,66 \text{ MPa}$ $\tau = 217,64 \text{ s}$	$E'(10\text{Hz}) = 152 \text{ MPa}$ $E''(10\text{Hz}) = 0,0009 \text{ MPa}$ $E'(75\text{Hz}) = 151 \text{ MPa}$ $E''(75\text{Hz}) = 0,0001 \text{ MPa}$	
$F_{max} = 1 \text{ mN}$ $r = 0,7 \text{ mN/s}$ $t_0 = 10 \text{ s}$	Creep 120 s $E_0 = 118,1 \text{ MPa}$ $E_1 = 409,52 \text{ MPa}$ $\tau = 25,776 \text{ s}$	$E'(10\text{Hz}) = 165 \text{ MPa}$ $E''(10\text{Hz}) = 0,017 \text{ MPa}$ $E'(75\text{Hz}) = 165 \text{ MPa}$ $E''(75\text{Hz}) = 0,0023 \text{ MPa}$	
$F_{max} = 7 \text{ mN}$ $r = 0,7 \text{ mN/s}$ $t_0 = 10 \text{ s}$	Creep 50 s $E_0 = 68,49 \text{ MPa}$ $E_1 = 241,74 \text{ MPa}$ $\tau = 11,548 \text{ s}$	$E'(10\text{Hz}) = 95 \text{ MPa}$ $E''(10\text{Hz}) = 0,02 \text{ MPa}$ $E'(75\text{Hz}) = 95 \text{ MPa}$ $E''(75\text{Hz}) = 0,0028 \text{ MPa}$	

3.3.3 The development of the VE model for the polymer under sliding contact

For structures made of polymer materials, and thermoplastic photoresists in particular, the corresponding surface deformation under tactile scan can be described by a linear superposition of (recoverable) elastic deformations D_L^e and strain-rate dependent visco-plastic deformation D_L^{vp} as proposed by PTB.

Within the purely elastic deformation region, i.e. $D_L \equiv D_L^e$, the contact pressure is:

$$\sigma_c = E_c^* \cdot \varepsilon_c = \frac{4}{3\pi} C_1 \cdot E_L^* \cdot \varepsilon_c$$

where E_c^* is the sliding contact modulus, E_L^* the effective instantaneous elastic modulus of the polymer under test, the contact strain

$$\varepsilon_c = \sqrt{\frac{D_L}{r_{tip}}}$$

and the coefficient C_1 is generally material dependent.

In case that the sliding contact pressure σ_c be far larger than the (minimum) scratch hardness H_0 , the surface deformation of the specimen under tactile scan becomes unrecoverable, i.e. $D_L = D_L^e + D_L^{vp}$. Under the same definition of the contact stress and strain, it can be assumed

$$\sigma_c = (1-b)H_0(v_{tip}) + b \cdot E_c^* \cdot \varepsilon_c,$$

in which the strain hardening ratio $b = \frac{3\pi}{4} E_p / E_L^*$, and E_p the strain hardening modulus of materials.

The material behaviour of polymers within elasto-viscoplastic region is, in general, quite complicated. However, since the investigation of the polymer deformation within elastic and visco-plastic regions is more valuable, this practical bi-linear material model was used for the following analysis as shown in Figure 45.

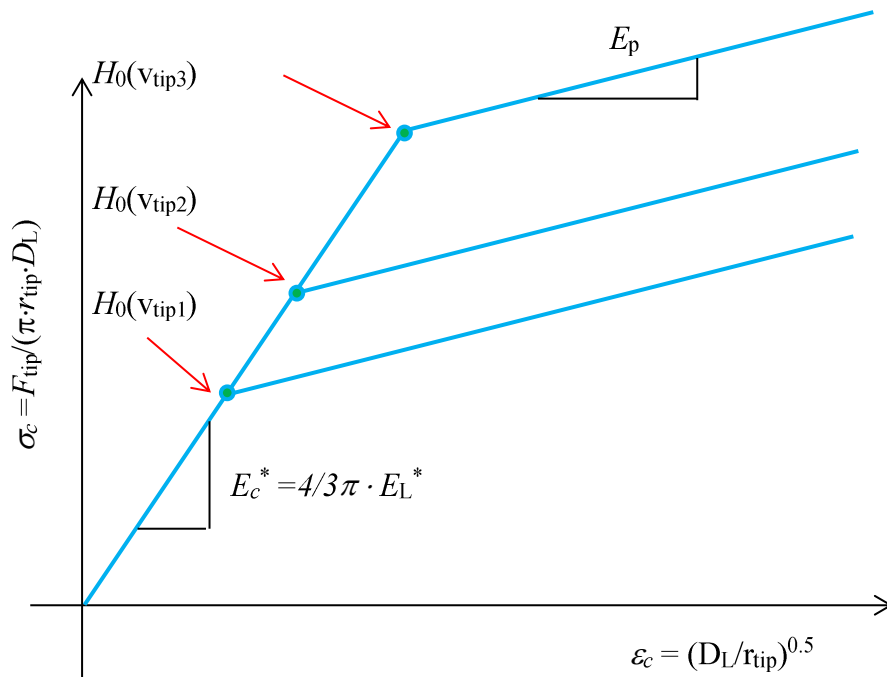


Figure 44: Bi-linear model used for describing the surface deformation of polymers under tactile scan, in which the scanning speed $v_{tip1} < v_{tip2} < v_{tip3}$.

3.3.4 Modeling of the surface deformation of SU-8 under sliding contact

Recent research on surface deformation of polymers under tactile scanning [13,14] was carried out by PTB. The results suggests that the systematic deviations of stylus profilometry for polymeric specimens can be modelled by a simplified elastic visco-plastic model, and then reduced by means of surface topography post-processing. Unfortunately, however, although different efforts [15–21] have been made in the past years to determine the mechanical properties of polymers used in micro-systems, the material properties of polymers, which are necessary for the aforementioned model, cannot be obtained easily and precisely, since none of the currently available testing methods for time-dependent mechanical properties of polymers have been validated [22]. In addition, it is not yet very clear how the friction between a (diamond) stylus tip and the polymer surface under test will contribute to the measurement deviation of stylus profilometry. In this paper, the effort to improve the measurement accuracy of contact-based profilometry for polymeric step-height micro-specimens on hard substrates is reported, in which pre-knowledges of the material properties and of tip–surface friction are not necessary.

The measurement results of typical stylus probe methods for determination of the dimensions of specimens, which consist of several different materials, especially of viscous materials, usually demonstrate considerably large deviation. Detailed analysis of the error sources within stylus step-height measurement method/system reveals that the potential dimensional measurement error is jointly determined by the mechanical properties of the substrate and of the viscous material and by the measurement conditions of the stylus instrument in use. Analysis of the error sources within stylus step-height measurement method/system reveals that the potential dimensional measurement error is jointly determined by the mechanical properties of the substrate and of the viscous material, the measurement performances of a stylus surface characterization instrument. In this project, numerical investigation of the surface deformation of polymer specimen under stylus surface profiling is realized with the help of the commercial Finite Element software Ansys®. To model the sliding deformation of polymer, the following variables will be firstly defined:

- (1) Averaged contact stress of the surface under stylus contact: $\sigma_c = \frac{F_{\text{tip}}}{A_c} = \frac{F_{\text{tip}}}{\pi r_{\text{tip}} \cdot d_L}$.
- (2) Contact strain: $\epsilon_c = \sqrt{\frac{d_L}{r_{\text{tip}}}}$.

The measured data can be recalculated on basis upon the aforementioned new variables, and depicted in Figure 45. The relationship between the contact strain and stress can be modelled by the following expression:

$$\frac{\epsilon_c}{\epsilon_0} = \frac{\sigma_c}{H_0} + \alpha_g \left(\frac{\sigma_c}{H_0} \right)^n,$$

where the parameters H_0 , α_g , and n have to be fitted from the experimental data.

Using the least-square fitting, the modelled curve (continuous curve in red) is shown in Figure 45. It can be seen that the experimental data can be well described by the nonlinear model proposed.

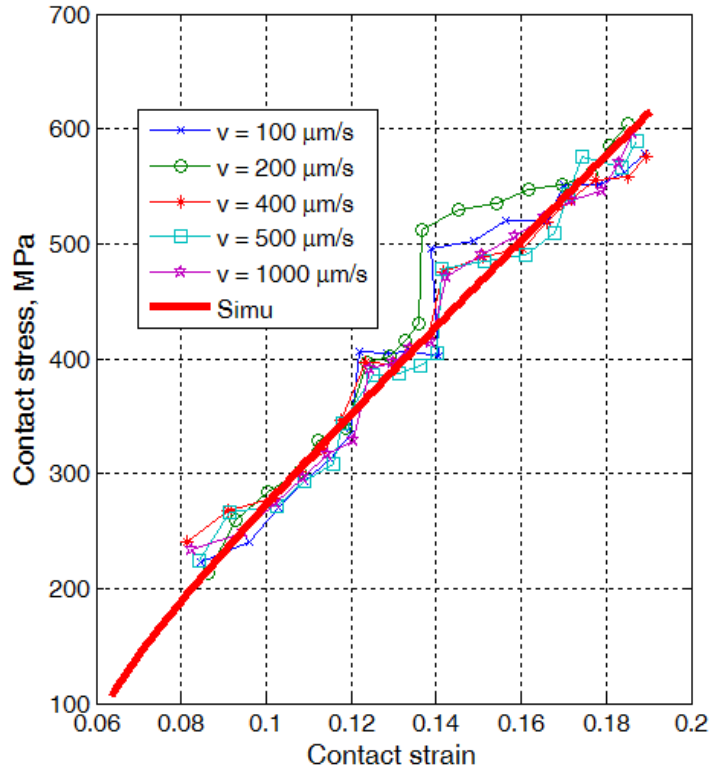


Figure 45: Modelling of the contact stress-strain curve of the photo resist SU-8 under different sliding contact.

3.3.5 Viscoelastic model used in 2D Finite Element analysis

In contrast to traditional structural materials like metals, polymers feature usually not only very weak mechanical properties, but also time-dependent deformation mechanism. To describe the visco-properties of polymer, there exist already a few different models, among them the Prony series might be one of the most popular models used in finite element simulation as chosen by PTB (see Figure 46).

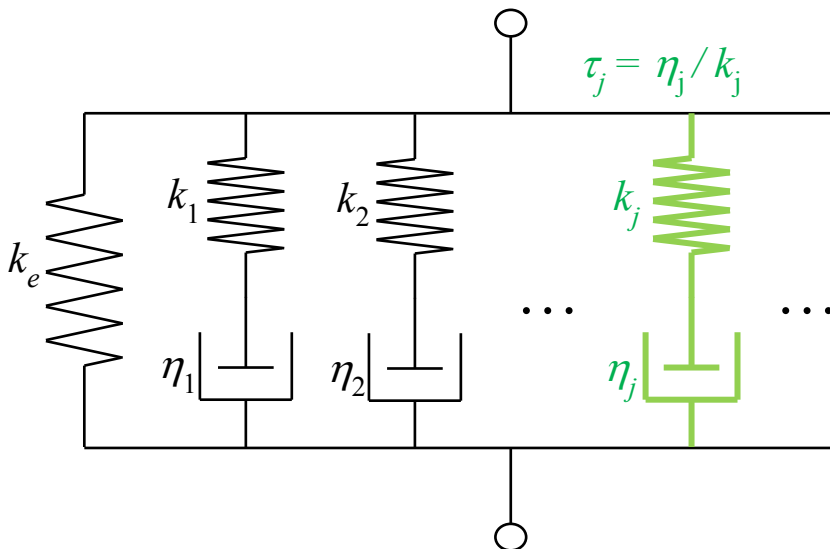
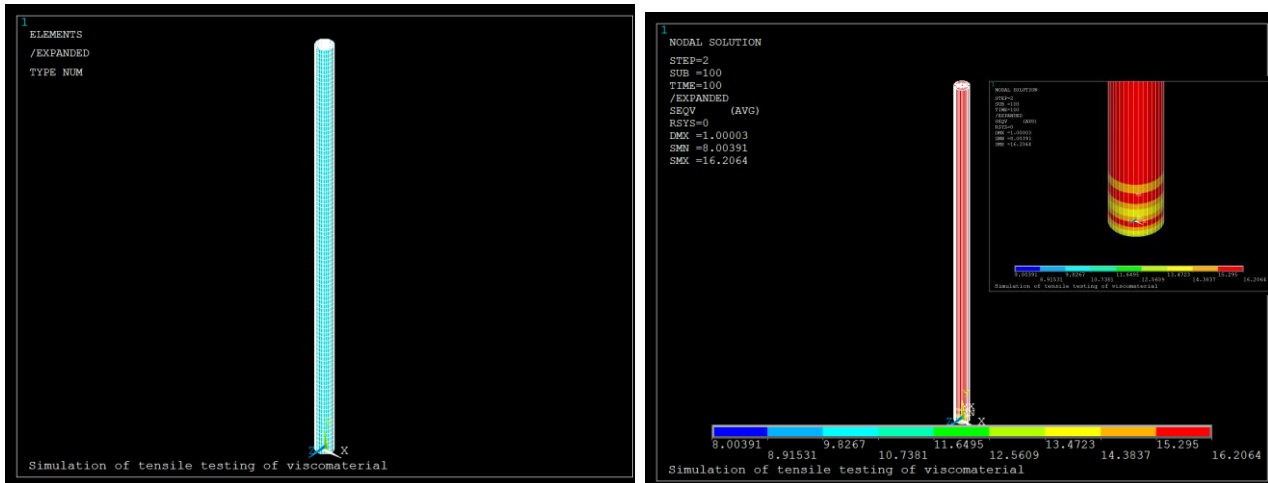


Figure 46 Standard linear solid (SLS) model used in Ansys for visco-elastic materials

a. Analytical verification of the visco-elastic model used in finite element simulation

For the purpose of validating the prony series used in FEA simulation, tensile testing of polymer rod is numerically investigated. It can be seen that the analytical result and the numerical simulation coincide well with each other. The coincidence of the numerical and analytical results for describing the relaxation response of Ormocomp specimen under different testing conditions proves that the viscoelastic model proposed in section 3.3 works well, can be further applied for contact-based analysis.



(a) Geometrical model

(b) Simulation result

Figure 47: 2D FEA modelling of tensile testing for viscous materials

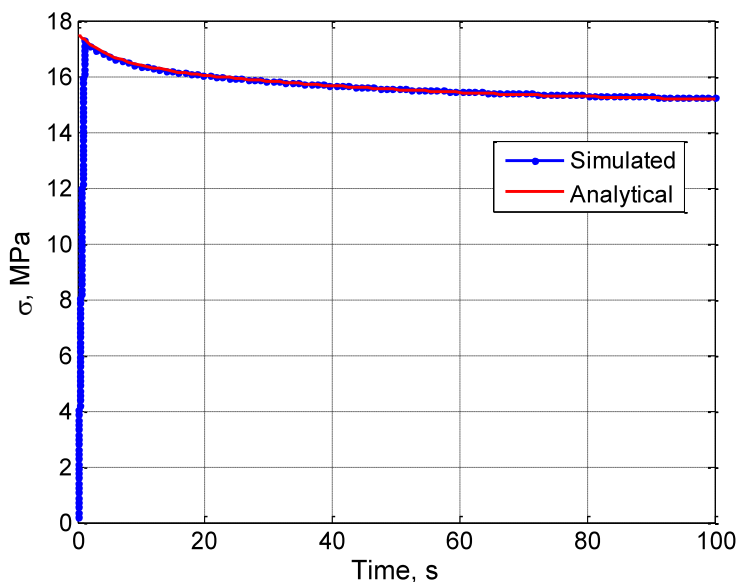


Figure 48: Validating the FEA simulation with analytical investigation: step-like load.

b. Numerical investigation of polymer surface deformation during tactile surface scan

The typical tactile surface scanning consists actually of two steps: (1) engagement and (2) surface scanning with predefined scanning speed and probing force. For the specimens of viscous materials, the final surface deformation suffers from the combined effect of the two procedures. Therefore, in the following, numerical investigation of the engagement and scanning procedure will be carried out subsequently.

Engagement procedure:

During the stylus-specimen engagement procedure, the surface deformation of a polymer specimen is symmetric with respect to the vertical axis of the stylus in use. Therefore the specimen and the spherical stylus tip can be described with a $\frac{1}{4}$ plane model, as shown in Figure 49 below:

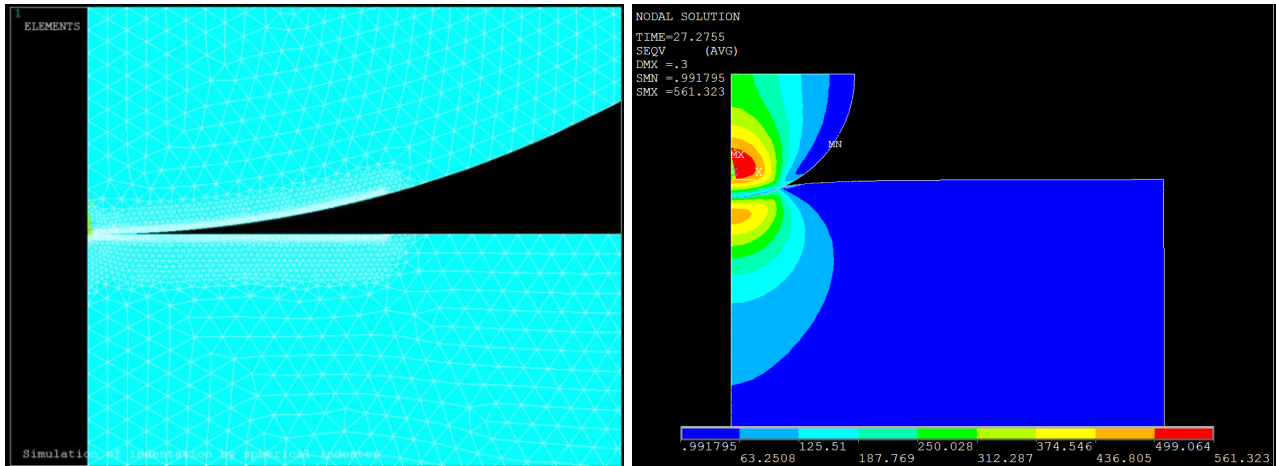


Figure 49: 2D FEA modelling of Stylus engagement: left: FEA model; right: Nodal solution of the stress distribution under stylus contact during engagement procedure.

Surface scanning procedure:

The FEM model is further applied for simulation of the surface scanning with a spherical stylus tip. Obviously, during the surface scan, the specimen surface suffers from sliding contact. The contact pair between the stylus tip and the specimen remains unchanged.

Figure 50 illustrates the typical cross-sectional contact stress distribution within the stylus-specimen pair. Compared with Figure 49, it can be seen clearly that during sliding contact, the contact stress under the specimen surface is no longer symmetric (with respect to the vertical axis of the spherical stylus). The FEM model is further applied for simulation of the surface scanning with a spherical stylus tip. Obviously, during the surface scan, the specimen surface suffers from sliding contact. The contact pair between the stylus tip and the specimen remains unchanged.

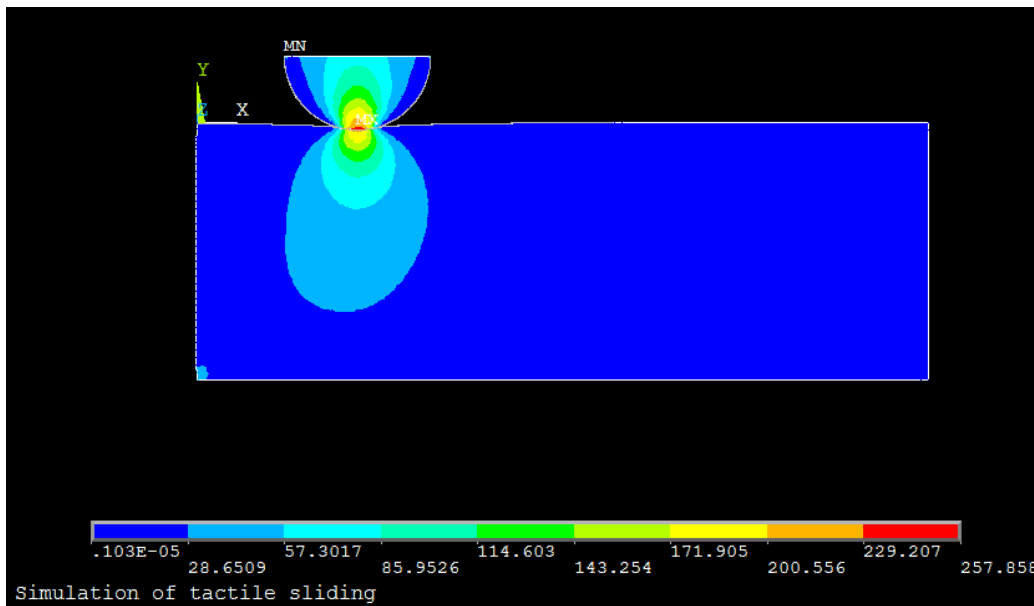


Figure 50: FEM simulation of the stylus surface scanning.

For the purpose of understanding of the surface deformation mechanism of viscous materials under tactile surface measurement, finite element simulation of the polymer deformation under spherical contact has been carried out. To describe the viscous properties of polymer, the traditional prony series on basis of Weichert rheological model has been used. The feasibility of this material model has been numerically investigated for tensile testing. It has been verified that the numerical result of tensile test for polymer, e.g.Ormocomp, coincides well with typical analytical result.

A two-dimensional simulation model has been presented in this report for numerical investigation of the polymer surface deformation under spherical sliding contact. A typical tactile scan is separated into two steps, i.e. engagement procedure and tactile scan with fixed probing force and scanning speed, and then numerically simulated subsequently.

Numerical results show that

- (1) In the range of shallow surface deformation, the specimen deformation is actually independent to the scanning speed, which should coincide well with the experimental results,
- (2) The stylus-surface interaction will fall into steady-state, only when the lateral scan length is far larger than the tip radius of a stylus in use.

The finite element simulation in this report lays a good foundation for further development of the analytical model for predicting the surface deformation of polymer under tactile geometrical measurement. Demands on quantitative characterisation of the dimensions of micro-scale polymer specimens require the further development of stylus profilometry. One of the main error sources within tactile dimensional measurement of polymer structures comes from the surface deformation of specimen under stylus scanning with a certain probing force. In this paper, a practical elastic-viscoplastic model has been proposed for modelling the (steady-state) polymer deformation during tactile surface scanning. To experimentally determine the (time-dependent) material properties of polymers necessary for the proposed analytical model, a stylus-profiling based methodology has been detailed. The feasibility of enhancing the measurement accuracy of currently available stylus pro- filometers for polymer based upon the aforementioned measuring methodology and analytical model has been experimentally tested. Preliminary experimental results for measuring the step height of polymer structures demonstrated that the tactile measurement deviation due to polymer surface deformation can be suppressed to less than 5 nm (1) within the whole probing force range of a commercial profilometer and under quite different scanning speeds. Although in the experimental investigations, only one of the typical photo-resists, Ormocomp, has been employed. Theoretical analysis indicates that the proposed tactile deformation correction model should be also effective for most thermal-plastic polymers.

3.3.6 Viscoelastic model used in 3D Finite Element analysis

For the purpose of understanding the surface deformation mechanism of viscous materials under tactile surface measurement, finite element simulation of the polymer deformation under spherical contact has been carried out by PTB. A three-dimensional simulation model has been presented in this report for numerical investigation of the polymer surface deformation under spherical sliding contact. A typical tactile scan is separated into two steps, i.e. engagement procedure and tactile scan with fixed probing force and scanning speed, and then numerically simulated subsequently. To describe the viscous properties of polymer, the traditional prony series on basis of extended Maxwell rheological model has been used. The finite element simulation in this report lays a good foundation for further development of the analytical model for predicting the surface deformation of polymer under tactile geometrical measurement. The feasibility and effectiveness of this FEM modeling will be further investigated with materials, whose viscous properties are well known.

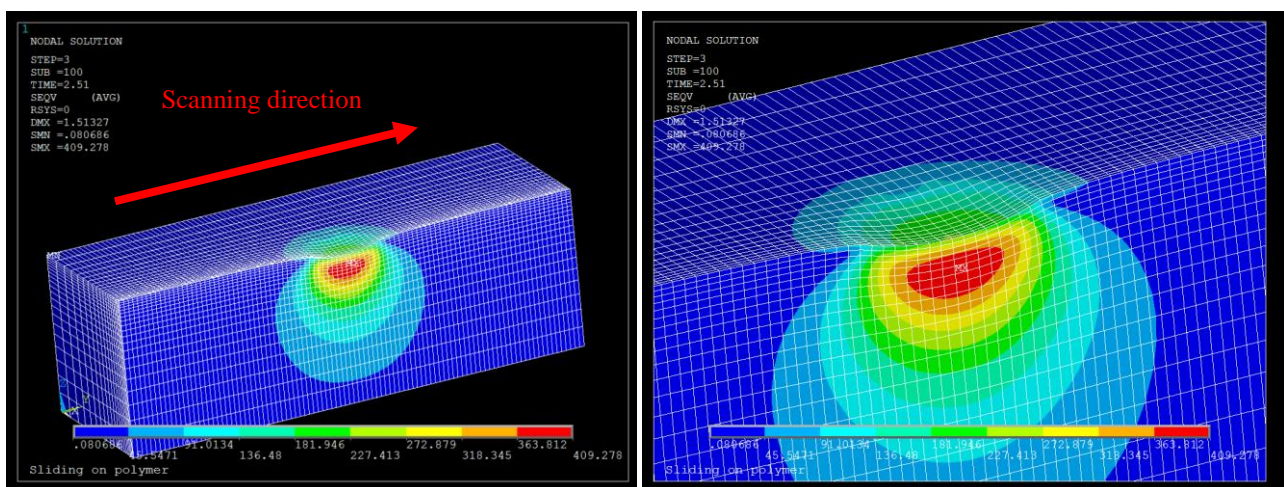


Figure 51 FEM simulation of the stylus surface scanning: left: Stress distribution within a polymer specimen during the tactile surface scan; right: Detailed view of the specimen stress distribution under a diamond stylus.

Key research outputs and conclusions

The objective was achieved, as new, time-enabled contact mechanics analysis methods were developed and validated for both dynamic (oscillating) and creep-compliance experiments. Open-source publication of the algorithms and source-code is intended, in order to facilitate direct use in ISO standards and rapid uptake in test instruments. The improved analytical models were developed and incorporated into SIOMECS software by the [Saxonian Institute of Surface Mechanics](#) for the analysis of mechanical surface measurements such as instrumented indentations, scratch tests and tribology tests. In addition, the project undertook initial work to identify suitable candidate reference materials that could be used to validate and calibrate apparatus used for long-term experiments for other users. Eight different polymeric materials were selected, and samples were distributed to project partner institutions for mechanical property testing. The new analysis methods were applied to the obtained data from macroscopic tests and both oscillating dynamic indentation and indentation creep tests.

3.4 Case Studies

3.4.1 Case study 1: Correction of step height measurement obtained using commercially available tactile probe methods

Owing to their unique advantages such as low cost, lightweight, ease of processing and excellent optical properties, polymer materials including SU-8, PMMA and PDMS have long been employed in micro-system technology. To date, various polymer micro-components and micro-systems have been developed, including micro-optics such as micro-lens arrays and diffractive micro-optical elements, micro-actuators and -sensors such as micro-grippers, micro-x-y stages and micro-polymer resonators. As one of the key points in quality control of these polymer micro-components and micro-systems, their geometrical dimensions have to be

quantitatively characterised. As for dimensional characterisation of structures in micro and nano-scale, there exist already various approaches, including non-contact (optical) methods and stylus profilometry. However, due to the quite low reflectance of most polymer microspecimens, optical approaches fail in many cases, especially when complex objects such as polymer specimens on silicon substrates have to be measured. Taken into consideration that contact-based stylus profilometry is, in principle, independent of the optical properties of the specimens to be measured, it is therefore expected that polymer micro-specimens could be quantitatively determined by tactile surface profilometry. Preliminary experimental investigations indicate, however, large systematic deviations when stylus profilometry is used for dimensional measurement of polymer specimens, especially polymeric structures on hard substrates (for instance, silicon wafers), since polymers have generally much weaker elastic modulus than metallic, ceramic and semi-conductor materials.

Commercial stylus instruments usually feature excellent vertical resolution and a quite large vertical measurement range (up to several millimetres). For the purpose of this project, i.e. quantitative measurement of the step height of micro-machined structures, nonlinearity within the whole vertical scan range (up to 50 micrometers) has to be well investigated. An optical flat with excellent flatness is employed to experimentally investigate the vertical nonlinearity of a stylus profilometer:

1. The glass flat is firstly well located (perfectly parallel to the horizontal scanning axis of the instrument), so that within the whole lateral scanning range of the profilometer (e.g. 6 mm) the absolute surface profile has tilting less than several micrometers.
2. Then, the glass flat is tilted slightly to yield profile variations up to 60 μm within the whole lateral scan.
3. By means of comparison of the measured surface profiles obtained by the stylus instrument under test, the vertical nonlinearity of the instrument can now be revealed.

Figure 52 below shows the measured surface profiles of an optical flat under different conditions using a stylus profilometer Tencor P11 located at PTB. Preliminary results indicate that the nonlinearity of the profilometer amounts to less than 0.3% within a vertical measurement range of up to 50 μm .

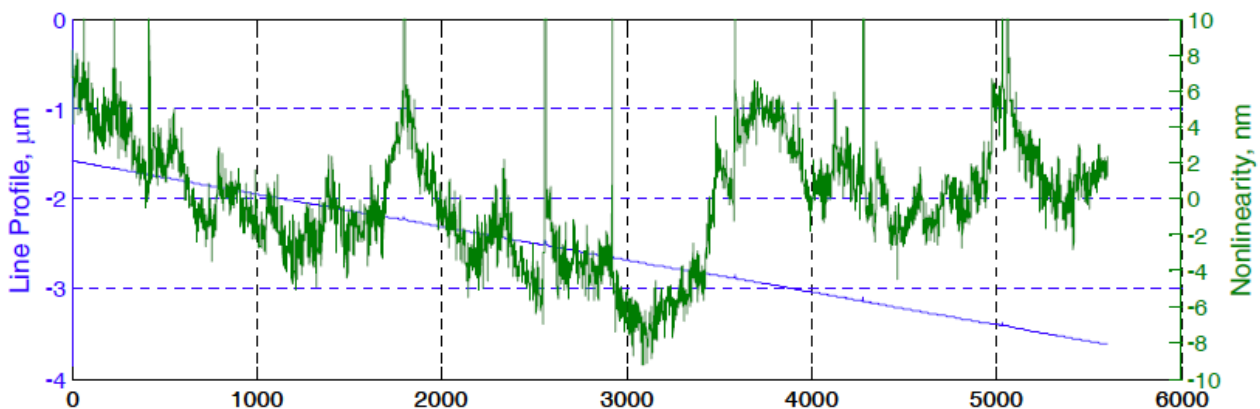


Figure 52 Investigation of the nonlinearity of the depth sensing system within a stylus profilometer (P 11, KLA Tencor) using an optical flat

A reliable tactile step-height measuring platform is now available, which features a probing force uncertainty less than 5 % and a step height measurement error of less than 5 nm (within 50 μm measurement range), and therefore offers quantitative measurements for the verification of the analytical model for tactile measurements of viscous specimens. The actual measurement accuracy of various tactile surface profilometers is determined not only by the fundamental specifications of the profilometers themselves, including the probing force in use, stylus' tip radius, scanning speed, etc, but also the mechanical properties of materials under test. The potential dimensional measurement error is jointly determined by the mechanical properties of the substrate and of the viscous material and by the measurement conditions of the stylus instrument in use.

To quantitatively investigate the measurement errors of tactile profilometry, and contact stylus profilometer in particular, in the Physikalisch-Technische Bundesanstalt (PTB, Braunschweig, Germany) a set of layered micro-structures on silicon substrates are fabricated, whose layered materials are of

- Aluminum, □ Gold, □ Cu, □ Su-8, □ maP

All the above materials are quite often employed in micro-/nano technology for practical applications. Furthermore, under the condition that the surface deformation of micro-structures under contact stress be relatively small, the first three metallic materials can be well described with traditional elastic-plastic models, and the behaviour of the latter two polymeric materials can be modelled with typical visco-elastic-plastic analysis.

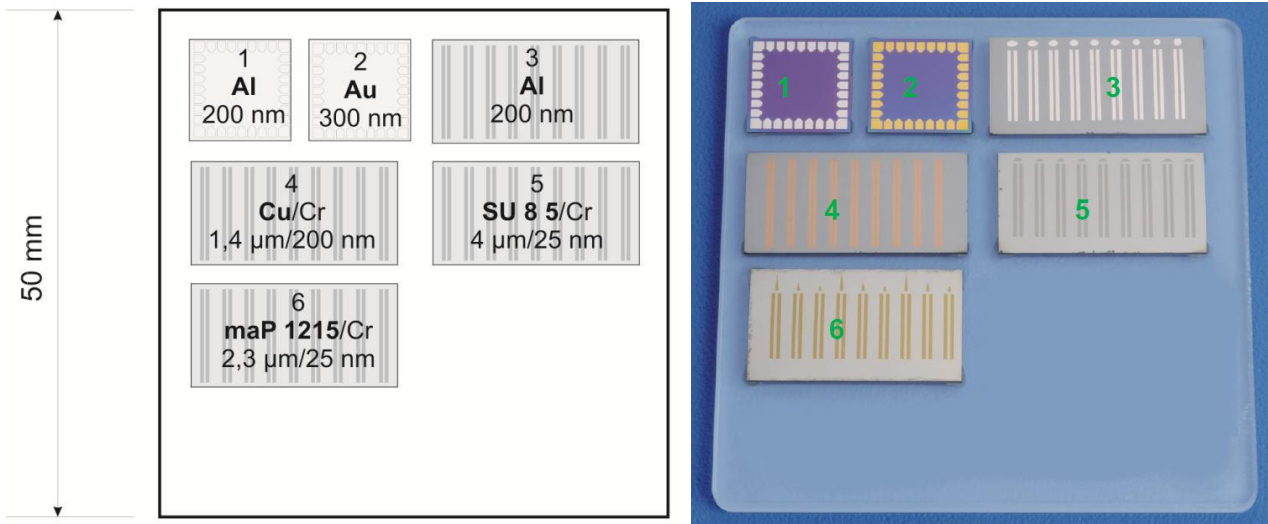
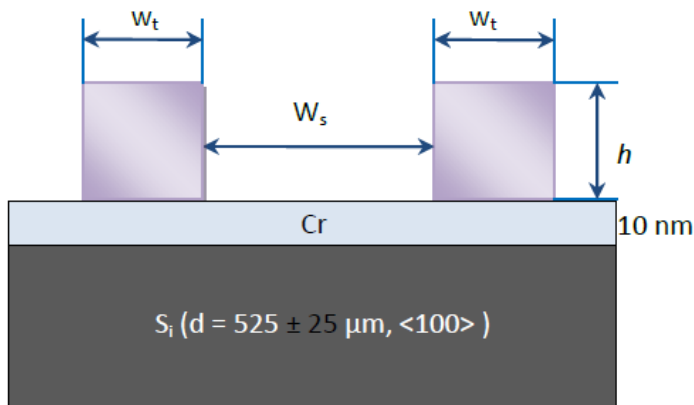
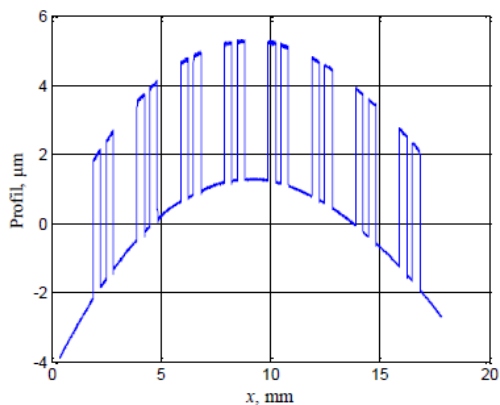


Figure 53 Photography of the PTB's layered step-height specimens (SdN7) and schematic of the layout.

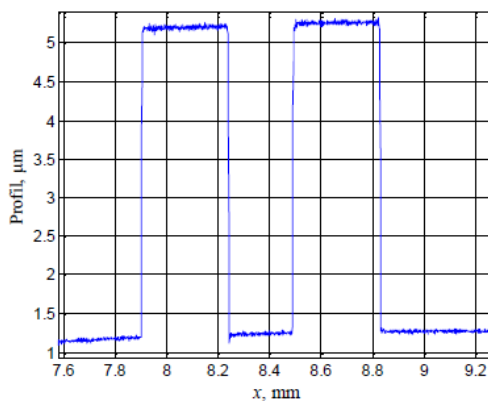


Chip No.	Layered material	$h, \mu m$	$W_t, \mu m$	$W_s, \mu m$
5	Su-8	4.1	375	300
6	maP	2.2	375	150

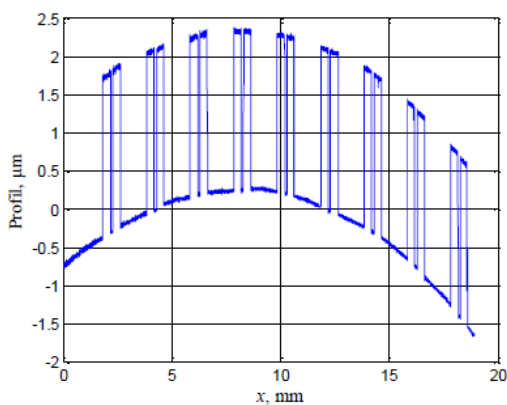
Figure 54 Cross-sectional configuration of the layered structures on Chip 5 and 6 respectively.



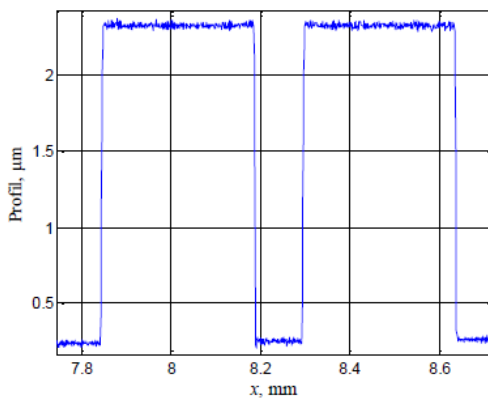
(a) Cross-sectional Profile chip 5



(b) detailed profile of the step height specimen (Chip 5)



(a) Cross-sectional Profile chip 6



(b) detailed profile of the step height specimen (Chip 6)

Figure 55 Cross-sectional profile of the layered structures on chip 6 measured by a stylus profiler (LD 120, Marsurf, Mahr GmbH, Germany, fundamental parameters: probing force = 500 μ N, stylus radius = 20 μ m, scanning speed = 100 μ m/s). The averaged step height of the Su-8-layer is found to be appr. 3.991 μ m. And the maP layer on chip 6 is about 2.080 μ m thick.

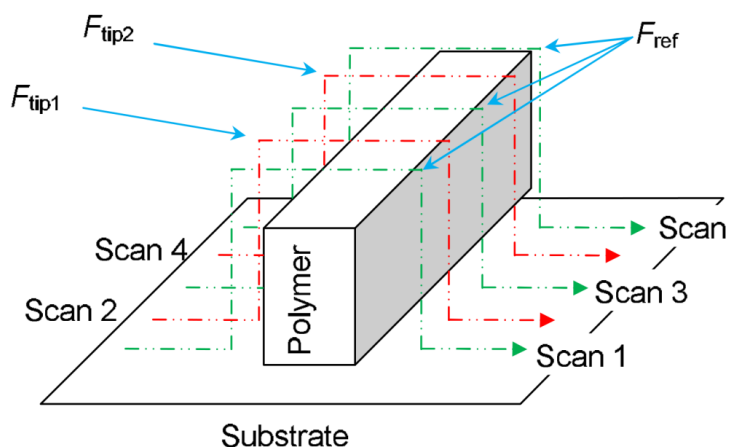


Figure 56 Strategy to scan a polymer surface using a stylus profilometer with known tip radius

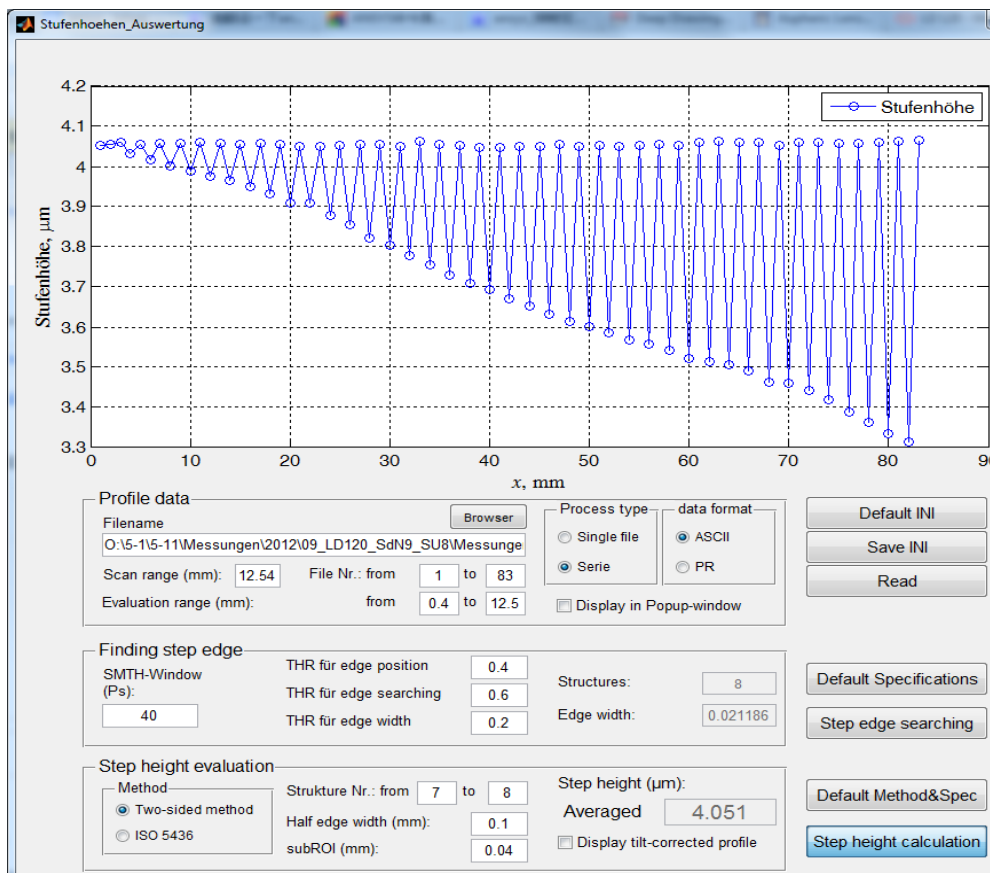


Figure 57 Typical measurement results using the stylus profilometer LD 120 with different probing forces.

Chips 5 and 6 employ the same wafer as a substrate, on which a thin chromium layer (appr. 10 nm thick) is coated so as to enhance the bonding strength of the polymer layers.

The polymer SU-8 used for chip 5 consists of three components: a base resin, solvent and photo-sensitive component. The polymer maP contains 2-methoxy-1-methylethyl acetate.

Since the specimens 5 and 6 consist of polymer as the structure materials, it can be imagined that relatively large deviation will be induced when the probing force becomes high.

To improve the measurement uncertainty of stylus profiling for soft materials, a series of surface scanning have been made, as illustrated in the Figure 56. The reference probing force used in the measurement $F_{ref} = 500 \mu\text{N}$, and the probing force F_m is increased from $500 \mu\text{N}$ to 8mN . The measured step height of the SU-8 structures under $v_{tip} = 100 \mu\text{m/s}$ is illustrated in Figure 57. It can be seen clearly that with increased probing force the measured step height becomes smaller. Under different scanning speeds, the aforementioned measurements have been undertaken. Finally the relationship between the surface deformation and different measuring conditions (i.e. varying probing force and scanning speed) is illustrated in Figure 58. It can be seen that the surface deformation of SU-8 specimens can be up to about 400 nm, when the probing force is increased to 8 mN, and a stylus with the tip radius of $2 \mu\text{m}$ is used for surface probing. In the meantime, it's also noticeable that the surface deformation of SU-8 specimens shows little influence of the scanning speed. The reason can be that the scanning speeds used in the measurements are generally quite fast, yielding that the tip-surface lateral contact time is much faster than the time constant of this material, therefore the viscoelastic effect of this material under test becomes very weak.

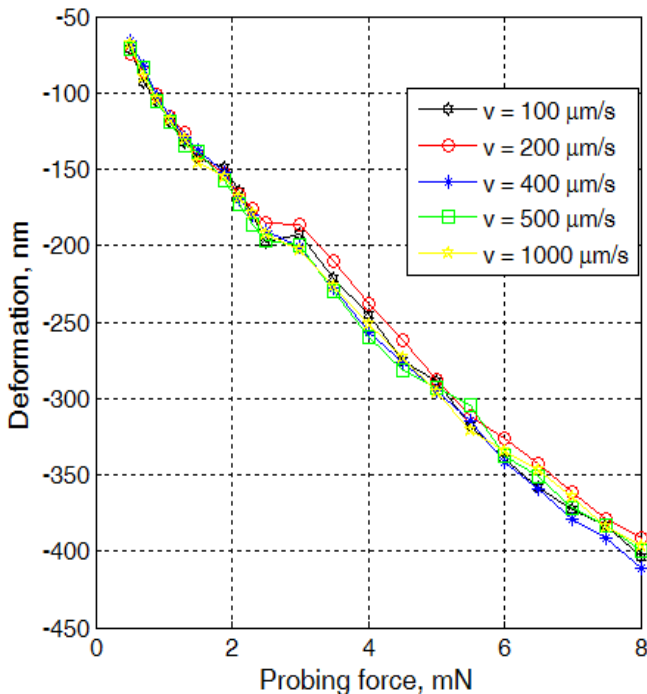


Figure 58 Systematic measurement deviation of surface profiler LD120 under different measurement conditions

3.4.2 Case study 2: Nano-Indentation Visco-Elastic Characterisation of Elastomers for Creep Prediction of Automotive Timing Belts.

The aim of this work was to use nano-indentation creep measurements to characterise the viscoelastic properties of elastomeric latex to predict the creep performance of timing belts provided by NGFE. The automotive cam timing belt has a critical role in controlling the CO₂ emissions and fuel economy of the internal combustion engine. With the advancement of timing belt technology the creep extension performance can be considered best-in-class at <0.1% during the service life of the belt (inside the engine, running in oil for the life of the engine: 320 000 km). In contrast a typical chain timing drive has creep extension of 0.3-0.5% over the same period which leads to deterioration of the environmental performance of the engine during use.

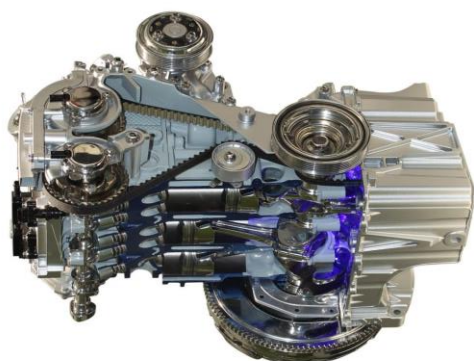


Figure 59 Modern automotive timing belts in-situ

The creep extension of a timing belt is restricted by the creep extension of the reinforcing glass cord. The cord is a composite structure where thousands of glass filaments are coated with elastomeric latex and twisted together. The creep of the high strength glass filaments is negligible. However, as the elastomer has viscoelastic properties the filaments can re-align within the twisted composite. A reduction in twist will cause an increase in length of the glass cord composite. Therefore, a good understanding of the long-term creep behaviour of the latex materials is the key to predict the product life and enable better design. This was investigated in this case study, using a reproducible “force-increase ramp and hold” indentation creep method. An instrumented indentation system (UNHT, CSM instruments) was used to perform these creep tests. The UNHT located in a controlled laboratory environment in NPL has demonstrated ultra-high stability; the average (drift+ creep) rate was observed to be smaller than 0.2 pm per second when contacting a piece of sapphire with a Berkovich indenter at a force of 9 mN over a period of 10 hours. This ultra-stability enables collection of valid, low-uncertainty, long-term creep data; orders of magnitude longer than previously possible.

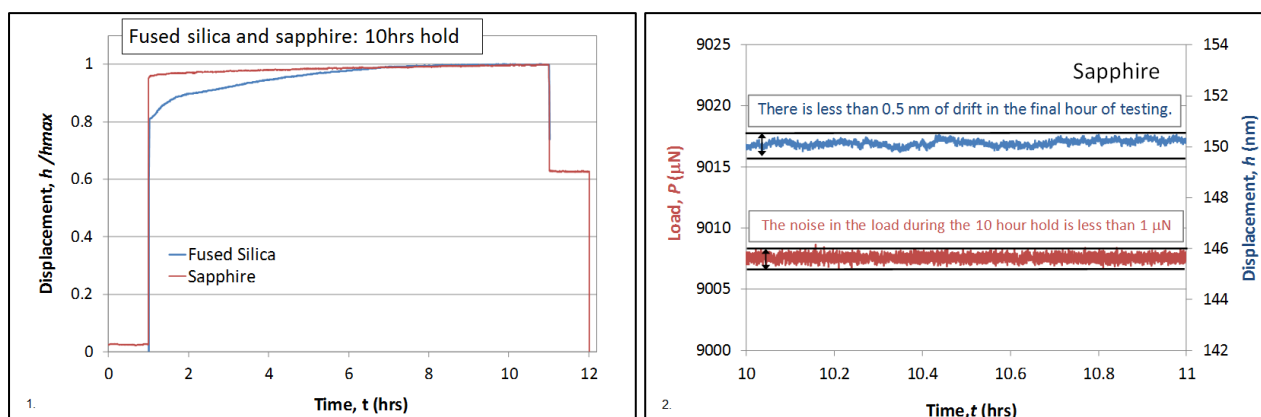


Figure 60 Left: shows the 10 hour nano-indentation creep of sapphire; Right: shows that during the last hour the load noise was <1µN, and the positional drift was <50 nm.

A Berkovich indenter was used to conduct creep experiments on solid films of the latex. A Designed Experiment with two levels and two factors was used to prepare latex systems for study:

Latex:	Standard Crosslinker	High Crosslinker
No Filler:	No Standard	No High
With Filler:	With Standard	With High

A maximum force of 0.2 mN was chosen for five different hold segments with creep time ranging from short experiments of 10 seconds, to longer experiments of 30,000 seconds. The n-element Kelvin-Voigt model, which is an extension of the standard linear model with extra Kelvin-Voigt elements, was used to analyse the indentation creep data obtained by NPL. The loss and storage modulus, and the time constant values were obtained by running the data through a fitting algorithm. The nano-indentation measurements were compared with Rubber Process Analyser (RPA) viscoelastic data at 10% shear strain at 150 °C for the same materials, obtained by NGFE.

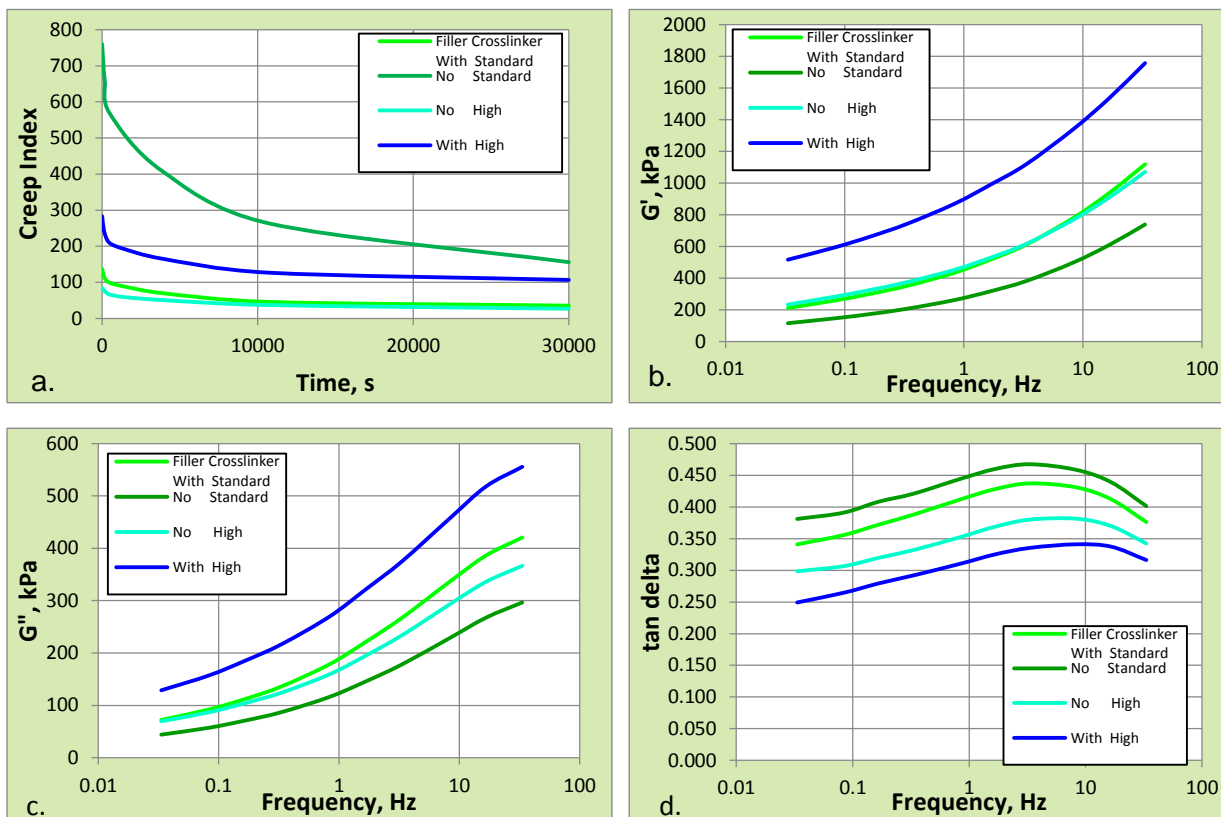


Figure 61 [a] shows the normalised nano-indentation creep of the four latex system; [b] shows the RPA elastic shear modulus dependence upon frequency; [c] shows the RPA viscous shear modulus dependence upon frequency; [d] shows the RPA tan delta dependence upon frequency.

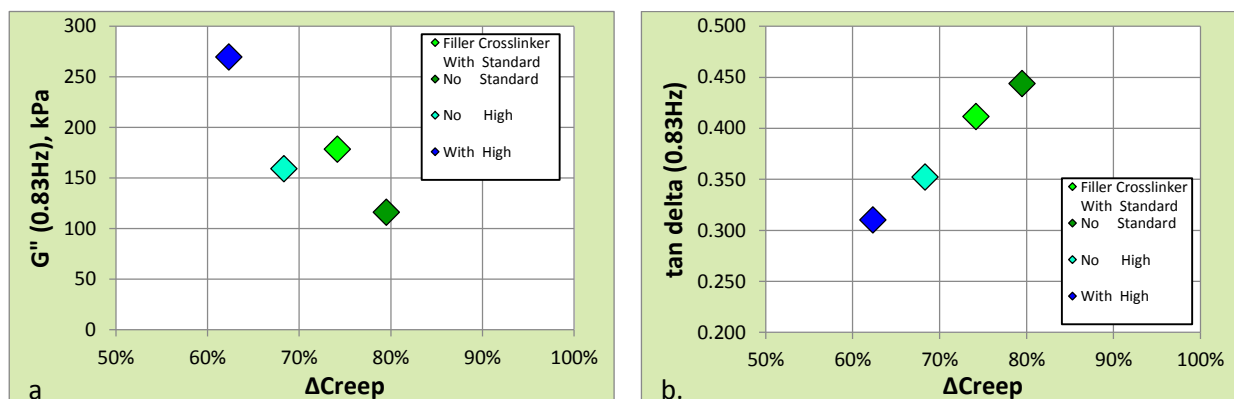


Figure 62 [a] shows the correlation between Δ creep and RPA viscous modulus; [b] shows the correlation between Δ creep and RPA tan delta.

The creep properties were expected to correlate to the RPA viscous (G'' or $\tan \delta$) properties. The % change of the starting indentation to the end of test (30000 seconds) indentation was used as the measure of creep. A loose correlation was observed between RPA viscous modulus and creep. An almost perfect correlation was observed between creep any hysteresis as measured by tan delta. The prediction from the creep and RPA measurements was that the latex with no filler and standard level of crosslinker would give the highest belt growth, and that the latex with filler and high crosslinker would give the lowest belt growth.

The UNHT nano-indentation instrument was shown to be incredibly stable, well suited to creep measurements. Creep measurements of cured latex were successfully completed. The nano-indentation creep data correlated to RPA tan delta data, and has predicted the system that would give the highest timing belt growth.

3.5 Certified reference materials

A few candidate certified reference polymer materials were investigated for instrumented indentation testing including PS-3, PS-8, LDPE, HDPE, PC and PMMA, These materials cover a range of modulus from hundreds of MPa to a few GPa. The time dependent properties were also studied extensively on these materials. As a result, a protocol was developed for indentation creep and dynamic testing of polymers, submitted to the VAMAS TWA 22 as a new project: “the international comparison of viscoelastic properties of polymers”. This new VAMAS project will further confirm the suitability of these selected materials as reference materials as a Round-robin exercise.

In this project, PTB designed and fabricated five test artefacts, Aluminium, Gold, Cu, Su-8, and maP; this set of layered micro-structures on silicon substrates were used to quantitatively investigate the measurement errors of tactile profilometry, and contact stylus profilometer. These artefacts have potentials to be used as reference materials for profilometry testing on polymers.

3.6 Summary of research results

- A new, highly-stable, optical interferometer system, with low-noise, high-sampling rate electronics, suitable for use in industrial settings was developed at NPL. Optical interferometers combine and overlap light-waves to intensify the waves, creating high-resolution, accurate images, suitable for measuring changes in the shape and dimensions of viscous materials. The stability of the optical interferometer was assessed and calibrated using an X-ray interferometer at NPL, the UK's National Measurement Institute (X-ray interferometers are more accurate but less suitable for industrial conditions than an optical interferometers). The optical interferometer demonstrated a measurement drift of 0.54 nanometres (approximately the width of two atoms) over a 64 hour period, a drift rate of one proton width per second – suitably accurate for measuring long-term changes in the properties of viscous materials. The optical interferometer system was made portable, to ensure it can be used to make in situ measurements, as a displacement calibration mean especially for the instrumented indentation systems at NMIs, DIs and industrial partners.
- Indentation creep testing, a technique that measures properties of a sample under pressure, was used to measure changes in shape and dimension, and to assess the elasticity and viscosity of samples. A new measurement capability was developed at NPL for long-duration, ultra-stable indentation creep measurements, using a UNHT nano-indenter (from [Anton Paar Ltd](#)). Displacement rates as low as 20 femtometres per second over a 66 hour period were demonstrated (less than two atomic nucleus widths per second), one of the longest nano-indentation creep tests ever performed.
- New correction algorithms were successfully developed for profilometer probes, which enabled correction for distortions created during soft material surface mapping. The project team also developed well-characterised step height change reference materials and organised a comparison exercise where in which they were used by profilometry instrument manufacturers to assess instrument performance. A tactile probe profilometer ISO standard is in preparation.
- New, time-enabled contact mechanics analysis methods were developed and validated for both dynamic (oscillating) and creep-compliance experiments. Open-source publication of the algorithms and source-code is intended, in order to facilitate direct use in ISO standards and rapid uptake in test instruments. The improved analytical models were developed and incorporated into SIOMECH software by the [Saxonian Institute of Surface Mechanics](#) for the analysis of mechanical surface measurements such as instrumented indentations, scratch tests and tribology tests.
- The project undertook initial work to identify suitable candidate reference materials that could be used to validate and calibrate apparatus used for long-term experiments for other users. Eight different polymeric materials were selected, and samples were distributed to project partner institutions for mechanical property testing. The new analysis methods were applied to the obtained data from macroscopic tests and both oscillating dynamic indentation and indentation creep tests. Candidate certified reference polymer materials for profilometry testing were also designed, fabricated and investigated.

4 Actual and potential impact

Dissemination of results

To promote the uptake of the methods and materials developed, project outputs were shared broadly with scientific and industrial end-users: 15 papers were published in international scientific journals (listed in the following section), including *Philosophical Magazine*, *Wear*, *Journal of Applied Polymer Science*, *Measurement Science and Technology*. Over 50 presentations were given at national and international conferences, meetings and seminars. 9 presentations were given to standards committees, including ISO/TC/SC3, ISO/TC/SC2, and CEN/TC 155 WG26. Discussions were held in these meetings on the development of new standards for measuring viscous materials, and have been progressed as new work items (ISO-14577 Part 6 and Part 7). 18 trainings sessions/workshops were held on testing viscous materials. Measurements were contributed to a study of the ultra-violet induced degradation of polypropylene, and have been included in a report by the UK Materials [Knowledge Transfer Network](#). Stakeholder meetings were held in September 2012 at the [PSE 2012](#) conference in Gernisch-Partenkirchen, Germany; April 2013 at NPL, Teddington, UK; October 2013 at the ECI Nano-Mechanics conference in Olhao, Portugal. To demonstrate the use of the methods developed here, two industrial case-studies were written; “*Correction of step height measurement obtained using commercially available tactile probe methods*” and “*Nano-Indentation Visco-Elastic Characterisation of Elastomers for Creep Prediction of Automotive Timing Belts*”.

Early impact on industry

[Mahr](#), a leading manufacturer of measurement equipment in the plastics processing industry, took part in the profilometry comparison exercise in objective 1. Results from this exercise, along with the project’s correction algorithm, have allowed Mahr to develop a new ‘low load’ profilometer suitable for viscous materials, which that can accurately measure a sample without altering or damaging it, and without material accumulating on the probe. The profilometer correction algorithms have also been incorporated in a German Institute for Standardization (DIN) standard, ensuring wider access to these techniques for instrument manufacturers and will ultimately lead to improved profilometry data for their customers.

Within objective 2, the project successfully developed a new method for measuring the creep properties of viscous materials, measuring creep rates in the 20 femtometres per second range. This method is being used by [SDS Limited](#), who design, manufacture and install water management systems, to better understand the long-term performance of their underground structural products, which must maintain their dimensional stability over decades of use. Long-term deformation measurements on materials used in the construction of underground water storage chambers are helping SDS to develop more durable and longer-lasting products. Additionally, SDS’s involvement in the project has allowed them to better understand and influence the work of standards committees, allowing SDS to help shape the development of other test methods relevant to their product range through CEN and ISO committees.

Detailed analyses of measurement errors and new calibration procedures were developed for a range of instruments used throughout the project. Results were shared with the instrument manufacturers, such as [Anton Paar](#) and [Micro Materials Ltd](#), at a workshop held in conjunction with the final project meeting at PTB in Germany. Anton Paar has used these results to develop a dedicated instrument specifically for the polymer testing market. Anton Paar have also upgraded their nano-test control and data processing software across their range to incorporate improved correction and mechanical property determination routines, ensuring their customers can benefit from the greater understanding of microscale testing that has resulted from the project. The [Saxonian Institute of Surface Mechanics](#) has used the results from objective 3 to enhance their range of software products, including algorithms and models. The software is widely acclaimed, and used by the indentation and scratch measurement communities for the study of surface properties of a wide range of materials. This software is a powerful tool for designers to use across a huge range of applications, confident in the knowledge that their designs will result in more durable products.

Two new work items have been proposed and accepted by ISO TC164/SC3I for hardness testing of materials. The development of these standards will ensure widespread uptake of the test and analysis methods developed in this project.

The project results have helped to finalize the German standard DIN 32567-3:2014-10: Production equipment for microsystems - Determination of the influence of materials on the optical and tactile dimensional metrology - Part 3: Derivation of correction values for tactile measuring devices.

In the year 2014 PTB has provided the project results and methods for stylus profilometry for further input to ISO TC 213 WG 16 where they are proposed to be incorporated into the new areal surface roughness standard ISO 25178. Within this drafted work item, a practical measurement method and strategy is suggested for the determination and correction of the systematic deviations of stylus instruments in the case of measuring the height of specimens of soft materials on hard substrates. The objective of this work item is to provide a material-independent tactile surface measurement approach with lower measurement uncertainty.

Potential future impact on industry

The new methods developed in this project will allow scientific and industrial researchers to accurately measure the properties of viscous materials, leading to the development and widespread use of polymeric components in lightweight, high-performance and low-cost products. The methods developed can also be applied to additional measurement needs, including creep testing of polymers, rubbers and composite materials, commonly used in the aerospace, automotive and wind-power sectors. Specifically the nano-indentation mechanical property mapping of nano-composites and graphene based products. This will quantify the improvement of the polymeric materials performance with addition of nano-particle fillers providing the critically important feedback in material development and quality control. The techniques developed could be used to develop new innovations in these industries, such as the replacement of thermoset matrix composite materials with more durable thermoplastic matrix composites. Ultimately, the techniques developed here will be used to develop new materials and products across a broad range of industries, supporting European industrial competitiveness.

5 Website address and contact details

Project website address: <http://projects.npl.co.uk/meprovisc>

Contact person: Dr Xiaodong Hou (xiaodong.hou@npl.co.uk)

6 List of publications

N.Schwarzer "Short note on the effect of a pressure-induced increase in Young's modulus", Philosophical Magazine 2012, Vol. 92, pp.1631-1648 [doi:10.1080/14786435.2012.667579](https://doi.org/10.1080/14786435.2012.667579)

F.Seibert et al "Comparison of arc evaporated Mo-based coatings versus Cr₁N₁ and ta-C coatings by reciprocating wear test", Wear 2013, Vol. 298-299, pp.14-22 [doi:10.1016/j.wear.2012.11.085](https://doi.org/10.1016/j.wear.2012.11.085)

T. Fischer-Cripps et al "Critical review of Claims for Ultra-Hardness in Nanocomposite Coatings", Philosophical Magazine 2012, Vol. 92, pp.1601-1630 [doi:10.1080/14786435.2011.652688](https://doi.org/10.1080/14786435.2011.652688)

J.G.Kohl et al "An investigation of scratch testing of silicone elastomer coatings with a thickness gradient" Journal of Applied Polymer Science 2012 Vol 124, pp.2978-2986 [doi:10.1002/app.35325](https://doi.org/10.1002/app.35325)

N.Schwarzer, "Analyse und Simulation der mechanischen Eigenschaften beschichteter Polymere unter Berücksichtigung der meist zeitabhängigen Materialparameter", Proceedings of the V2011 Industrieausstellung & Workshop-Woche, Dresden, Germany, 17–20 October 2011; pp. 96–101, (In German).

N.Schwarzer and P.Heuer-Schwarzer "Qualitative failure analysis on laminate structures using comprehensive analytical linear elastic contact modelling", SEECCM-proceedings 2013

Z.Li et al "In-situ characterisation of the probing force of contact stylus profilers using a micromachined nanoforce actuator", Proceedings of the 12th euspen International Conference, Stockholm, June 2012

Z.Li and U.Brand "Towards quantitative characterisation of the small force transducer used in Nanoindentation Instruments", Modern Instrumentation 2013, Vol. 2, pp.61-67 [doi:10.4236/mi.2013.24009](https://doi.org/10.4236/mi.2013.24009)

Z.Li et al "In-situ traceable characterization of the depth sensing system of a nanoindentation instrument", 11th International Symposium on Measurement and Quality Control 2013

Z.Li et al "Towards quantitative modelling of surface deformation of polymer micro-structures under tactile scanning measurement", Measurement Science and Technology 2014, Vol. 25, 044010 [doi:10.1088/0957-0233/25/4/044010](https://doi.org/10.1088/0957-0233/25/4/044010)

Zhi Li, Thomas Ahbe, Sai Gao, Uwe Brand "In-situ characterisation of the probing force of contact stylus profilers using a micromachined nanoforce actuator", Proceedings of the 12th euspen International Conference

N.Schwarzer "From interatomic interaction potentials via Einstein field equation techniques to time dependent contact mechanics", Materials Research Express, 2014, 2053-1591 [doi:10.1088/2053-1591/1/1/015042](https://doi.org/10.1088/2053-1591/1/1/015042)

P. Heuer-Schwarzer, N. Schwarzer, "Investigation, quality control and optimization of laminate-structures – example: windsurfing boards, Proceedings of OPTI 2014

N.Schwarzer "Completely Analytical Tools for the Next Generation of Surface and Coating Optimization", Coatings 2014, Vol. 4, pp. 253-281 [doi:10.3390/coatings4020253](https://doi.org/10.3390/coatings4020253)

N. Schwarzer, "About Stress Field, Time and Temperature Dependent Contact Mechanics for Thin Film Structures – Especially the Role of Intrinsic Stresses", Proceedings of TechCon 2014

J.G.Kohl et al "Determining the viscoelastic properties obtained by depth sensing microindentation of epoxy and polyester thermosets using a new phenomenological method", Materials Research Express 2015, Vol. 2, 015301 [doi:10.1088/2053-1591/2/1/015301](https://doi.org/10.1088/2053-1591/2/1/015301)

Schiavi, AS, Cuccaro, RC and Troia, AT, "Strain-rate and temperature dependent material properties of Agar and Gellan Gum used in biomedical applications", Journal of the mechanical behavior of biomedical materials 2016, 53, 119-130 [doi:10.1016/j.jmbbm.2015.08.011](https://doi.org/10.1016/j.jmbbm.2015.08.011)

N. Schwarzer, "Scale invariant mechanical surface optimization applying analytical time dependent contact mechanics for layered structures, Proceedings SMT-28, 2014

Li, ZL; Brand, UB; Popadic, RP, "In-situ traceable characterization of a depth sensing system of a nanoindentation instrument", Proceedings of 11th International Symposium on Measurement and Quality Control 2013

Reference

-
- [1] C. Weichert, P. Kochert, R. Koning, J. Flugge, B. Andreas, U. Kuetgens and A. Yacoot. "A heterodyne interferometer with periodic nonlinearities smaller than ± 10 pm" *Meas. Sci. Technol.* **23** (2012) 094005
- [2] P L M Heydemann, "Determination and correction of quadrature fringe measurement errors in interferometers" *Appl. Opt.* **20** (1981) 3382–4
- [3] K.P. Birch and M.J. Downs. "An updated Edlén equation for the refractive index of air." *Metrologia* 30 (1993) p.155.
- [4] J. Nohava, N.X. Randall and N. Conte, "Novel ultra nanoindentation method with extremely low thermal drift: Principle and experimental results" *J. Mater. Res.* (2009) **24**, p. 873-882
- [5] Ruprecht R, Hanemann T, Piotter V, Haußelt J. Polymer materials for microsystem technologies. *Microsyst Technol* 1998;5:44-48
- [6] Z. Li, U. Brand, T. Ahbe, "Towards quantitative modelling of surface deformation of polymer micro-structures under tactile scanning measurement", *Measurement Science and Technology* 25(4):044010, 2014
- [7] <http://www.simetrics.de/pdf/FS-B.pdf>
- [8] H. Shinzawaa et al. Rheo-optical near-infrared (NIR) spectroscopy study of lowdensity polyethylene (LDPE) in conjunction with projection two-dimensional (2D) correlation analysis *Vibrational Spectroscopy* Volume 70, January 2014, Pages 53–57